



Theoretical Investigation of the Influence of Atmospheric Transmission on Commercial-Off- The-Shelf (COTS) Night Vision Scopes

Wayne C. King

Alliance for Education, Wright-Connection
2100 Kettering Tower
Dayton Oh 45423

August 1997

FINAL REPORT FOR 06/05/97-08/15/97

APPROVED FOR PUBLIC RELEASE; DISTRIBUTION UNLIMITED.

Sensors Directorate
Air Force Research Laboratory
Air Force Materiel Command
Wright-Patterson Air Force Base, OH 45433-7322

19980723 009

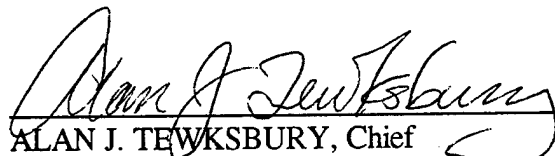
NOTICE

WHEN GOVERNMENT DRAWINGS, SPECIFICATIONS, OR OTHER DATA ARE USED FOR ANY PURPOSE OTHER THAN IN CONNECTION WITH A DEFINITELY GOVERNMENT-RELATED PROCUREMENT, THE UNITED STATES GOVERNMENT INCURS NO RESPONSIBILITY OR ANY OBLIGATION WHATSOEVER. THE FACT THAT THE GOVERNMENT MAY HAVE FORMULATED OR IN ANY WAY SUPPLIED THE SAID DRAWINGS, SPECIFICATIONS, OR OTHER DATA, IS NOT TO BE REGARDED BY IMPLICATION, OR OTHERWISE IN ANY MANNER CONSTRUED, AS LICENSING THE HOLDER, OR ANY OTHER PERSON OR CORPORATION; OR AS CONVEYING ANY RIGHTS OR PERMISSION TO MANUFACTURE, USE, OR SELL ANY PATENTED INVENTION THAT MAY IN ANY WAY BE RELATED THERETO.

THIS REPORT IS RELEASABLE TO THE NATIONAL TECHNICAL INFORMATION SERVICE (NTIS). AT NTIS, IT WILL BE AVAILABLE TO THE GENERAL PUBLIC, INCLUDING FOREIGN NATIONS.

THIS TECHNICAL REPORT HAS BEEN REVIEWED AND IS APPROVED FOR PUBLICATION.


JAMES G. GROTE, Proj. Engineer
MULTI-CHIP INTEGRATION BRANCH
AEROSPACE COMPONENTS DIVISION


ALAN J. TEWKSBURY, Chief
MULTI-CHIP INTEGRATION BRANCH
AEROSPACE COMPONENTS DIVISION


ROBERT T. KEMERLEY, Chief
AEROSPACE COMPONENTS DIVISION
SENSORS DIRECTORATE

IF YOUR ADDRESS HAS CHANGED, IF YOU WISH TO BE REMOVED FROM OUR MAILING LIST, OR IF THE ADDRESSEE IS NO LONGER EMPLOYED BY YOUR ORGANIZATION, PLEASE NOTIFY AFRL/SNDI, WRIGHT-PATTERSON AFB OH 45433-7322 TO HELP MAINTAIN A CURRENT MAILING LIST.

COPIES OF THIS REPORT SHOULD NOT BE RETURNED UNLESS RETURN IS REQUIRED BY SECURITY CONSIDERATIONS, CONTRACTUAL OBLIGATIONS, OR NOTICE ON A SPECIFIC DOCUMENT.

REPORT DOCUMENTATION PAGE			Form Approved OMB No. 0704-0188	
<small>Public reporting burden for this collection of information is estimated to average 1 hour per response, including the time for reviewing instructions, searching existing data sources, gathering and maintaining the data needed, and completing and reviewing the collection of information. Send comments regarding this burden estimate or any other aspect of the collection of information, including suggestions for reducing the burden, to Washington Headquarters Services, Directorate for Information Operations and Reports, 1215 Jefferson Davis Highway, Suite 1204, Arlington, VA 22202-4302, and to the Office of Management and Budget, Paperwork Reduction Project (0704-0188), Washington, DC 20503.</small>				
1. AGENCY USE ONLY (Leave blank)		2. REPORT DATE 15 Aug 97		3. REPORT TYPE AND DATES COVERED Final Report, 5 Jun 97 - 15 Aug 97
4. TITLE AND SUBTITLE Theoretical Investigation of the Influence of Atmospheric Transmission on Commercial-Off-The-Shelf (COTS) Night Vision Scopes			5. FUNDING NUMBERS PE: 62204F PR: 2001 TA: 05 WU: 12	
6. AUTHOR(s) Wayne C. King				
7. PERFORMING ORGANIZATION NAME(s) AND ADDRESS(es) Alliance for Education, Wright-Connection 2100 Kettering Tower Dayton OH 45423			8. PERFORMING ORGANIZATION REPORT NUMBER	
9. SPONSORING/MONITORING AGENCY NAME(s) AND ADDRESS(es) Avionics Directorate Wright Laboratory Air Force Material Command Wright-Patterson AFB OH 45433-7322 POC: James G. Grote (937)255-4557			10. SPONSORING/MONITORING AGENCY REPORT NUMBER WL-TR-97-1186	
11. SUPPLEMENTARY NOTES This effort was conducted in part under a NSF Grant to the Wright Connection. The author is associated with Miamisburg High School, 1860 Blvo Rd. Miamisburg, OH 45342				
12a. DISTRIBUTION AVAILABILITY STATEMENT Approved for public release, distribution unlimited			12b. DISTRIBUTION CODE	
13. ABSTRACT (Maximum 200 words) This report provides details on the analytical procedures utilized to predict the performance ultraviolet, visible, and near-infrared detectors under various atmospheric visibilities. All the analytical tools and product information are commercially available. Key to this effort was the utilization of the Phillips Laboratory Expert Assisted User Software (PLEXUS) program. The work clearly demonstrates that a high school teacher, using the current analytical, analysis, software, and computer tools can predict the "all weather" performance of selected commercial-off-the-shelf electro-optical components.				
14. SUBJECT TERMS COMMERCIAL-OFF-THE-SHELF (COTS), NIGHT VISION SCOPES, ATMOSPHERIC LIMITATIONS, ELECTRO-OPTICS			15. NUMBER OF PAGES 92	
			16. PRICE CODE	
17. SECURITY CLASSIFICATION OF REPORT U	18. SECURITY CLASSIFICATION OF THIS PAGE U	19. SECURITY CLASSIFICATION OF ABSTRACT U	20. LIMITATION OF ABSTRACT U	

Table of Contents

List of Figures	iv
Foreword	v
Section 1: Introduction	1
Section 2: Range Determination of Electromagnetic Spectrum for Detector Utilization	5
2.1: Theory	5
2.2: Application	9
Section 3: Visibility Range Determination	14
Section 4: Overview of Procedures for Determining Night Vision Detector Responses Under Atmospheric Conditions	15
4.1: Atmospheric Transmittance Values Generated By PLEXUS	16
4.2: Scan the Manufacturer's Response Curves	17
4.3: Determination Of The "X" And "Y" Values From The Manufacturer's Detector Response Graphs (Digitize)	18
4.4: Determine The Polynomial Fit Using Mathematica	18
4.5: The Convolution Of Transmittance And Detector Response Curve	25
Section 5: Conclusions	41
Appendix A: Plexus Procedural Details	43
Appendix B: Scanmaker II Procedural Details	56
Appendix C: Un-Scan-It Procedural Details	59
Appendix D: Procedural Detail for Determination of Polynomial Fit Using Mathematica and Excel for Graphing Comparisons	63
Appendix E: Procedures for Convolution and Final Results	77
End Notes	85

List Of Figures

Figure	Page
1. Head Mounted Russian Night Vision Binocular With Infrared Illuminator	3
2. Hand-Held Night Vision Binoculars	4
3. Electromagnetic Spectrum (Hecht, Eugene, "Physics", Brooks / Cole Publishing Co., Pacific Grove, California, 1994, Page 849).	6
4. 0.2 To 2.0 μ M Atmospheric Transmittance For A Clear Day	11
5. 2.0 To 100.0 μ M Atmospheric Transmission On A Clear Day	12
6. Plot Of The Data For R-Scope 85345 Based On Manufacturer's Data	19
7. Plot Of The Polynomial $Y = 38.0556 + 0.148354 X - 0.000185853 X^2 + 5.12486 \cdot 10^{-8} X^3$	20
8. Comparison Of R-Scope 85345 With Third Order Polynomial Fit	21
9. Comparing R-Scope 84499 With Polynomial Fit Of 10 Terms	22
10. Comparing R-Scope 84499 With Polynomial Fit Of 20 Terms	23
11. Comparing R-Scope 84499 With Polynomial Fit Of 30 Terms	24
12. R-Scope 84499 Illustrating Composite Of Trials To Match Detectors Response	25
13. Convolution Of Transmittance And R-Scope 84499 Response For 0.2 Km Visibility	27
14. Convolution Of Transmittance And R-Scope 84499 Response For 0.5 Km Visibility	28
15. Convolution Of Transmittance And R-Scope 84499 Response For 1.0 Km Visibility	29
16. Convolution Of Transmittance And R-Scope 84499 Response For 5.0 Km Visibily	30
17. Convolution Of Transmittance And R-Scope 84499 Response For 23.0 Km Visibility	31
18. Convolution Of Transmittance And R-Scope 84499 Response For 50.0 Km Visibility	32
19. Convolution Of Transmittance And R-Scope 85345 Response For 0.2 Km Visibility	33
20. Convolution Of Transmittance And R-Scope 85345 Response For 0.5 Km Visibility	34

List Of Figures Continued

Figure	Page
21. Convolution Of Transmittance And R-Scope 85345 Response For 1.0 Km Visibility	35
22. Convolution Of Transmittance And R-Scope 85345 Response For 5.0 Km Visibility	36
23. Convolution Of Transmittance And R-Scope 85345 Response For 23.0 Km Visibility	37
24. Convolution Of Transmittance And R-Scope 85345 Response For 50.0 Km Visibility	38
25. Sum Of Individual R-Scope Responses After Convolution With The Atmospheric Transmissions With The Different Visibility Ranges	40
26. Transmission Through The Atmosphere For 0.2 – 1.0 μM	48
27. Transmission Through The Atmosphere For 1.0 – 100.0 μM	49
28. Radiance From 0.2 To 1.0 Micrometers	50
29. Radiance From 1.0 To 100.0 Micrometers	51
30. Mathematica Output Graph For The R-Scope 85345 Detector Response File	64
31. Comparison Of R-Scope 85345 With Mathematica Polynomial Fit	66
32. Trial 1 Match Of R-Scope 85345	67
33. Trial 2 Match Of R-Scope 85345	67
34. Trial 3 Match Of R-Scope 85345	68
35. Trial 1 Match Of R-Scope 84499	69
36. Trial 2 Match Of R-Scope 84499	69
37. Trial 3 Match Of R-Scope 84499	70
38. Trial 4 Match Of R-Scope 84499	70
39. Trial 5 Match Of R-Scope 84499	71
40. Trial 6 Match Of R-Scope 84499	71

List Of Figures Continued

Figure	Page
41. Trial 7 Match Of R-Scope 84499	72
42. Trial 8 Match Of R-Scope 84499	72
43. Trial 9 Match Of R-Scope 84499	73
44. Trial 10 Match Of R-Scope 84499	73
45. Trial 11 Match Of R-Scope 84499	74
46. Trial 12 Match Of R-Scope 84499	74
47. Trial 13 Match Of R-Scope 84499	75
48. Overview Of 3 Trials For R-Scope 85345	75

SECTION 1

INTRODUCTION

Present military search and rescue operations utilize a variety of methods to locate the general area where a downed crewman's position may be. To enable effective rescue to occur, a method is needed to pinpoint his exact position without jeopardizing his safety in a hostile environment. The objective of this report is to determine the most effective wavelength range of near infrared ($< 2 \mu\text{m}$) radiation that can be transmitted through our atmosphere and detected by a commercial, off-the-shelf, night vision scope. Discussion will be limited to the detection methodology only and no tactical considerations will be given for actual rescue operations.

Microwave and other radio frequency systems could utilize radar capabilities to accomplish the above objective, but it is believed an optical, line-of-sight system has certain advantages in covert operations. Consider the following:

- a. Precise angular tracking capability
- b. Precise range accuracy
- c. Close range operation
- d. Day or night operations
- e. Secure and covert operation (infrared radiation)
- f. Small radiation source
- g. No multipath signal problems (as in RF homing systems)
- h. No dead zone over the target (as in RF homing systems)

- i. Does not degrade or restrict the existing RF rescue channels for direction finding or communication.

The prime disadvantage of an infrared detecting system is the need for an unobstructed line-of-sight to the detector. Under certain conditions this is not considered to be a prohibitive limitation since rescue operations usually require visual identification of the rescue prior to pickup. Rescue operations are further limited to "visual flight rules" since the flight vehicle must maneuver within 100 to 200 feet of the ground. However, in some environments such as a tall rain forest canopy, this system would not be effective.

This report will document the efforts in developing the methodology used in determining the effectiveness of using COTS systems in adverse conditions and give results of two such detectors analyzed in this study for developmental purposes. Figures 1 and 2 illustrate examples of COTS night vision viewers already available. It should be made clear that the reason for the COTS investigation in night vision detectors is purely that of cost reduction since developmental costs of the detector system would be eliminated.

The methodology used in this investigation was that of computer modeling with PLEXUS software to generate transmittance values for atmospheric conditions under varying conditions and to convolve that data with manufacturer's detector response graphs which were digitized. Mathematica was used to establish polynomial equations enabling the convolution at all points generated by PLEXUS over the entire spectral range of interest.

The time factor significantly impacted the depth of this study in regards to the number of detectors analyzed and also the validation of analyses through experimentation. Other limiting factors were hardware and software capabilities for this study. Using a 486 computer, an older

version of Excel, and the need to break the spectrum into many sub-spectral ranges, the developmental effort was greatly protracted. Given new computers with at least six times the operational speed and spreadsheet programs which can graph all the points generated by PLEXUS in one operation, a detector analysis could be performed in only a few hours. As a result of this modeling "tool" the decision-making capabilities for selection of night vision detectors, or any other detectors subjected to atmospheric conditions, should be greatly enhanced.

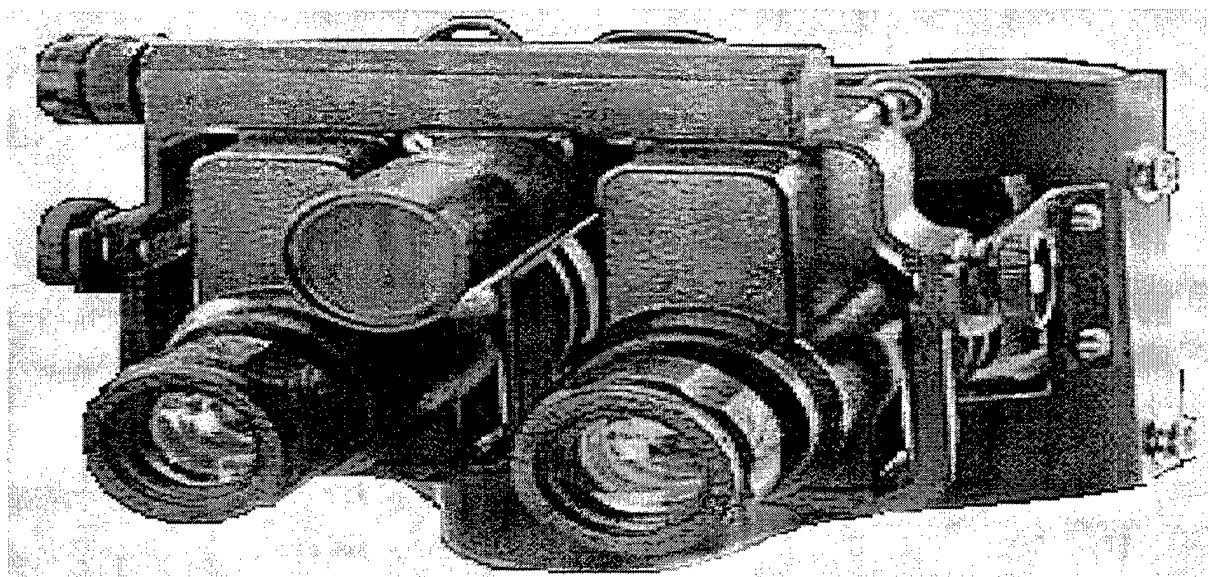


Figure 1. Head Mounted Russian Night Vision Binocular With Infrared Illuminator

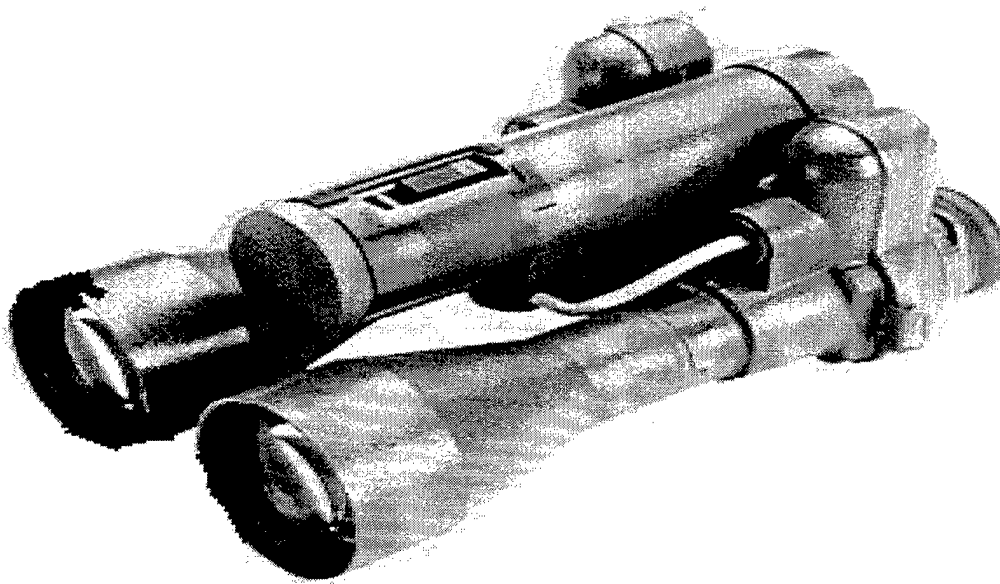


Figure 2: Hand-Held Night Vision Binoculars

SECTION 2

RANGE DETERMINATION OF ELECTROMAGNETIC SPECTRUM FOR DETECTOR UTILIZATION

2.1 THEORY:

Light and all other forms of electromagnetic radiation, interacting with matter in the processes of emission and absorption, behave like streams of particle-like concentrations of energy that exist only at the speed “c”, and which otherwise propagate in a wavelike fashion. The electromagnetic wave is really an illusion of continuity since, on the fundamental level, there is no such thing as a continuous electromagnetic wave. However, torrents of photons behave exactly as if they were dissolved into a smooth classical electromagnetic wave. Figure 3 illustrates the various classifications of electromagnetic waves (gamma, x-ray, etc.) and the approximate ranges for each. This figure also illustrates the sources for each type of photon energy and methods for detection.

The most important mechanism for the emission and absorption of radiant energy is the electron, a bound charge confined within the atom. Most of the optical behavior of a substance is determined by only the outer electrons of the atom, with the inner electrons formed into an essentially closed, unresponsive set of shells bound tightly to the nucleus. Light is absorbed and emitted during the outer charge distribution of the electron cloud and is responsible for almost optical phenomena in nature.

When just the right amount of energy (ΔE) is imparted to valence electrons of an atom, it can respond by suddenly jumping from a lower to a higher energy level. Since the energy absorbed by an atom is quantized, the electron will be enabled to jump to a higher, but specific



MICROSCOPIC SOURCE:

Atomic Nuclei Inner Electrons Inner & Outer Electrons Outer Elec. Molecular Vibra. & Rotat. Electron Spin Nuclear Spin Currents

ARTIFICIAL SOURCE:

Accelerators X-ray tubes Synchro-Tron Lasers, Arcs, Sparks Hot Bodies Magnatron Traveling-Wave Tubes AC-Generators

DETECTION METHODS:

Geiger & Scintillation Counters Ionization Chamber Photo-electric Photo-multiplier Eye meter Bolometer Thermopile Crystal Electronic Circuits

Figure 3: Electromagnetic Spectrum (Hecht, Eugene, "PHYSICS", Brooks / Cole Publishing Co., Pacific Grove, California, 1994, Page 849).

energy level. After approximately one nanosecond, the excited electron will begin a downward migration. Light or other photon phenomena is released, which exactly matches the quantized energy decrease in going from one energy level down to another. The amount of downward transition could be the full amount of energy absorbed and hence the electron now resides at the level it started from. The same electron could also drop to intermediate levels, with each transition giving off a photon equal to the ΔE for that drop. Multiple drops in energy levels will occur until the electron reaches the ground state with comparable amounts of photon energy released for each downward transition. The sum of all ΔE in the downward transition will equal the total energy absorbed. The emitted photons are not necessarily emitted in the same direction as the incoming photon, hence a scattering phenomena is achieved.

For solids or liquids the above scenario is not necessarily accurate since the excitation energy is often not re-emitted in the form of photons but is transferred by way of collisions to random KE of the atom where the photon vanishes and its energy is converted into thermal energy. This process of taking up a photon and its conversion into thermal energy is called dissipative absorption. For example, an apple in white light will have resonance in the blue and absorb out the yellow-blue. It will reflect mostly the red.

The process whereby an atom absorbs a photon and emits another photon is known as scattering since the emitted photon will probably go in a different direction from that of the absorbed photon. It is this absorption of photon energy and re-emission that gives our sky the blue color. Since the sunlight, which was originally going across the sky, is now absorbed and re-emitted in all directions, it enables our eyes to see light instead of the blackness of the sky like

on the moon where there is no atmosphere. The blue light of our sky occurs because of the scattering effect of light given by the following equation:

$$E = NE_o^2\rho^2/\lambda^4$$

E_o is the intensity of the sunlight

ρ is the scattering constant of an atom

λ is the wavelength of light

N is the number of air molecules.

Notice that the light is scattered in inversely proportional to the fourth power of the wavelength of light. This means that the shorter the wavelength the greater the scattering and since blue light has the shortest wavelength it is scattered most giving a blue sky. If we looked directly into the sunlight it would appear white since all frequencies of light are received. For light traveling at any other angle, the path of the sunlight is NOT directed into our eyes and we would see darkness such as when a flashlight is shined in a dark room. If no dust is present, the beam is not seen except as it bounces off the wall. Therefore, it is because the sunlight in our atmosphere interacts with air molecules that we see the scattered light, which is primarily the blue light according to the above equation.

It is interesting that Avogadro determined the number of air molecules in a mole of gas (6.02×10^{23}) by using the above equation. He determined the ratio of sky light intensity to sunlight intensity, and knowing the value of ρ by refraction studies, and the known wavelength of light, he was able to determine the number of air molecules in 1 cm^3 of air, and therefore in a mole of gas.

If photon energy is too small to cause an excitation up into any of the higher energy states the electromagnetic field can drive the electron cloud into oscillation. There will be no resulting atomic transitions but the electron cloud will vibrate at the frequency of the incident light. Once the electrons begin to oscillate, we have an accelerating charge which will replace the increased KE with the radiation of photon energy according to a basic law of physics. The excited atom becomes essentially a little dipole oscillator producing omnidirectional scattering and creating the appearance of a source of spherical wavelets. This is a process called “nonresonant elastic scattering.” (Reference: Hecht, Eugene, “PHYSICS”, Brooks / Cole Publishing Co., Pacific Grove, California, 1994, Page 844).

2.2 APPLICATION:

The above theory helps to explain some of the considerations made in the PLEXUS software program. Two sets of output values generated by this program need to be defined.

- a. Transmittance is the intensity or relative amount of photons reaching a destination through our atmosphere and is a unitless value, a percentage of the total per micrometer of wavelength.
- b. Radiance is the amount of energy per unit of time per area, per steradian, reaching a destination through our atmosphere. The units are watts, per square centimeter, per stridden, per micrometer of wavelength.

Transmittance and radiance values generated by PLEXUS utilized a combination of atmospheric aerosol scattering ratios, solar activity, cloud, and rain models. The atmospheric model included over 13 separate gas molecular profiles for oxygen, nitrogen, water vapor, ozone,

methane, carbon monoxide, carbon dioxide, nitrous oxide, nitric oxide, nitrogen dioxide, ammonia, and nitric acid, sulfur dioxide, and others with all as a function of altitude. (Reference: Dr. Frank Clark, U.S Air Force, "PLEXUS User Guide", ver 2.1, Mission Research Corporation, Nashua, NH < Phillips Laboratory, Bedford, MA., 1996, Page 5-26 & 8-1). The meteorologist at Wright Patterson, and other U.S. Air Force facilities use the PLEXUS program. It has an overall validity in prediction of transmittance and radiance in our atmosphere, under a variety of conditions, of approximately 97% and even better results are obtained in the infrared range. Comparisons of PLEXUS results with satellite observations of the more difficulty modeled ultraviolet range showed a better than 90% correlation. Results are especially predictable for altitudes of less than 80 km since the air has a homogenous mixing of the gases. Above that altitude stratification occurs which will skew the results. (The source of that information is discussions with Captain Paul Gehred, August 7 & 8, 1997, who is a member of the Meteorology department at Wright Laboratories.)

The opacity in the electromagnetic spectrum results from the proper frequencies of photons absorbed by the various molecules in the atmosphere, therefore prohibiting of the transmission of electromagnetic energy. Regions of transparency exist because the proper quantum of energy associated with the excitation of electrons in the air molecules for that wavelength do not exist, permitting the transmission of electromagnetic energy.

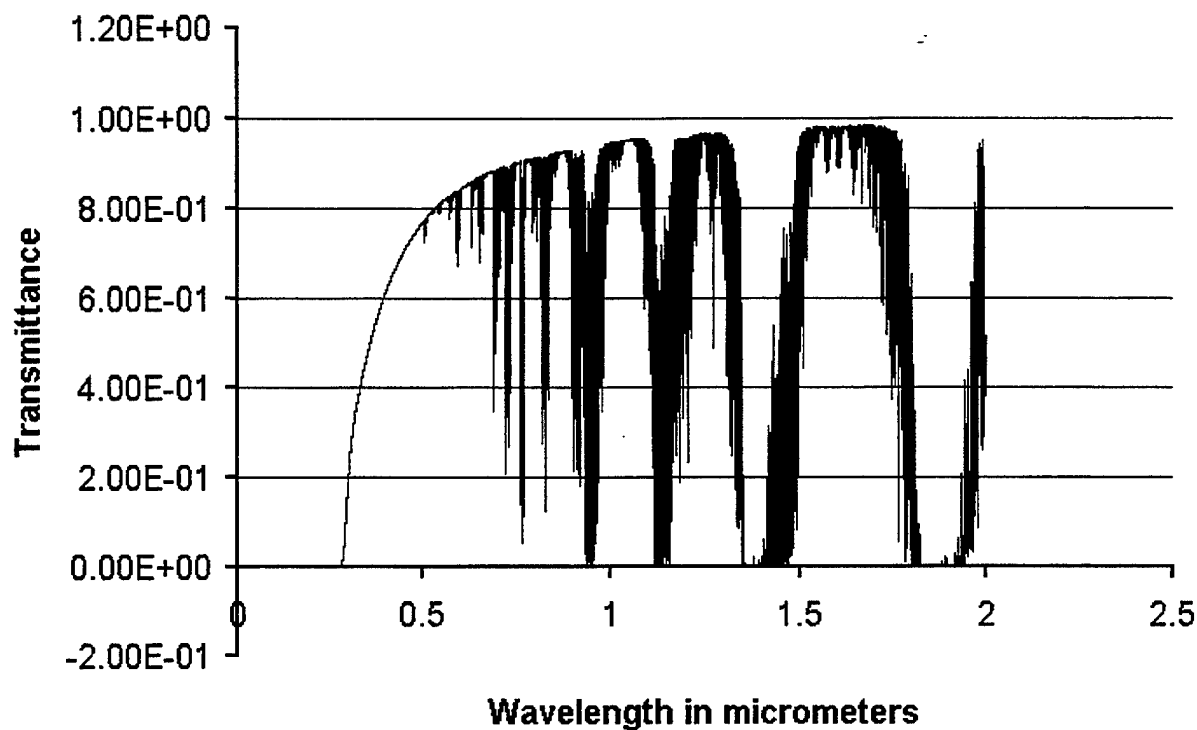


Figure 4: 0.2 to 2 μm Atmospheric Transmittance For a Clear Day.

Figures 4 and 5 illustrate transmittance graphs from PLEXUS for the spectral range, 0.2 μm through 100 μm . The portions of the electromagnetic spectrum where the earth's atmosphere is opaque is for wavelengths less than 0.29 μm and greater than 25 μm where it appears that no transmission occurs. The same figures also indicate that there is some absorption of photon energy from 0.52 through 25.0 μm but the amount is minimal until 1.0 μm where the amount of absorption becomes significant.

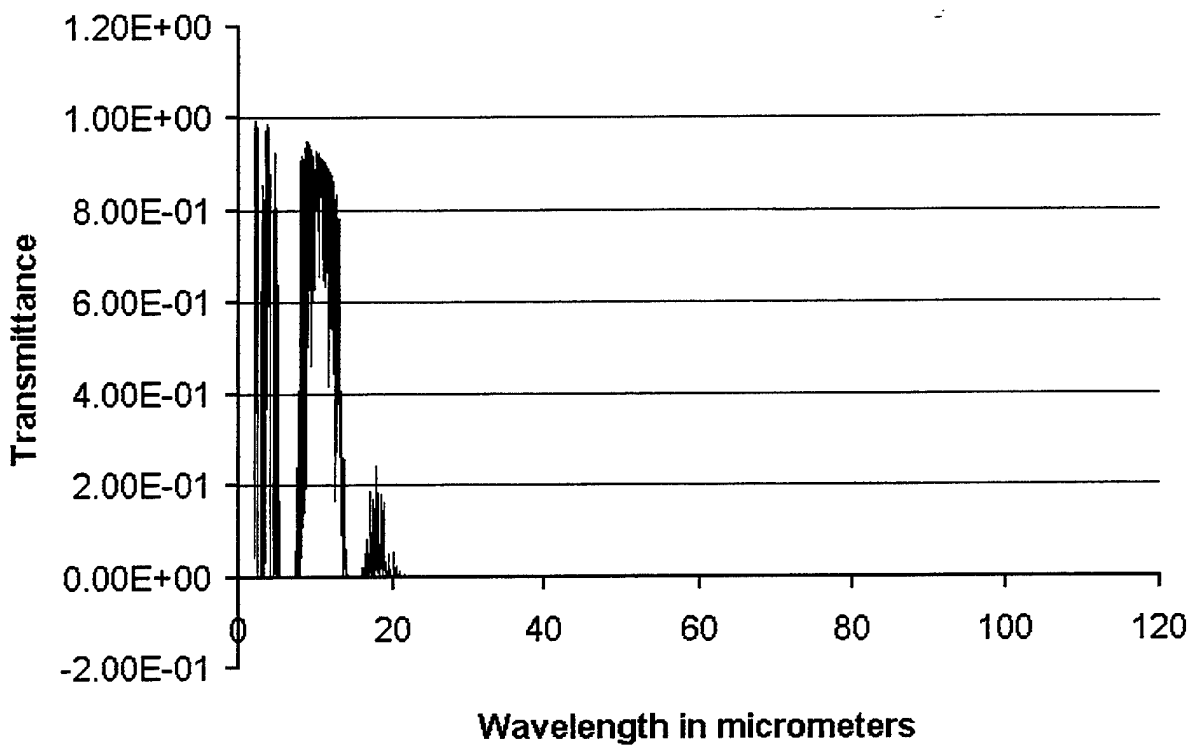


Figure 5: 2.0 to 100 μm Atmospheric Transmission on a Clear Day.

The radio range of radiation was rejected since the waves are too long for use in imaging in a real as opposed to synthetic aperture. Radio communication is not point specific and in covert operations these signals could be picked up by unwanted persons. An equation indicating the amount of “fanning-out” of the signal is:

$$\alpha = (2.1 \text{ E}+5 \times \lambda)/d \text{ in seconds of arc}$$

α = resolution or spread in seconds of arc

λ = wavelength (same unit as “d”)

d = receiver diameter (same unit as “ λ ”)

Notice that as the wavelength increases, the worse the resolution. Hence, radio waves are far worse than infrared or visible photons for resolution purposes.

To conclude this section, it is obvious why the infrared or visible range of the spectrum was chosen. Since the atmosphere attenuates most electromagnetic signals because of atomic/molecular absorption of photon energy, only portions of the visible/infrared range and the microwave/radio range are useful for detection purposes. Since the radio waves are not point specific, they would have limited feasibility for quick detection and rescue operations. The visible photon range has the disadvantage of being easily seen by undesirable persons. The infrared range becomes the most probable photon candidate for night vision detection. Night vision scopes are utilized throughout the visible spectrum as well as the near infrared spectrum. Therefore, the visible range was also examined.

SECTION 3

VISIBILITY RANGE DETERMINATION

The visibility is an important factor in the consideration of the COTS night vision infrared detector. When atmospheric conditions generated by PLEXUS are convoluted with the manufacturers detector response curves, significant modifications result in those curves.

The term "visibility" is defined as the degree of clearness of the atmosphere or the quality or state of being visible. It is the greatest distance toward the horizon that prominent objects can be identified visually with the naked eye. It is a subjective term in most areas since it is an approximate value given by a human determination of marker posts located in the horizontal direction, 360 degrees around, with the naked eye. Some airfields use electronic means where photons are sent to a receiver and an algorithm set up by the receiver to give results which makes the results a little less subjective.

The typical visibility in most places in our country is 7 miles where limiting factors are the humidity in the air and the terrain. The early morning is usually the worst part of the day because of fog and related dew point issues where visibility ranges from 3 to 7 miles. It is rare to have less than 3-mile visibility except in big city smog areas and other abnormal conditions such as heavy rain, snow, dust storms, forest fires, etc. For desert areas, visibility is typically greater than 10 miles and is frequently 50 miles or more.

SECTION 4

OVERVIEW OF PROCEDURE FOR DETERMINING NIGHT VISION DETECTOR RESPONSES UNDER ATMOSPHERIC CONDITIONS

To arrive at the proper night vision detector response intensity, the transmittance values of the atmosphere were convoluted with the detector response values over the range of $0.4\mu\text{m}$ - $2.0\mu\text{m}$ for each detector. The mathematical relationship that explains the process is:

$$R = \int T(x)D(x)dx$$

where T is atmospheric transmittance generated by PLEXUS and D is the detector response given by the manufacturer. Finding the response intensities for various visibility ranges (0.2 km, 0.5 km, 1.0 km, 5.0 km, 23 km, 50 km) gives a fairly clear indication of which detector is best suited for the job.

The task was achieved by generating atmospheric transmittance values, scanning the manufacturer's commercial detector response curves and obtaining calculable values from the bitmap. A polynomial equation was then determined for this manufactures response curve from which "response" values were determined for each of the wavelength points. The final task was to convolute the response values with the transmittance values for each point along the "x" axis, the independent variables. The overview will be given for each step in the process with details given in the appendices for each of the steps.

The initial developmental work was performed with a 486 computer having a machine speed of 33 Mhz. This hardware limitation along with the graphing limitation of the older Microsoft-Excel, version 7 software established the parameters that had to be worked within. Other software packages used in the analysis included Mathcad, Mathematica, PLEXUS, Corel

Photo Paint-6, and Un-Scan-It. These working parameters necessitated the dividing of the spectral range of $0.4\mu\text{m}$ - $2.0\mu\text{m}$ into 15 subdivisions. Utilizing these 15 divisions for each of the 6 visibility ranges required a total of 90 sets of calculations for one detector. It can be seen why only two detectors were analyzed during this study.

The complexity of analysis can be greatly simplified for the typical engineer/researcher at Wright Patterson Laboratory where possessing the proper hardware and software, as mentioned in the introduction, will enable him to perform a complete analysis within a few hours for each detector. This can be accomplished since only one set of data can be analyzed all the way through the analysis for each visibility range. The one exception will be where the manufacturer's graph of detection responses will probably have to be divided up into sections such that a proper polynomial fit could be found for the entire curve. However, software does exist where one operation could probably determine the polynomial fit over the entire equation, reducing the time and steps necessary to determine this part of the analysis as well. This software was not available to the current researcher.

4.1. ATMOSPHERIC TRANSMITTANCE VALUES GENERATED BY PLEXUS

Enter the PLEXUS program for atmospheric generation. The following data must be entered at the appropriate prompts:

- a. Select: Novice or casual user
- b. Select: Moderate resolution
- c. Altitude: 1km
- d. Select: Venice as location
- e. Looking down (Zenith = 180 degrees)

- f. Range to end of path: 1km
- g. Time: July 4, 1997 at 12 noon
- h. Select: Clear day
- i. Range: 0.2 km, 0.5 km, 1.0 km, 5.0 km, 23 km, 50 km
- j. Select: Urban Environment
- k. Select: No unusual atmospheric conditions prior to investigation

The PLEXUS program was run for each of the visibility ranges, with all other parameters remaining constant. The output from this program, which was used in the successive steps of this analysis, was the AIM $\alpha\beta\gamma$.trn file. This file has the "x" and "y" points generated for transmittance. The "x" was the position along the spectral wavelength and "y" is the actual transmittance magnitude, in percent of the whole originally emitted. It is these values which are convolved with the manufacturer's data for the detector.

See Appendix A for details.

4.2. SCAN THE MANUFACTURER'S RESPONSE CURVES

The manufacturer's detector response graphs were put on the ScanMakerII flatbed scanner located in the laboratory used by Mr. Crespo. A bitmap was determined using the Corral Photo-Paint-6 program where the following procedure should be followed:

- a. Place the graph in the scanner with graph up-side-down
- b. Under FILE menu select "Acquire Image"
- c. Select ACQUIRE
- d. Then select PREVIEW
- e. Move the dotted square and resize until desired area of the graph is selected

- f. Select 300 dpi (dots per inch) resolution and operate under the Line-Art format
- g. Press SCAN and wait until it finishes (a few minutes wait)
- h. Save in PCX extension

If there is a grid in the graph, go into Paintbrush and erase portions of it which intersect with the graph curve since the scanner will move off on the grid lines, deviating from the intended path. If there is a graph with intersecting lines be sure to erase a small part of the intersecting line above and below the line you are scanning because the scanner will leave the main line as mentioned for the grid lines.

See appendix B for details.

4.3. DETERMINATION OF "X" AND "Y" VALUES FROM THE MANUFACTURER'S DETECTOR RESPONSE GRAPHS (Digitize)

Enter the UN-SCAN-IT program and load the PCX file saved in the scanning program. This is done by selecting the DIGITIZE menu. (Do NOT use the FILE menu, as is usually the procedure in most programs.) Follow the many prompts that are very user-friendly. Upon completion of the digitizing, save as an ASCII file with the tab delimiting option. Use the same PCX extension.

See Appendix C for details.

4.4. DETERMINE THE POLYNOMIAL FIT USING MATHEMATICA

The next step of the procedure is to associate a polynomial equation with the manufacturer's detector response graph, which has been digitized. This is necessary so dependent ("y") values can be determined at each of the independent ("x") values generated by

PLEXUS in the AIM $\alpha\beta\gamma$.trn program. Mathematica was the best software program to perform this task available to the researcher. However, Mathematica, version 3.0 is not very user-friendly and is very particular of the kind of external file it will read and also how things are typed since it is also case sensitive.

It is suggested that a plot of the data be obtained in Mathematica before determining the polynomial equation fitting the line. This is to assure all of the digitized data is being read into the program. Figure 6 is an illustration of an output graph when data is read in.

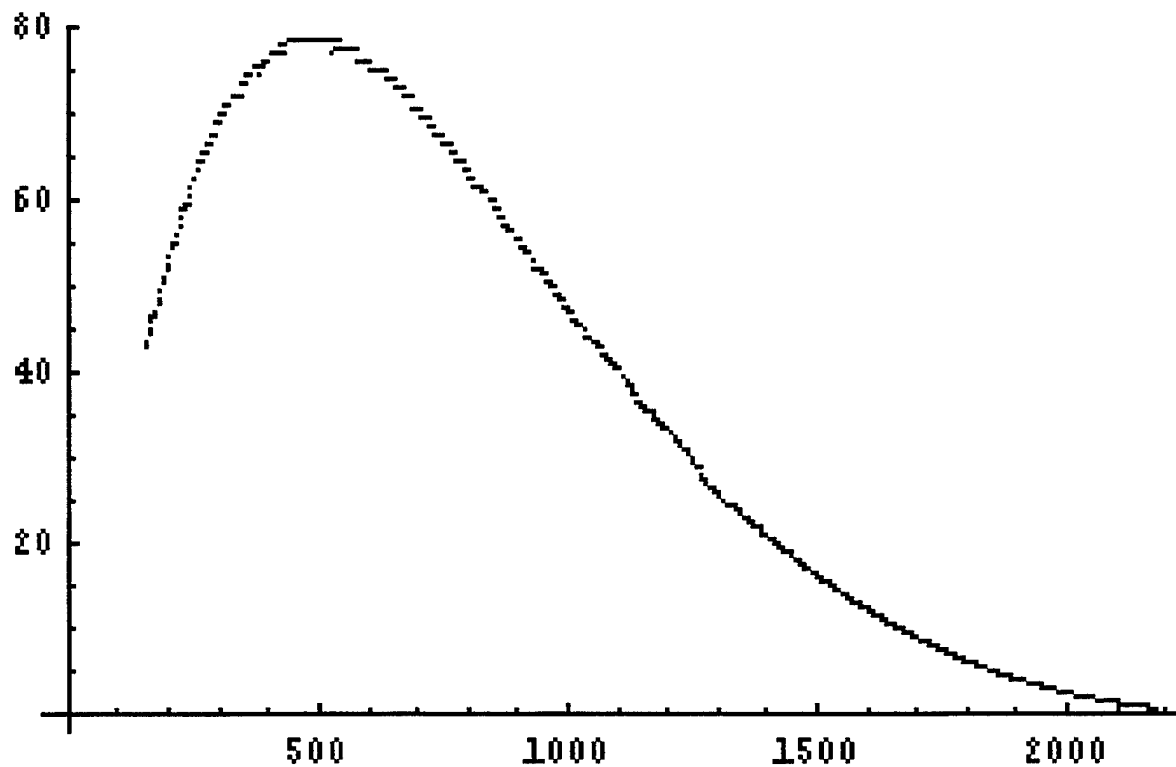


Figure 6: Plot of the data for R-scope 85345 based on manufacturer's data.

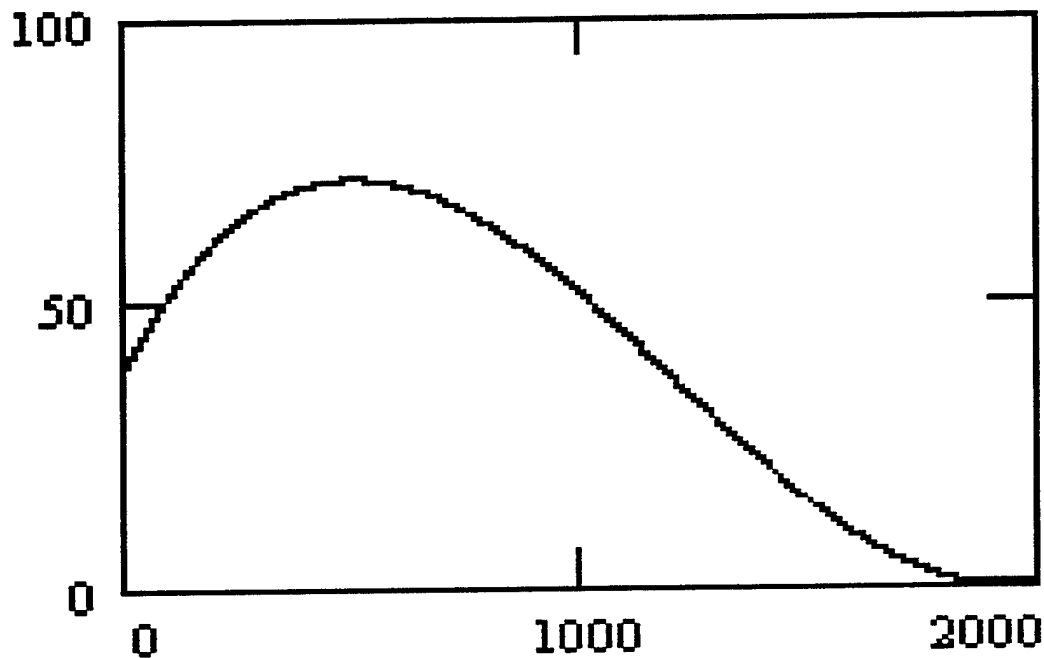


Figure 7: Plot of the polynomial $y = 38.0556 + 0.148354 x - 0.000185853 x^2 + 5.12486 \cdot 10^{-8} x^3$.

can be expected. Most of the statements used in obtaining the plot will also be used in deriving the polynomial equation describing the graph so those efforts are not wasted. If the procedure for using Mathematica is not known see the Appendix D or the manual for details.

Once the polynomial equation is determined for the manufacturer's graph, it must be determined if it is a proper fit. This is accomplished by using the abscissa values to the digitized, manufacturer's curve as the "x" values of that equation to calculate the Y value for each "x". The results of the generated values from the equation are compared with the digitized values from the manufacturer's graph on a comparison graph using the Excel graphing capabilities of the spreadsheet program.

See Figure 8 for a comparison fit for the simpler R-Scope 85345 and Figures 9-11 for three comparisons of the polynomial fit for R-Scope 84499. In all cases the comparisons were not adequate so the larger graph was divided into sections and a polynomial fit was associated with each section. The entire graph was then composed of a composite set of polynomial equations. Figures 12 and 13 show the trial composite response function which will be used in the convolution. See Appendix D for details.

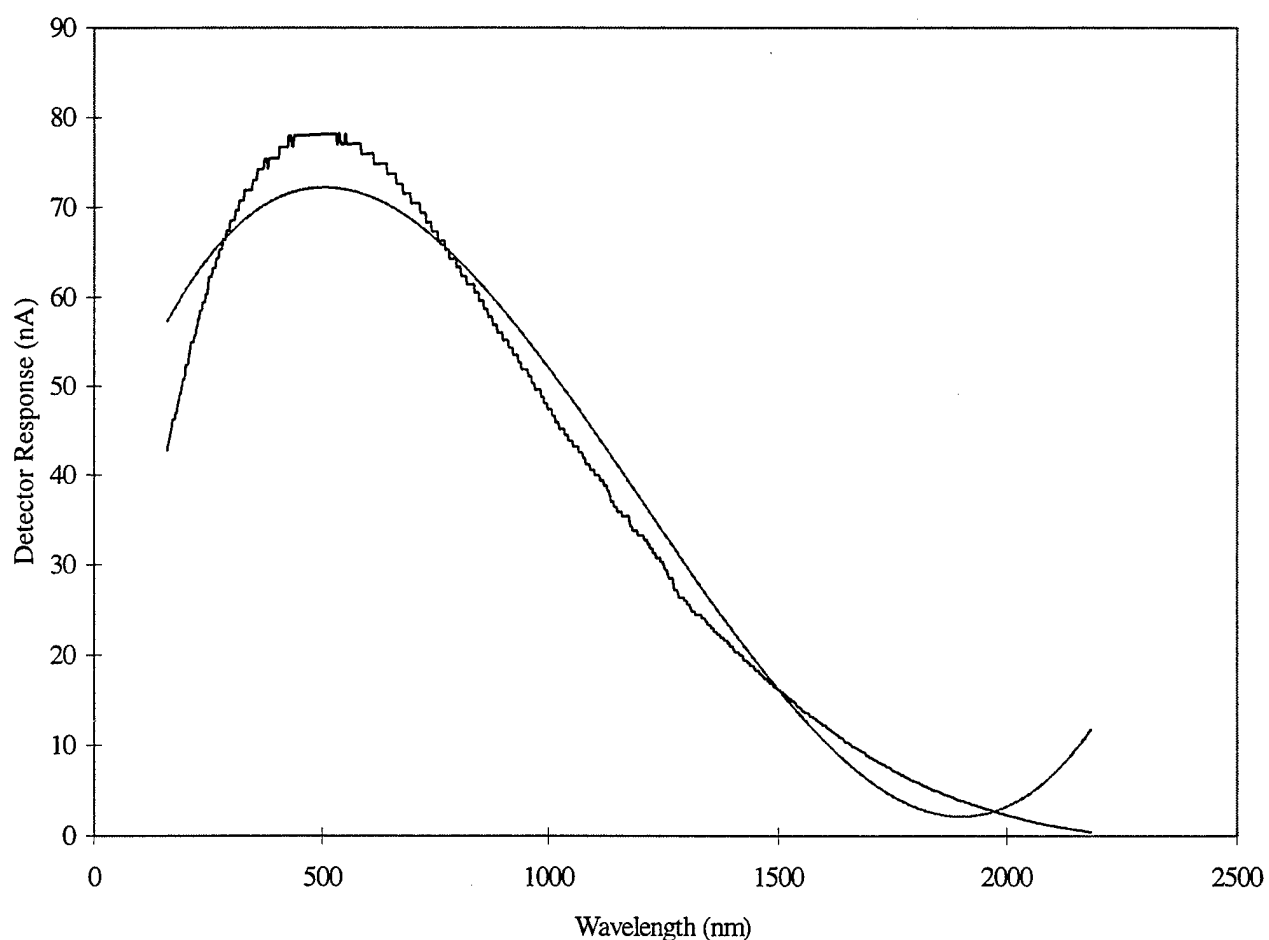


Figure 8: Comparison of R-Scope 85345 with third order polynomial fit.

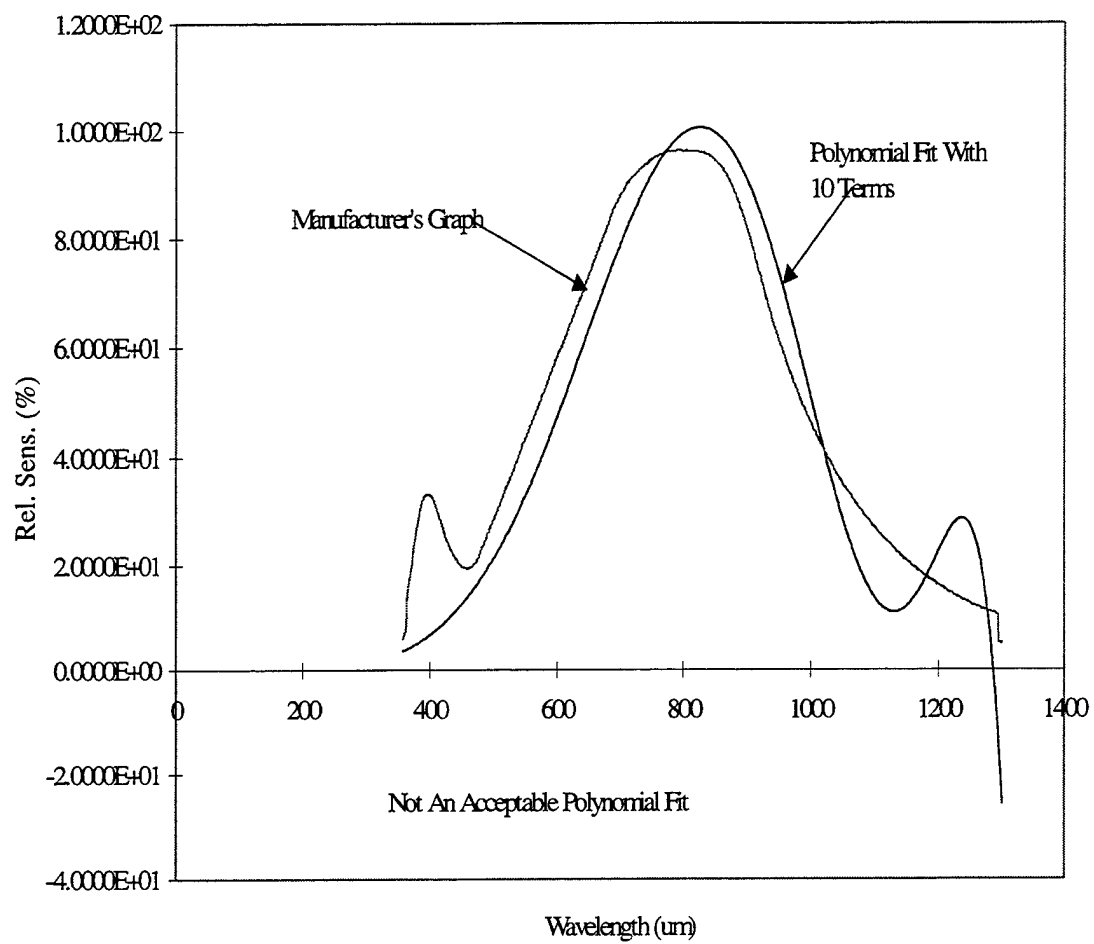


Figure 9: Comparing R-Scope 84499 With Polynomial Fit Of 10 Terms.

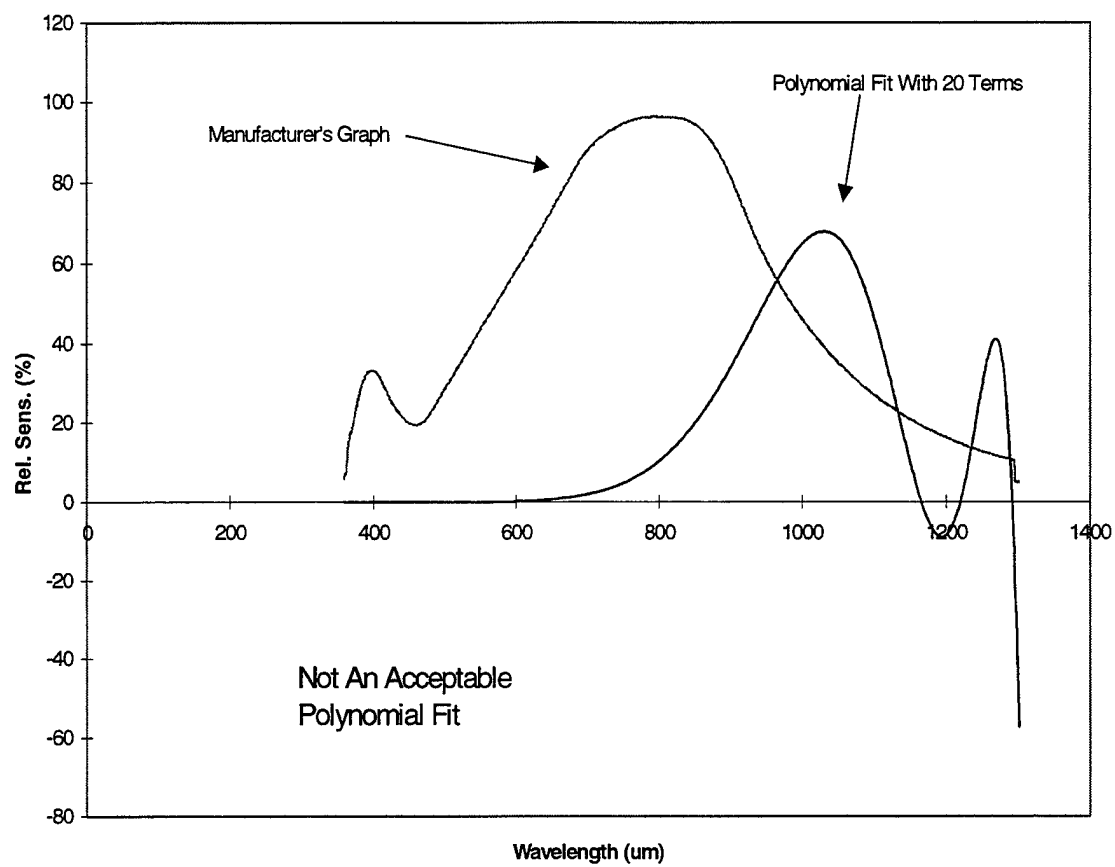


Figure 10: Comparing R-Scope 84499 With Polynomial Fit Of 20 Terms.

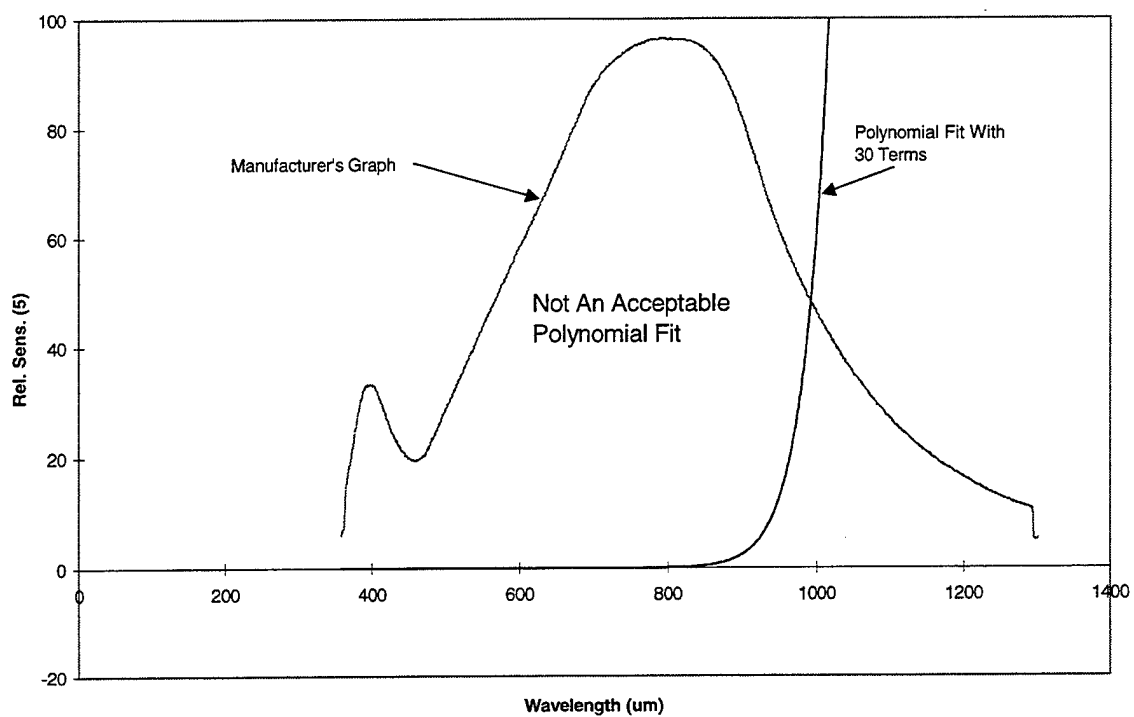


Figure 11: Comparing R-Scope 84499 With Polynomial Fit Of 30 Terms.

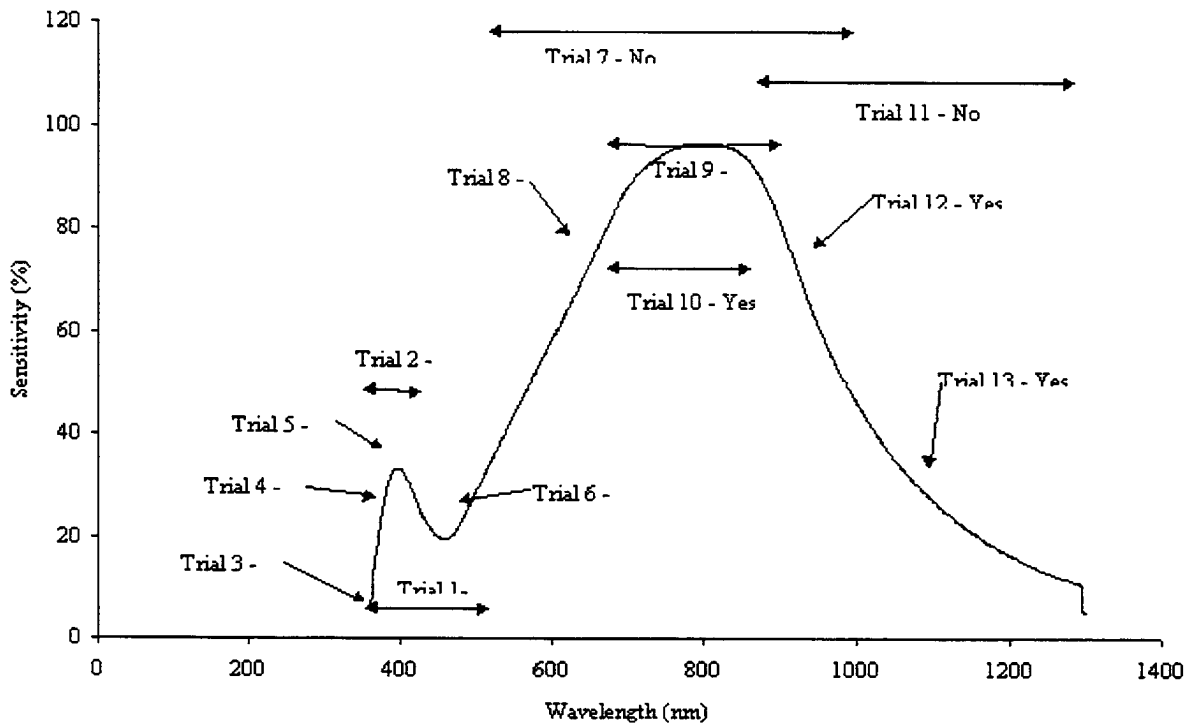


Figure 12: R-Scope 84499 illustrating composite of trials to match detectors response.

4.5 THE CONVOLUTION OF TRANSMITTANCE AND DETECTOR RESPONSE CURVE.

The final phase of the analysis is the convolving together the atmospheric transmittance data generated by PLEXUS with the detector response curve data interpolated by the polynomial equations. 20,000 data points will be convolved using the Excel Spreadsheet program.

The AIM $\alpha\beta\gamma$.trn file is brought into the Excel spreadsheet where the “x” values must be converted to nanometers since that is the abscissa unit used in the manufacturer’s detector graph. This nanometer value of “x” is multiplied by the polynomial equation applicable for that range of congruency to give the dependent value “y” for each value of “x.” (Three polynomial equations

for the 85345 R-Scope and eight for the 84499 R-Scope.) There are fifteen AIM $\alpha\beta\gamma$.trn files for each visibility range or a total of 90 files for this analysis for each detector. As has been mentioned several times already, it is conceivable that with proper hardware and software this could be done with one file for each visibility range.

The final convoluted value for each value of “x” is obtained by multiplying the polynomial interpolated value of the detector by the ordinate value from the AIM $\alpha\beta\gamma$.trn file, which is the atmospheric transmittance. The current sensitivity for the R-Scope 85345 was already a part of the detector sensitivity so the product of the two values gave the final detector response value. For the R-Scope 84499, the manufacturer’s response curve was a relative scale, so the peak nanoamp response sensitivity (15 nanoamps in this case) had to have been also multiplied by the convolving of the atmospheric transmittance and the relative detector response.

When all convolution values are graphed, a detector response curve is now generated which reflects atmospheric conditions for a given visibility over the entire spectral range specified.

The convolutions step is that simple for Excel-97, which can do all calculations on 65,536 points at once, and graph approximately 32,000 points. However, for the older version of Excel, or other smaller spreadsheet programs, the convolution had to be performed on subsets of data, and then combine all that data into one large file in Mathcad.

See Figures 13 – 25 for a graph of the convoluted detector responses for each visibility range, for each detector.

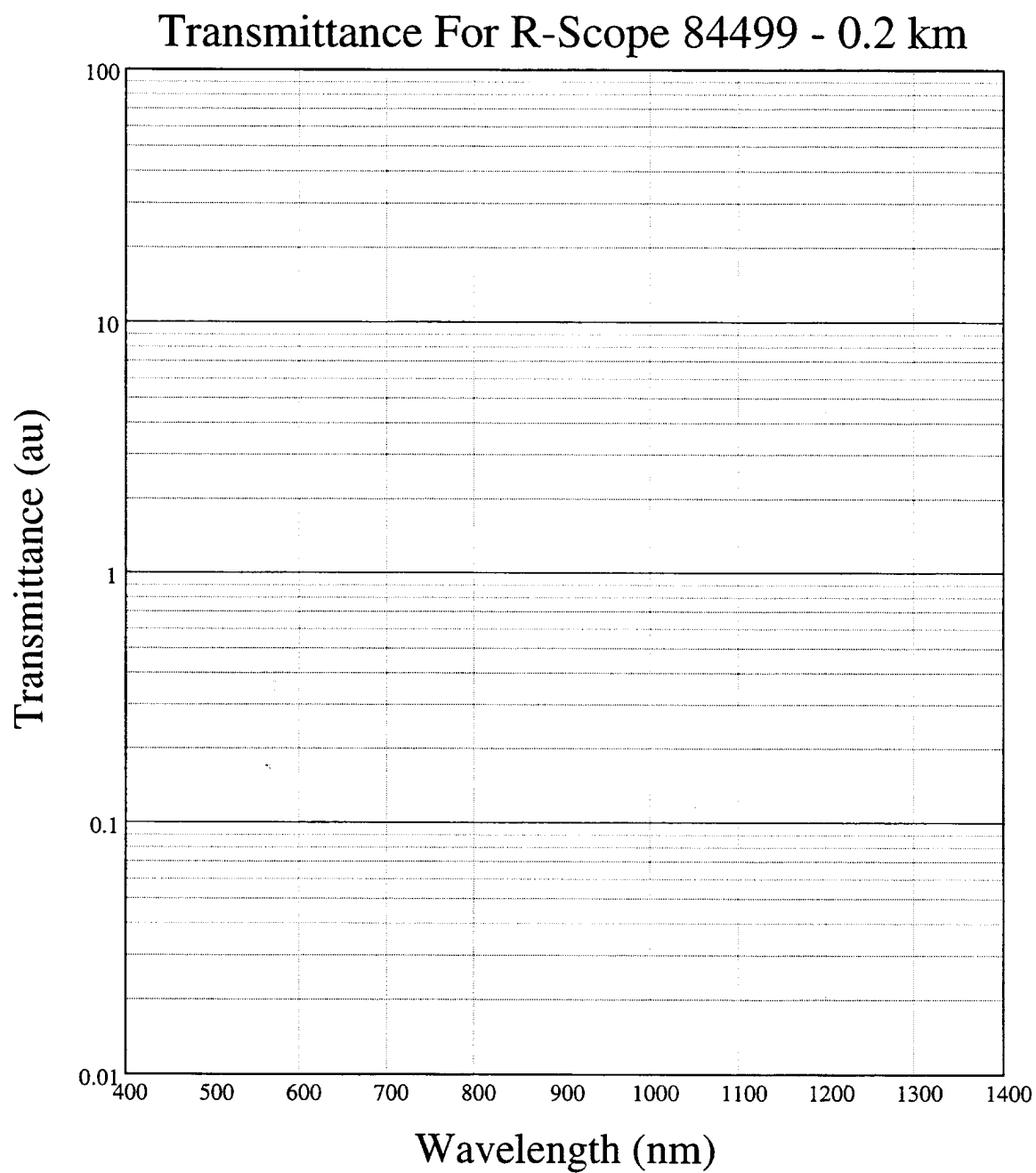


Figure 13: Convolution of Transmittance and R-Scope 84499 Response for 0.2 km Visibility.

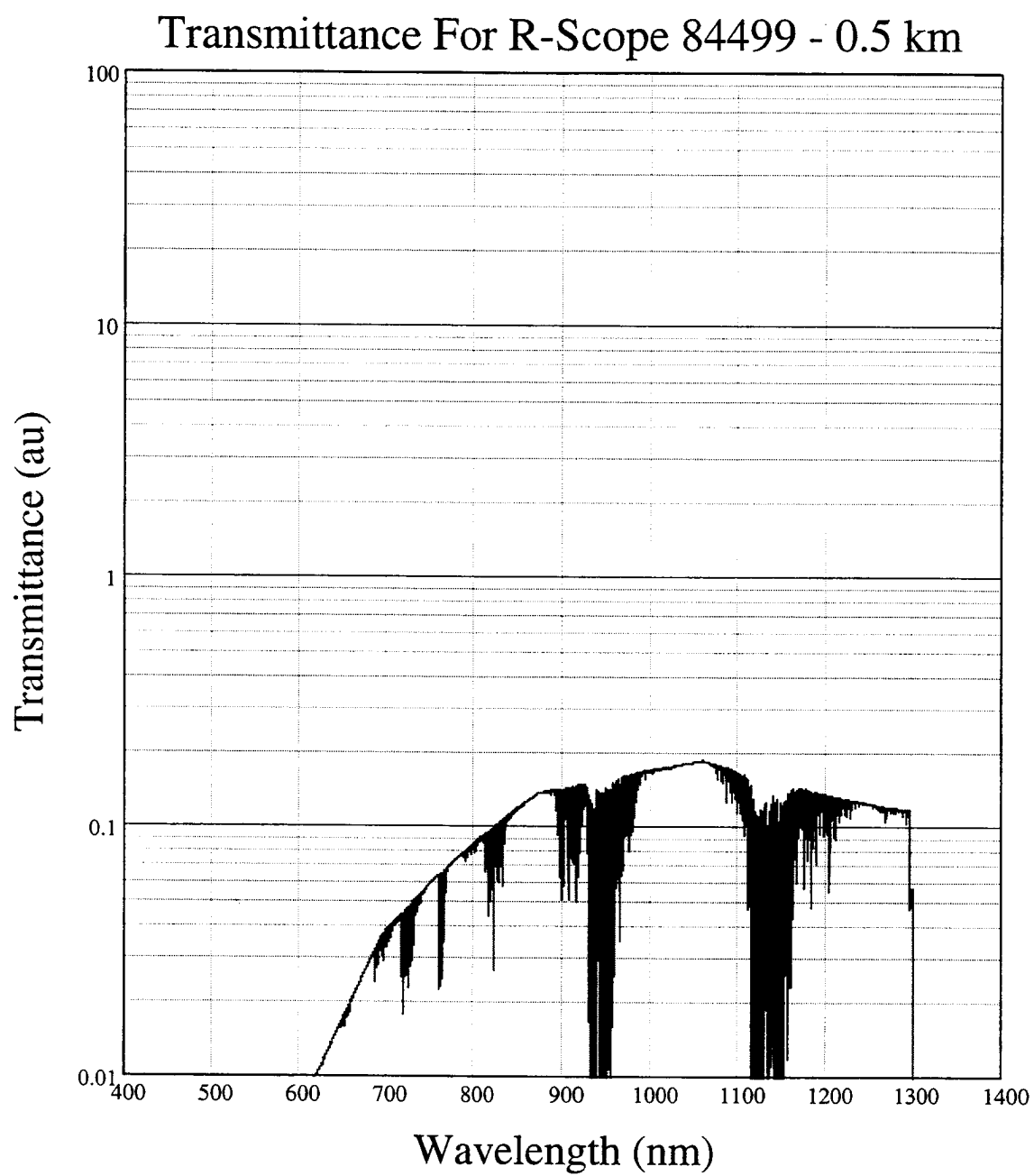


Figure 14: Convolution of Transmittance and R-Scope 84499 Response for 0.5 km visibility.

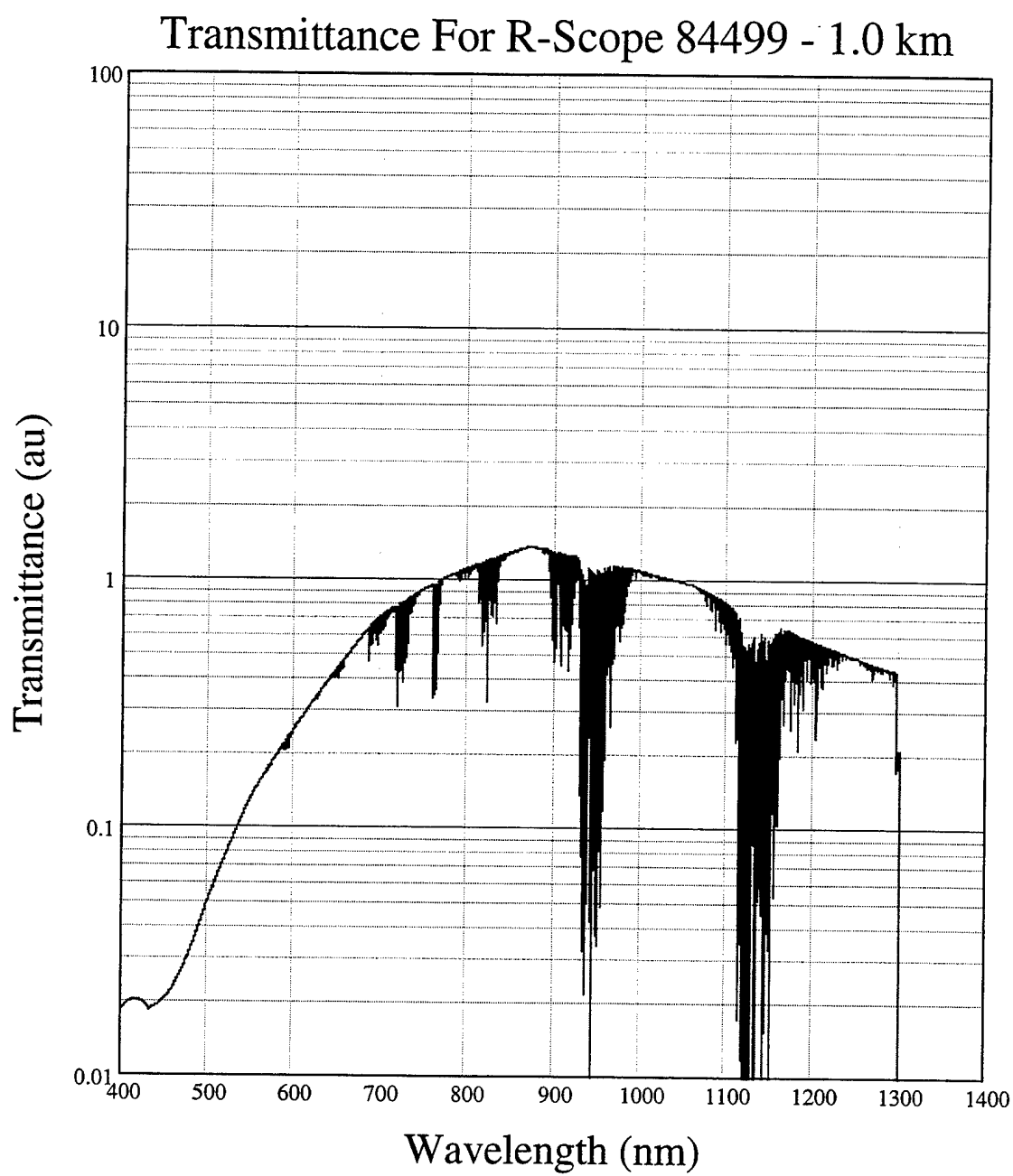


Figure 15: Convolution of Transmittance and R-Scope 84499 Response for 1.0 km visibility.

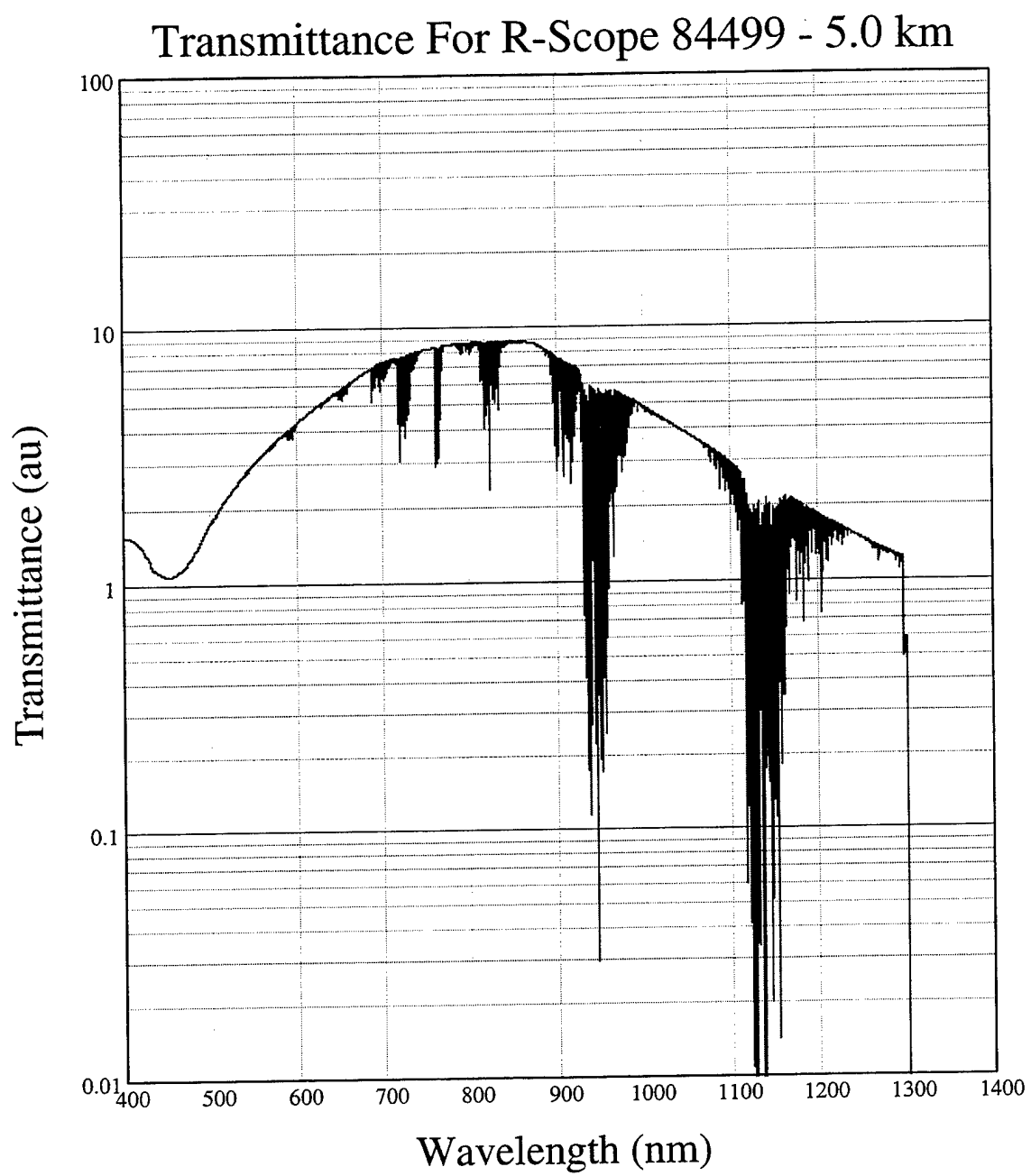


Figure 16: Convolution of Transmittance and R-Scope 84499 Response for 5.0 km visibility.

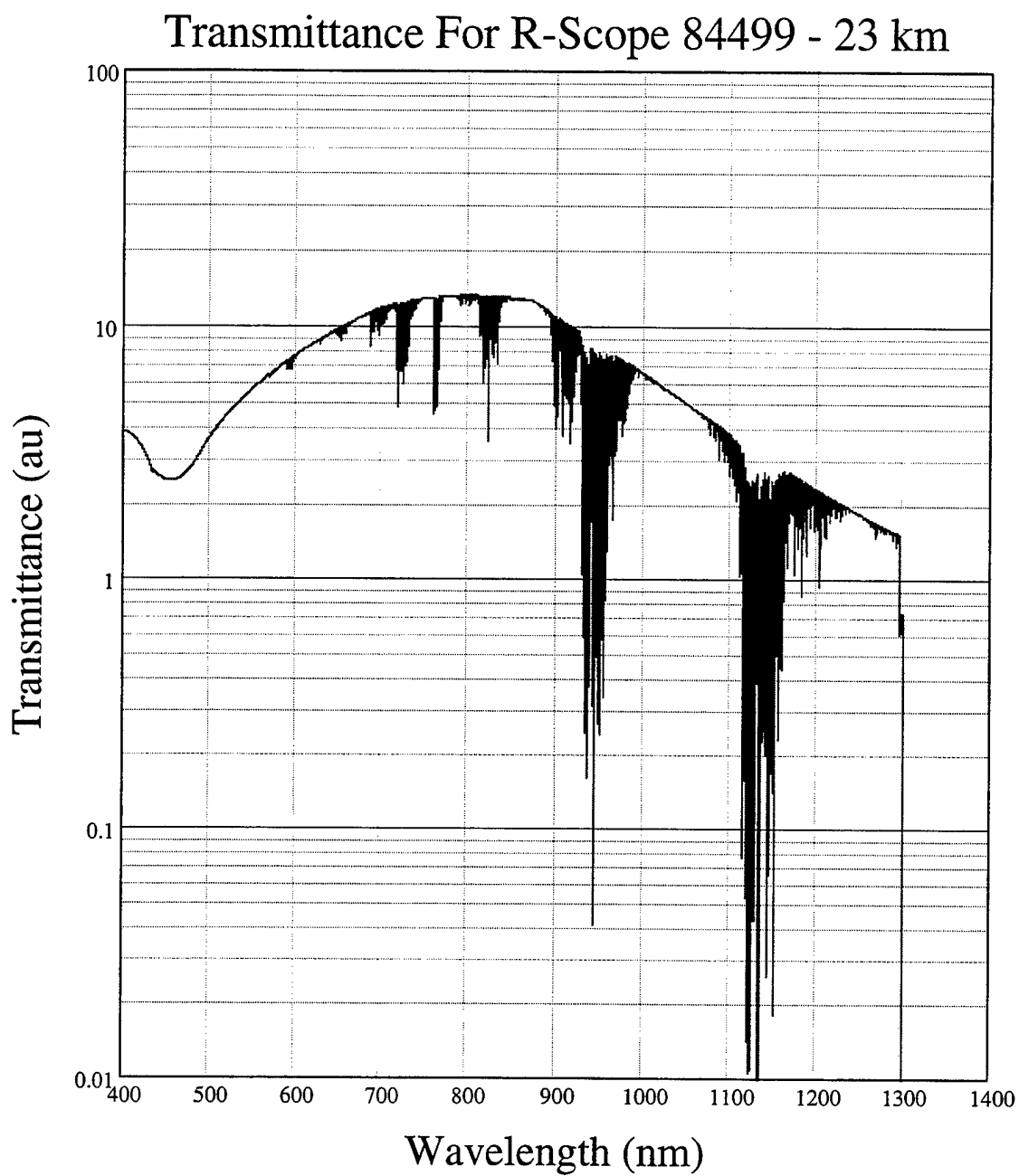


Figure 17: Convolution of Transmittance and R-Scope 84499 Response for 23.0 km visibility.

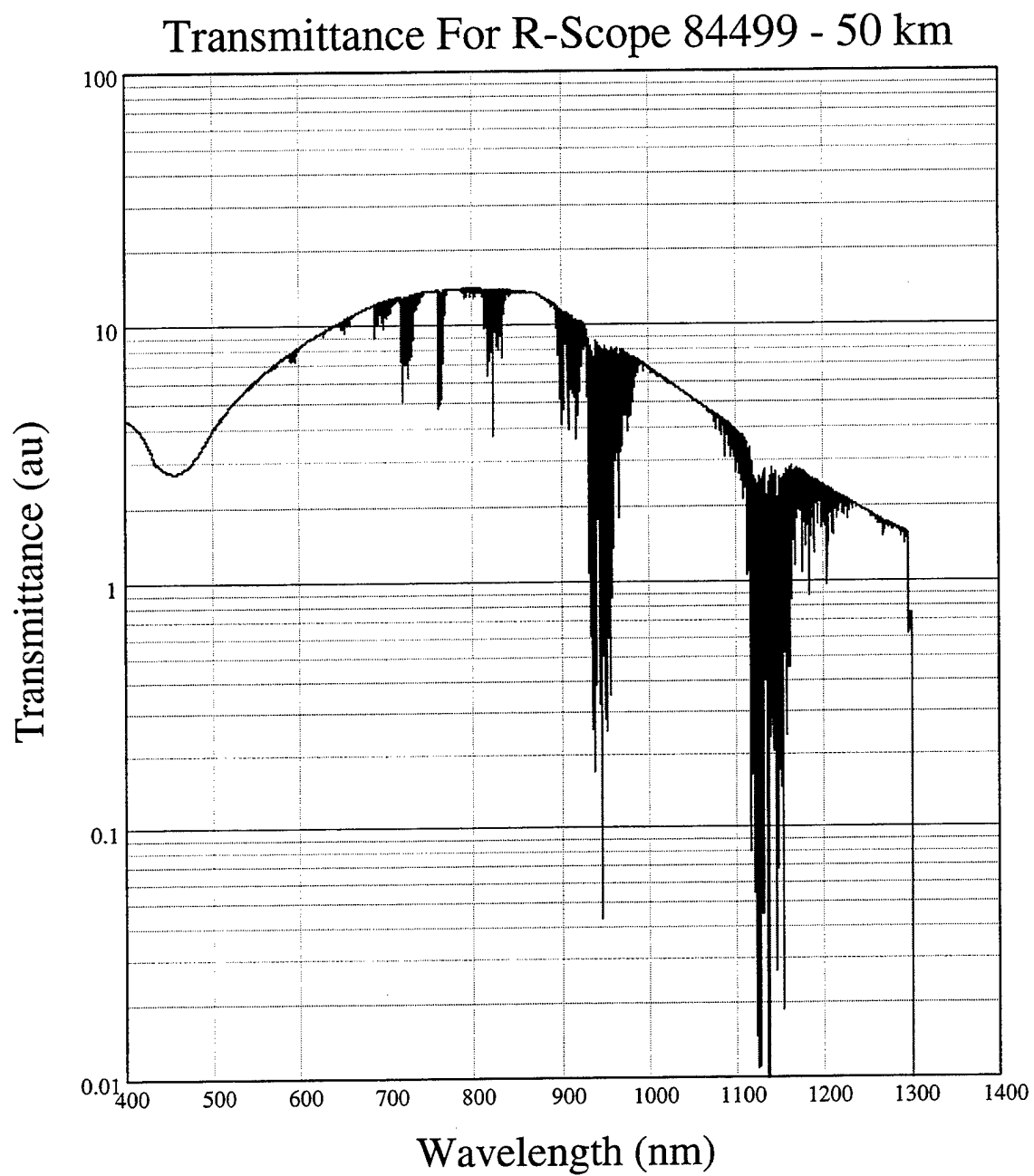


Figure 18: Convolution of Transmittance and R-Scope 84499 Response for 50.0 km visibility.

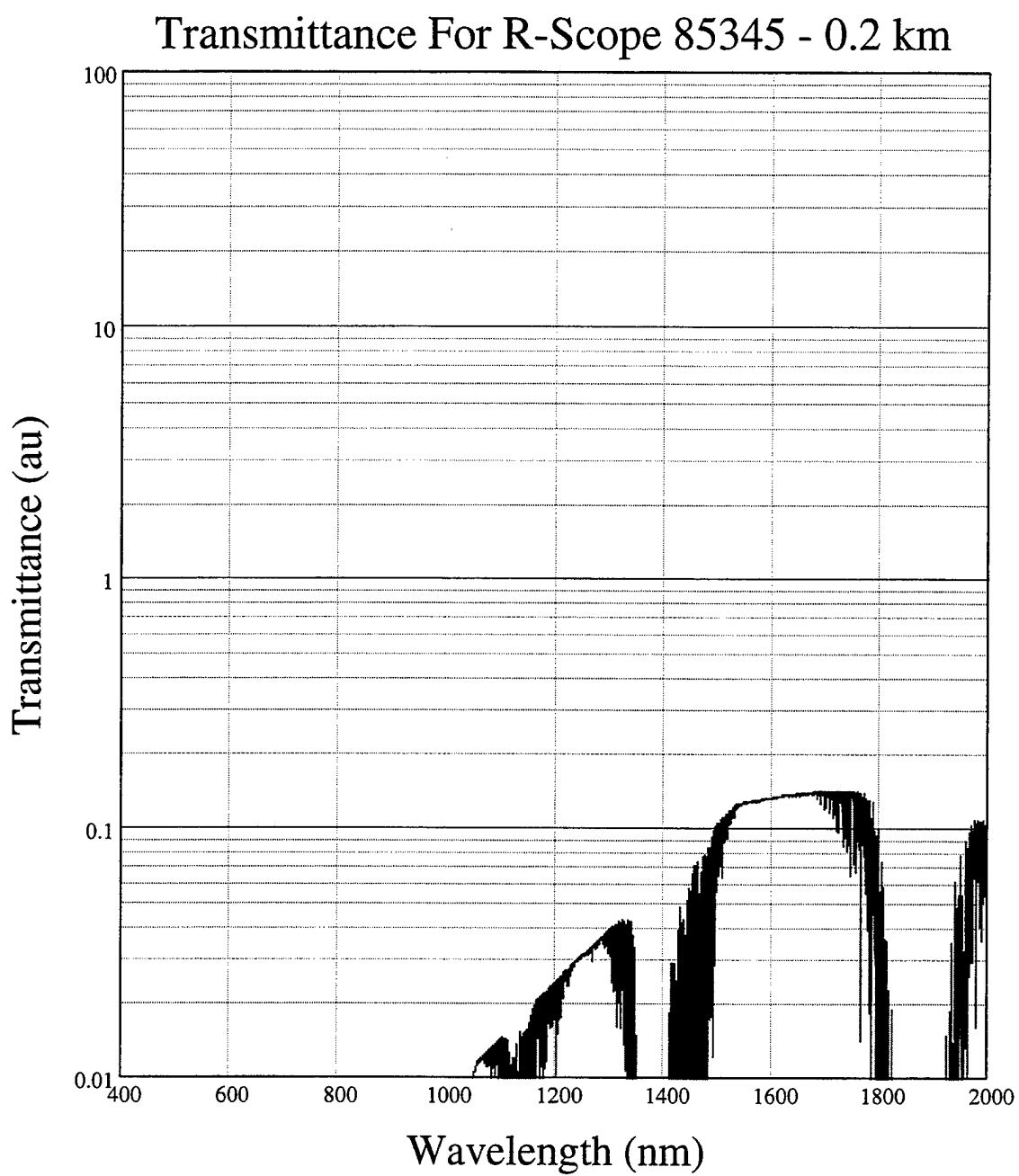


Figure 19: Convolution of Transmittance and R-Scope 85345 Response for 0.2 km visibility.

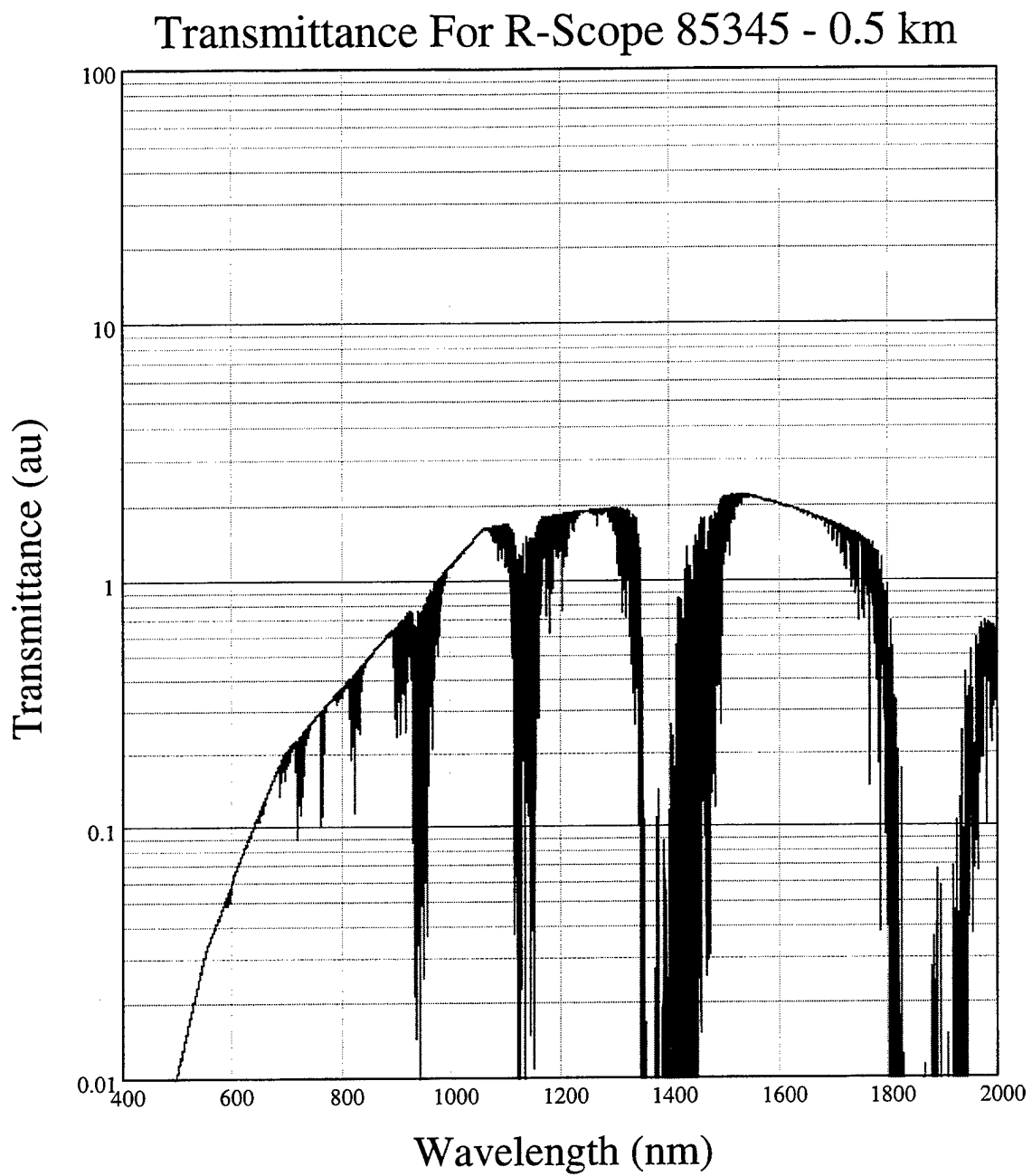


Figure 20: Convolution of Transmittance and R-Scope 85345 Response for 0.5 km visibility.

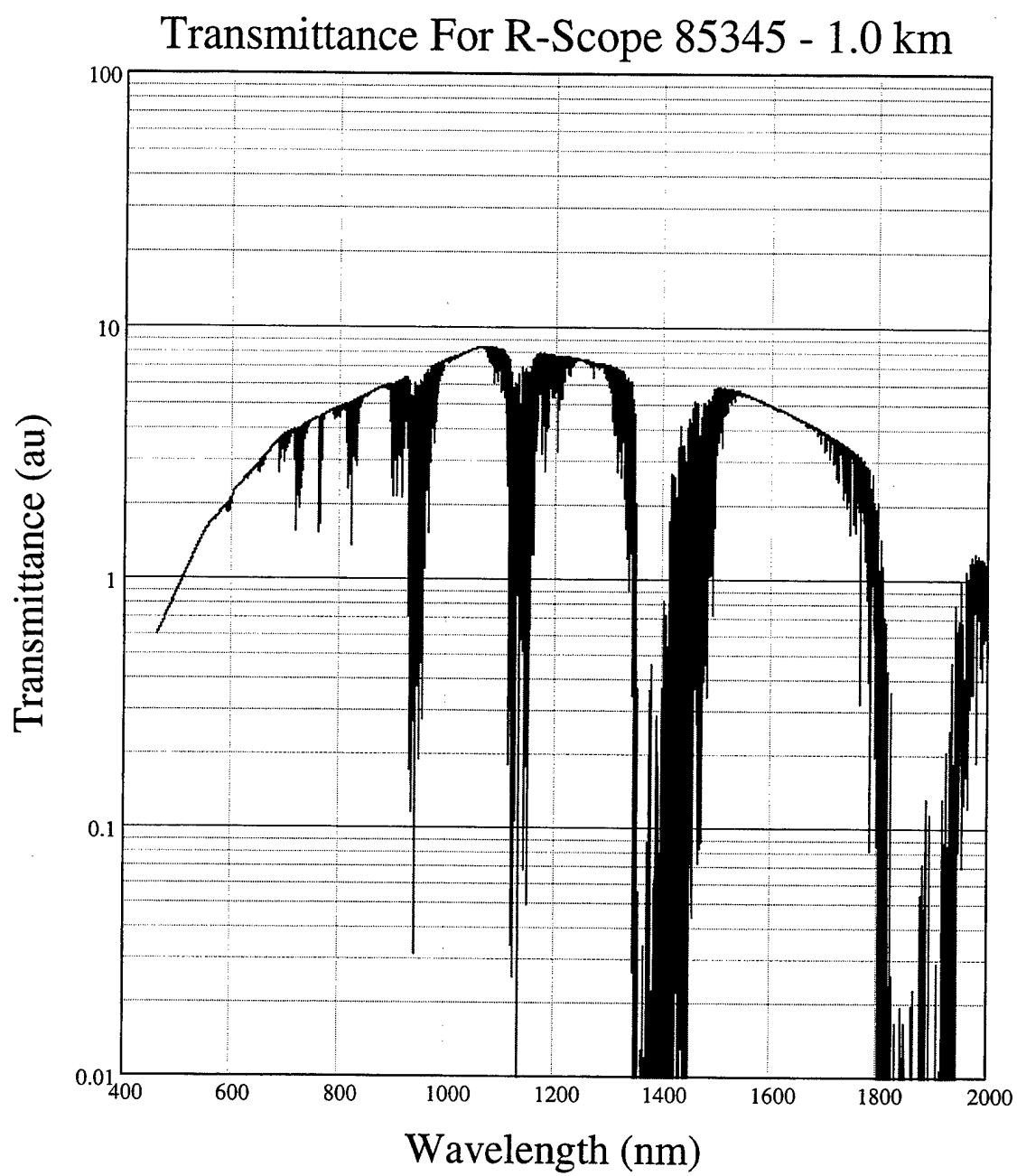


Figure 21: Convolution of Transmittance and R-Scope 85345 Response for 1.0 km visibility.

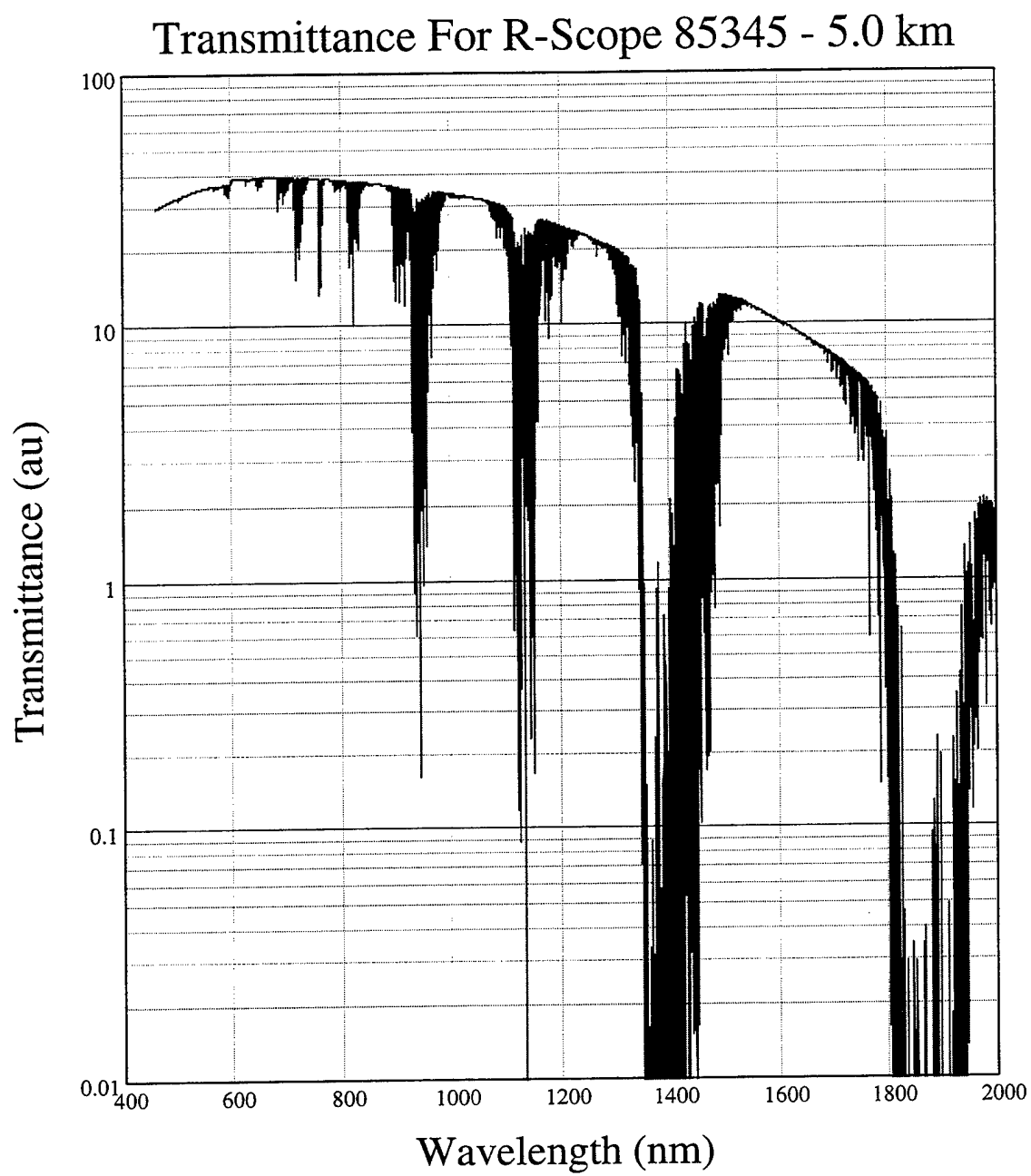


Figure 22: Convolution of Transmittance and R-Scope 85345 Response for 5.0 km visibility.

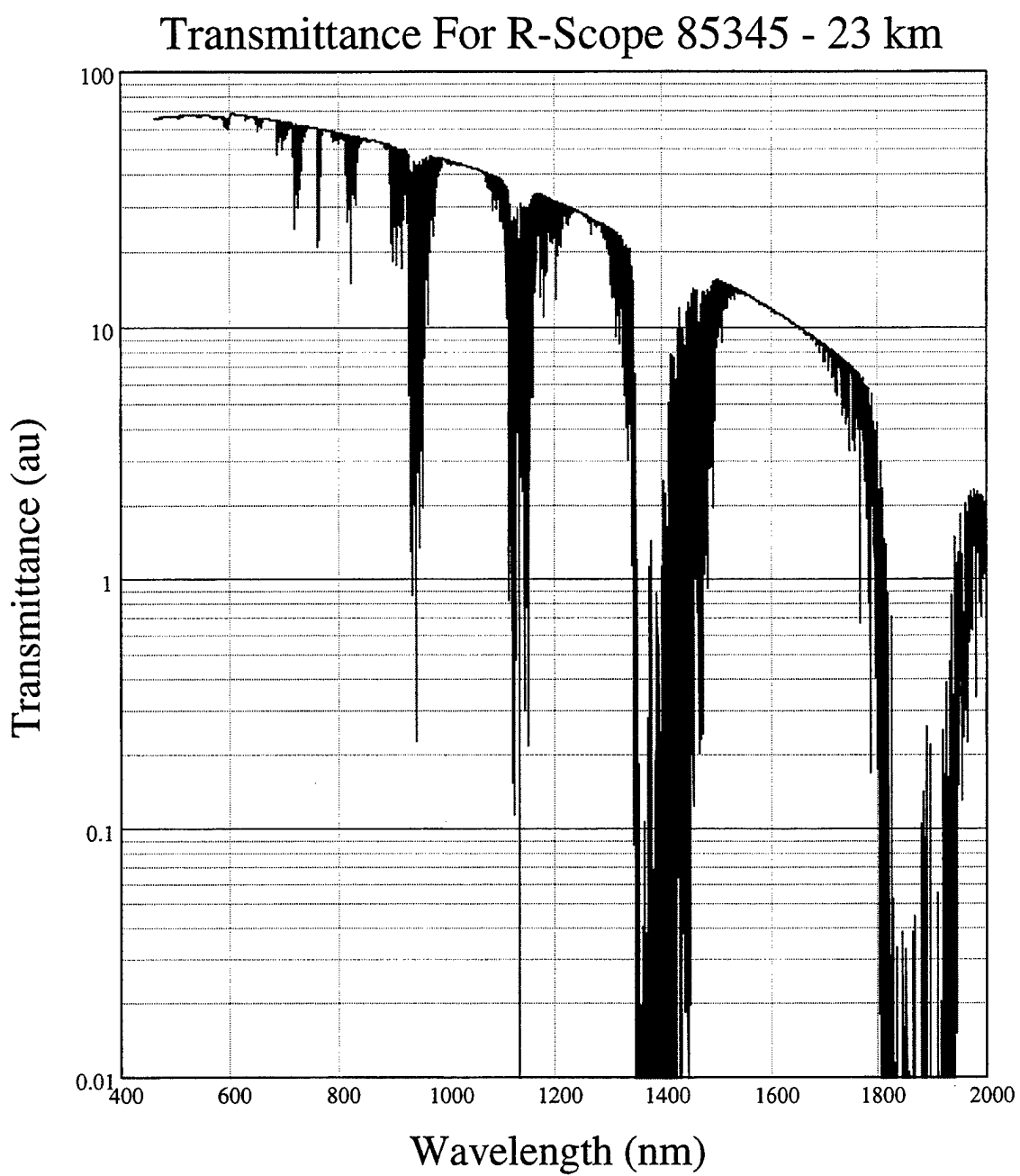


Figure 23.: Convolution of Transmittance and R-Scope 85345 Response for 23.0 km visibility.

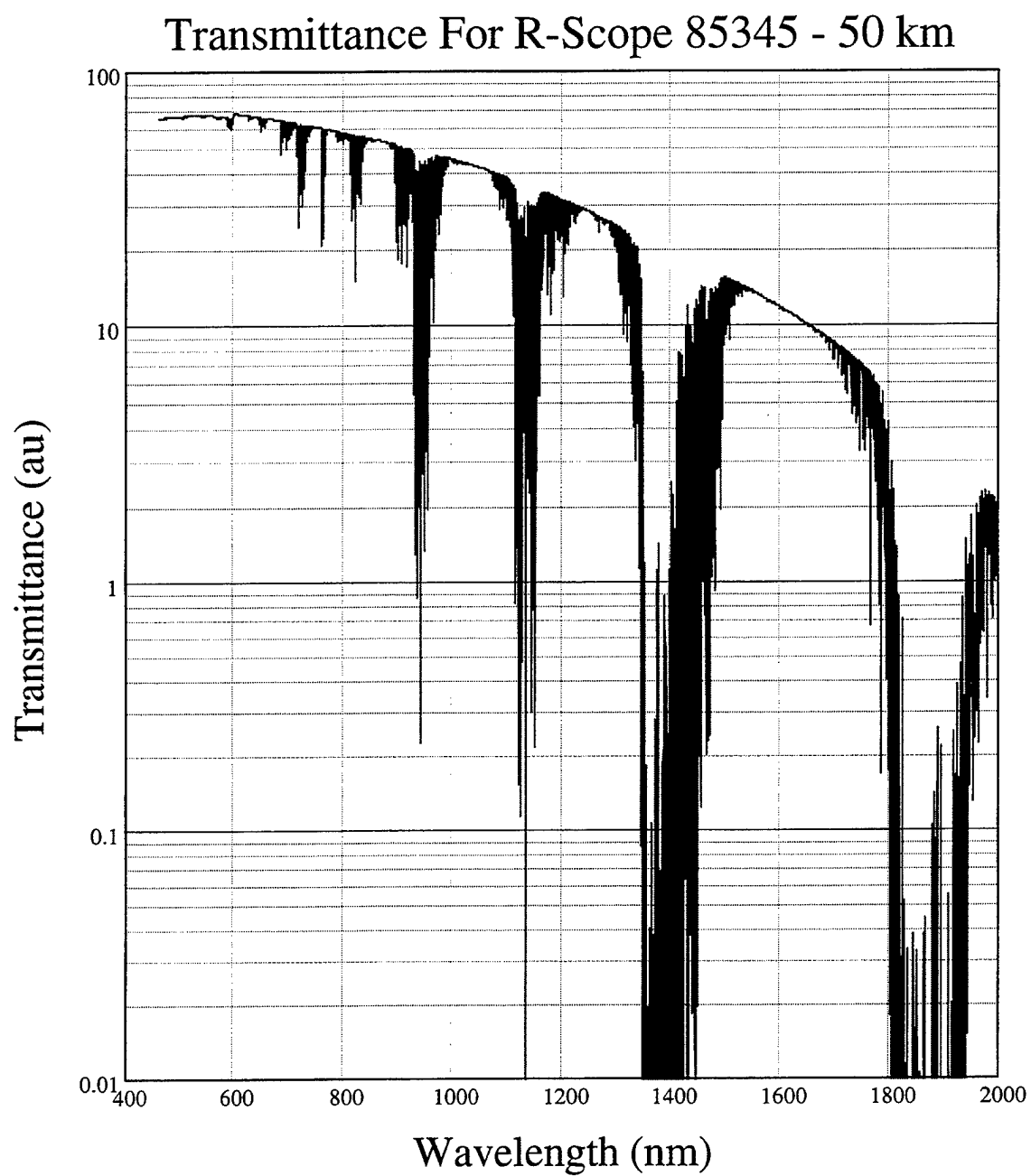


Figure 24: Convolution of Transmittance and R-Scope 85345 Response for 50.0 km visibility.

One final graph must be generated which represents the sum of all transmittance received by each detector for each visibility range. This is a composite graph showing all such data on the same graph for comparison purposes. This is accomplished by recording the sum of all convoluted transmittance values for a given detector for a given range. Having the six visibility ranges recorded in Excel with the recording of the transmittance sum for each range, for each detector in the next two columns, enables a summation graph/chart to be made. See Figure 25 for this graph summarizing the current analysis.

See Appendix E for details of doing the convolution with a smaller spreadsheet capability and also for a hard copy of results. This would also illustrate the simpler methodology for the larger Office-97 spreadsheet program. Also discussed is the summation graph.

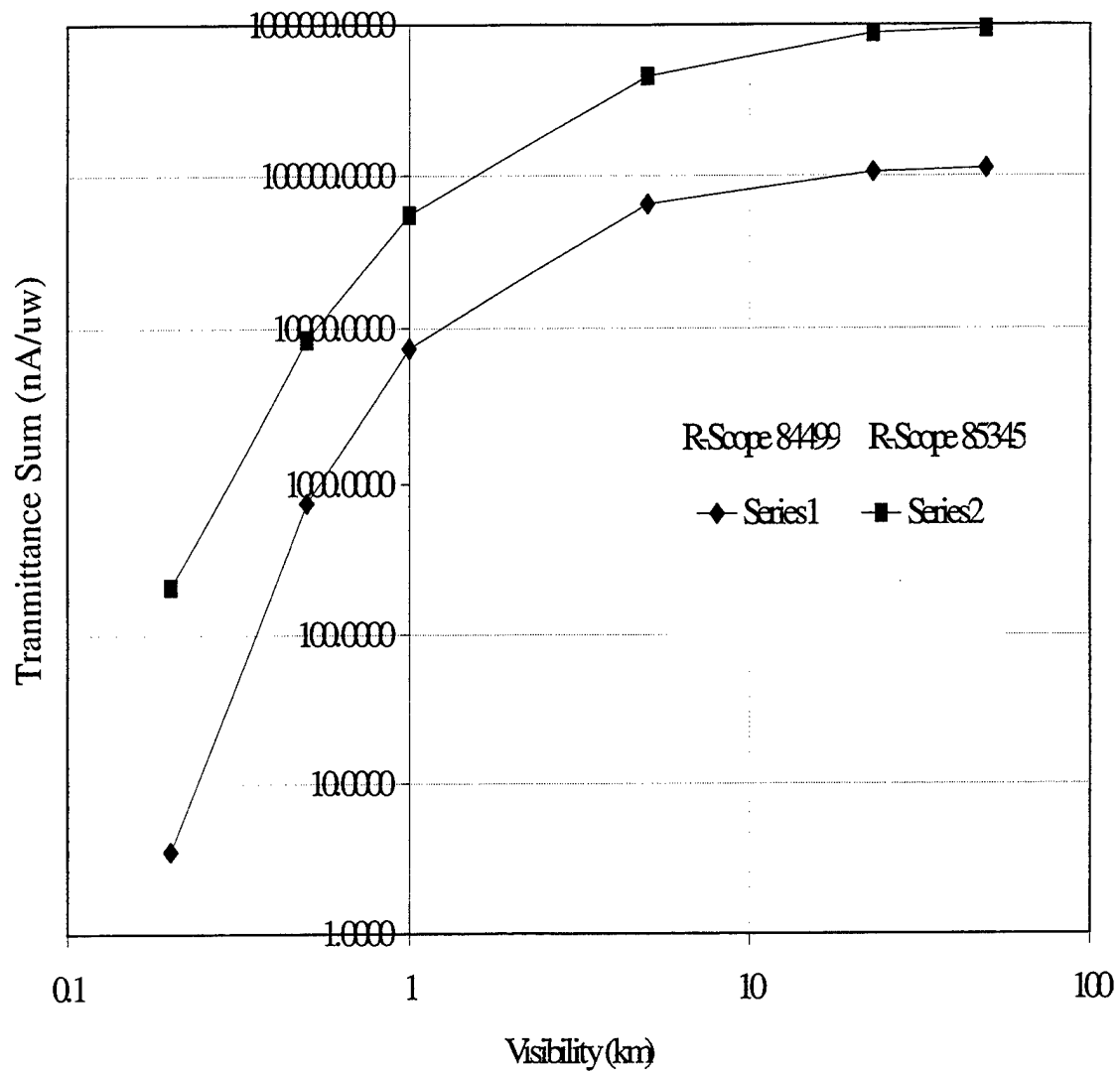


Figure 25: Sum of Individual R-Scope Responses After Convolution With The Atmospheric Transmissions With The Different Visibility Ranges.

SECTION 5

CONCLUSIONS

A study of graphs in Figures 13 - 24 enables the reader to see how this modeling tool can be utilized. We can first compare the various visibility ranges for a given detector and in both cases it is obvious that the greater the visibility the better the detector response for that condition. That result is obvious and not very meaningful.

A second set of comparisons can be made by comparing a given visibility range for each detector (i.e., comparing 0.2 km for each detector with each other). Here it can be seen that there is approximately one order-of-magnitude difference between the two detectors. The R-Scope 85345 costs approximately five times more than the R-Scope 84499 but only shows one order-of-magnitude improvement. This calls into question the value of spending that extra money.

However, it is found that for the 0.2 km visibility range, the more expensive 85345 detector has two orders-of-magnitude advantage, which implies now that there is a substantial difference for this condition. Upper management must determine if that low visibility range is a dominant factor in the decision making process.

Figure 25 is a comparison graph illustrating, in one succinct view, the facts presented above but with a simpler format.

It can be concluded that methodology of convolving night vision detector response values with atmospheric transmittance values of approximately 99% accuracy can be a good tool in decision making. This technique, using computer modeling, can save millions of dollars in field-testing and at the same time gives reasonable results with minimal effort and time.

The mathematical relationship that explained the process was $R = \int T(x)D(x)dx$ where T is atmospheric transmittance generated by PLEXUS and D is the detector response given by the manufacturer. It is believed that this methodology can be used in a variety of ways with a variety of detectors over a large part of the electromagnetic spectrum since the mathematical relationship should be always valid.

It is also realized that it canNOT be concluded from this study which detector is best or most suitable for the intended purpose. Only two detectors were analyzed for purposes of developing an effective technique with the available software tools. As a result of the minimal number of scenarios investigated and the failure to compare analytical results with field-testing, this can only be considered a pioneer effort in modeling development. It is realized that many other scenarios must be considered and that field-testing must be performed.

Given that all of the above is performed, it still remains for management at higher levels to supply additional information needed to make a final decision as to under what conditions the detector system will be used and what risk factor is acceptable. Hence, it is recognized that this methodology is only one of several tools which may be used in the decision making process.

APPENDIX A

PLEXUS PROCEDURAL DETAILS

The procedure for using the PLEXUS software program is relatively simple for the novice option since most all parameters are calculated for the user and are based upon values derived from a few input values. Some critical input data is required which means the user must be knowledgeable of his responsibilities for input. Two significant limitations to this program exist which should not impact its use in most cases.

- a. The first limitation is that altitudes above 80 km are subject to error because of stratification of the gases in the air. PLEXUS assumes a homogenous mixing of the various types of air molecules in its modeling characterization.
- b. The second limiting parameter is that it will not generate data for wavelengths less than approximately 0.29 μm , which is in the ultraviolet range.

The procedure for using PLEXUS is as follows:

1. Enter the PLEXUS software program where a screen will enable the user to select the desired level of specialization. Novice was the level used in this study since no specialization was required
2. Screen #2 - Spectral Limits Screen:
 - a. Resolution: Most applications will use the moderate resolution. Only where extremely well resolved spectra are used can the High-Resolution and Laser Line options be used which take extremely long run times.
 - b. Spectral Limits: Type in the spectral limits that define the output spectrum. The Band Center and Bandwidth respond automatically to the spectral limit input. This study

established 15 subdivisions of the overall spectral range of $0.4 \rightarrow 2.0 \mu\text{m}$ where 20,001 points were utilized over the whole range. For purposes of the developmental work, increments were established at less than 2,000 points each. Increment breaks occurred at the following micron ranges: 0.425, 0.450, 0.475, 0.500, 0.550, 0.600, 0.650, 0.700, 0.800, 0.900, 1.000, 1.200, 1.400, 1.700, 2.000 μm . It is recommended that with Office 97 version of Excel, Mathcad 6.0, and Mathematica 3.0, or better for each software package, the spectral range need not be subdivided.

- c. Spectral Interval & Scanning Function: For moderate resolution, the spectral interval is defaulted to 1 cm^{-1} and no scanning is applied.
- d. Express Keys: For version 2.1 they are not operational.

3. Screen #3 - Line-of-Sight Specifications Screen:

- a. Express Keys: Select the World Icon in the upper left of the screen to select Europe and then select Venice, Italy. This will automatically give the latitude of 45.43 degrees and a longitude of 12.07 degrees for the Initial Observer Location. Venice was chosen because it is at sea level and has humid, atmospheric conditions. The other Express Keys are optional with the manual explaining their function.
- b. Set New Path Type Keys: Icons located in the upper right side of the screen, these keys are also optional for line-of-sight input.
- c. Ground Altitude Above Mean Sea Level: For Venice, Italy this value would be zero.
- d. Reference Input Altitude To: Either ground or sea level is acceptable, since for Venice they are both the same.
- e. Initial Observer Location: This is the geographic location of the rescuing aircraft.

- 1) Altitude: 1 km was used since that is a reasonable distance above ground for a rescue plan to begin searching..
 - 2) Latitude & Longitude: These values could be typed in or they are automatically entered by way of the city location from the World Icon.
- f. Sensor Geometry: This also is referenced to the rescuing aircraft but is referring to the orientation of the detector and the path length of the signal being monitored.
- 1) Azimuth: This is the direction of orientation and since the signal is being directed straight up and the detector directed straight down this value is of no significance in this case.
 - 2) Zenith: This is very significant and refers to the angle of pointing the detector. Straight up in the air is 0.0 degrees and straight down is 180 degrees. The Zenith value is given for reference purposes. 180 degrees was used in this case.
 - 3) Range To Path End: Use 1 km since the person being rescued is on the ground and the plane is hovering 1 km above. If the zenith were set to 0.0 then the range to path end would be about 384 km for everything else being the same.

4. Screen #4: Time of Observation Screen

- a. Month: Use mouse to select the month of the year. July was arbitrarily used throughout this study.
- b. Day: Use the mouse to select the day of the month on the calendar. The 4th was arbitrarily used throughout this study.

- c. Time: Either type in or use the mouse to determine the time of interest. 12 noon was arbitrarily used throughout this study.
 - d. Selection of the Sun Icon would show the information about the sun which is already calculated. The resulting screen shows data that will be recorded in the output report.
5. Screen #5: Boundary Layer - Aerosol Parameters
- a. Choose clear day
 - b. Select the range - all six were used in the study
 - c. Choose Urban terrain
 - d. Choose No Significant Condition - refers to weather conditions
6. Screen #6: Run The PLEXUS Code
- a. Type in a numbering system that is appropriate.
7. Screen #7: Rapid Response Screen
- a. If modeling output is already available then a quick response may occur; otherwise it will take perhaps 20 minutes or more depending on the speed of the computer. The 486 which was used for this study would take 25 minutes for a run where the new 200 Mhz computers takes less than 5 minutes.
8. Program results are as follows:

The output from the program gives five AIM files. The AIM $\alpha\beta\chi$.fit file gives the transmittance and radiance graphs. Figure 26, gives the transmittance graph over the spectral range 0.2 μm through 1.0 μm and Figure 27 gives the transmittance graph for the spectral range 1.0 μm through 100 μm . Figures 28 & 29 give the radiance graphs over the same two spectral ranges.

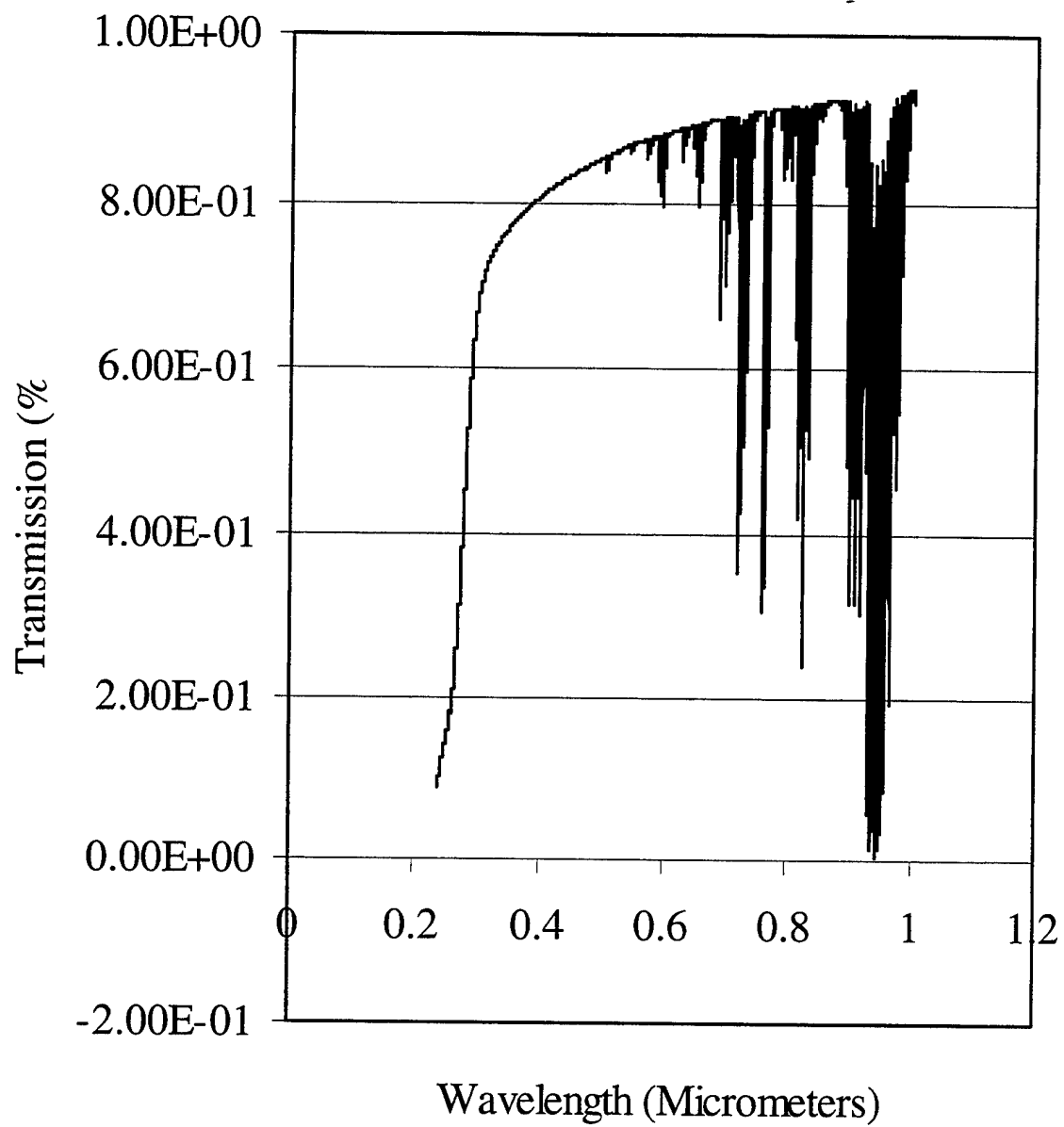


Figure 26: Transmission Through The Atmosphere For 0.2 – 1.0 μm .

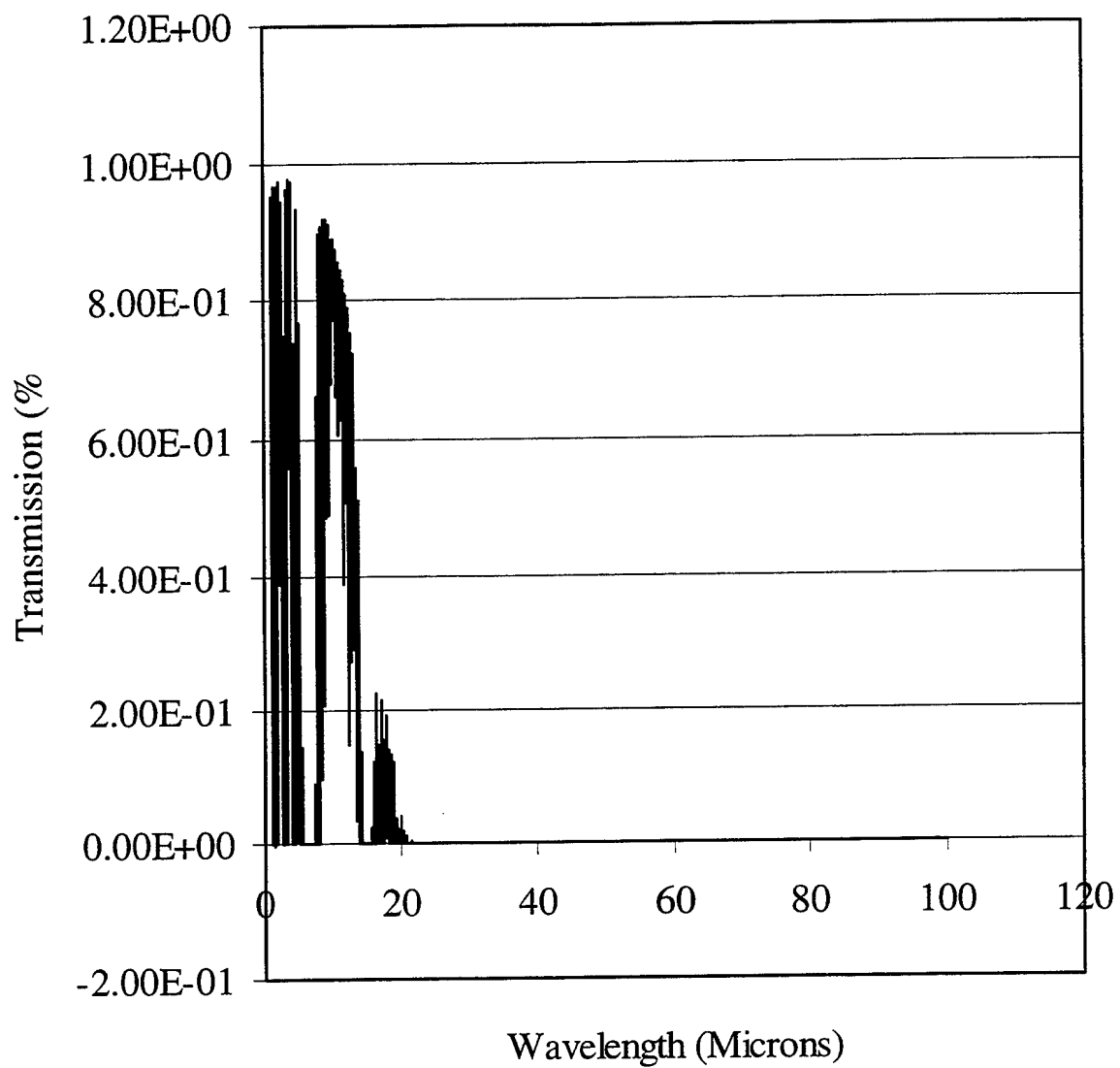


Figure 27: Transmission Through The Atmosphere for 1.0 – 100.0 μm .

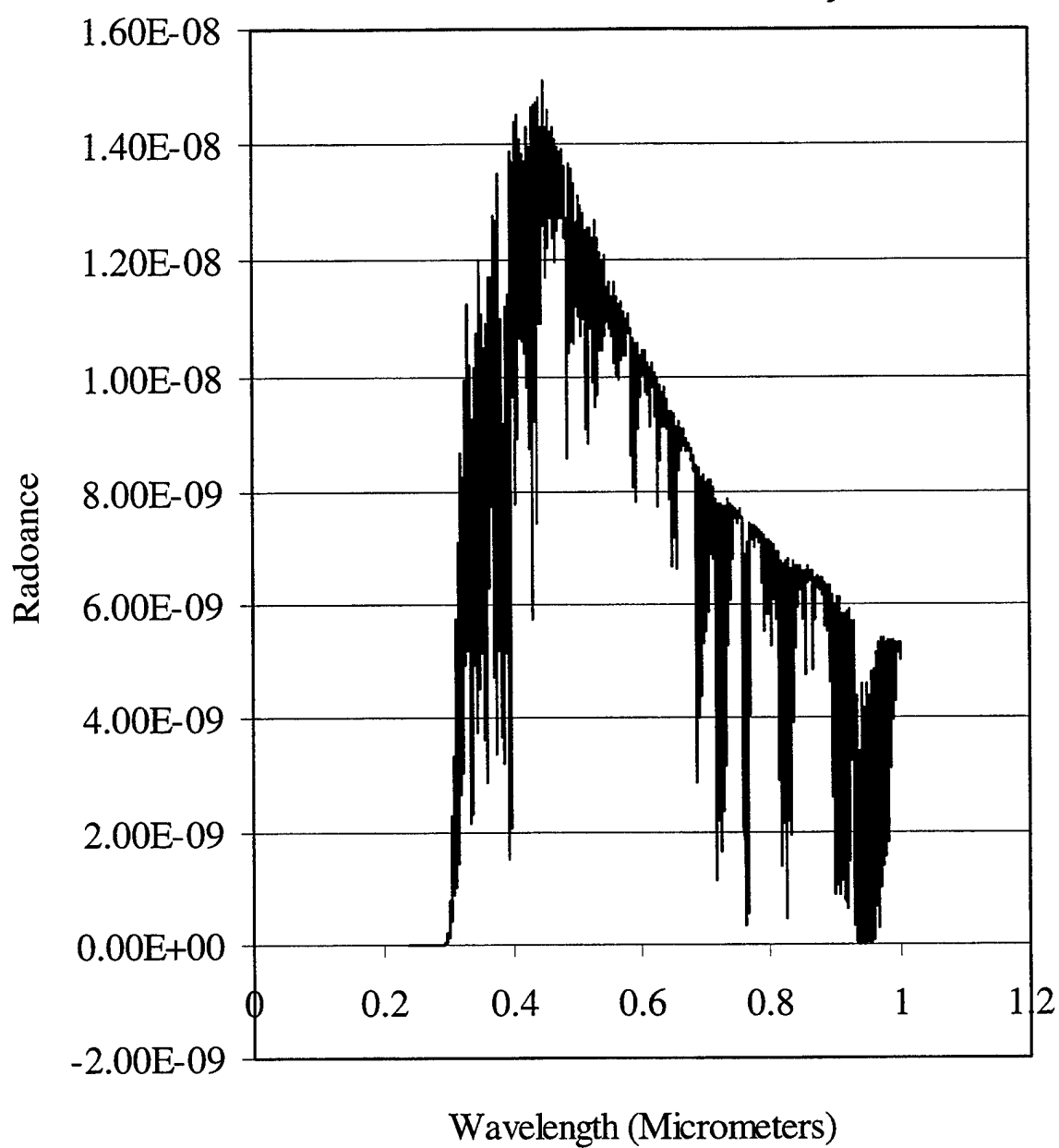


Figure 28: Radiance from 0.2 to 1.0 Micrometers.

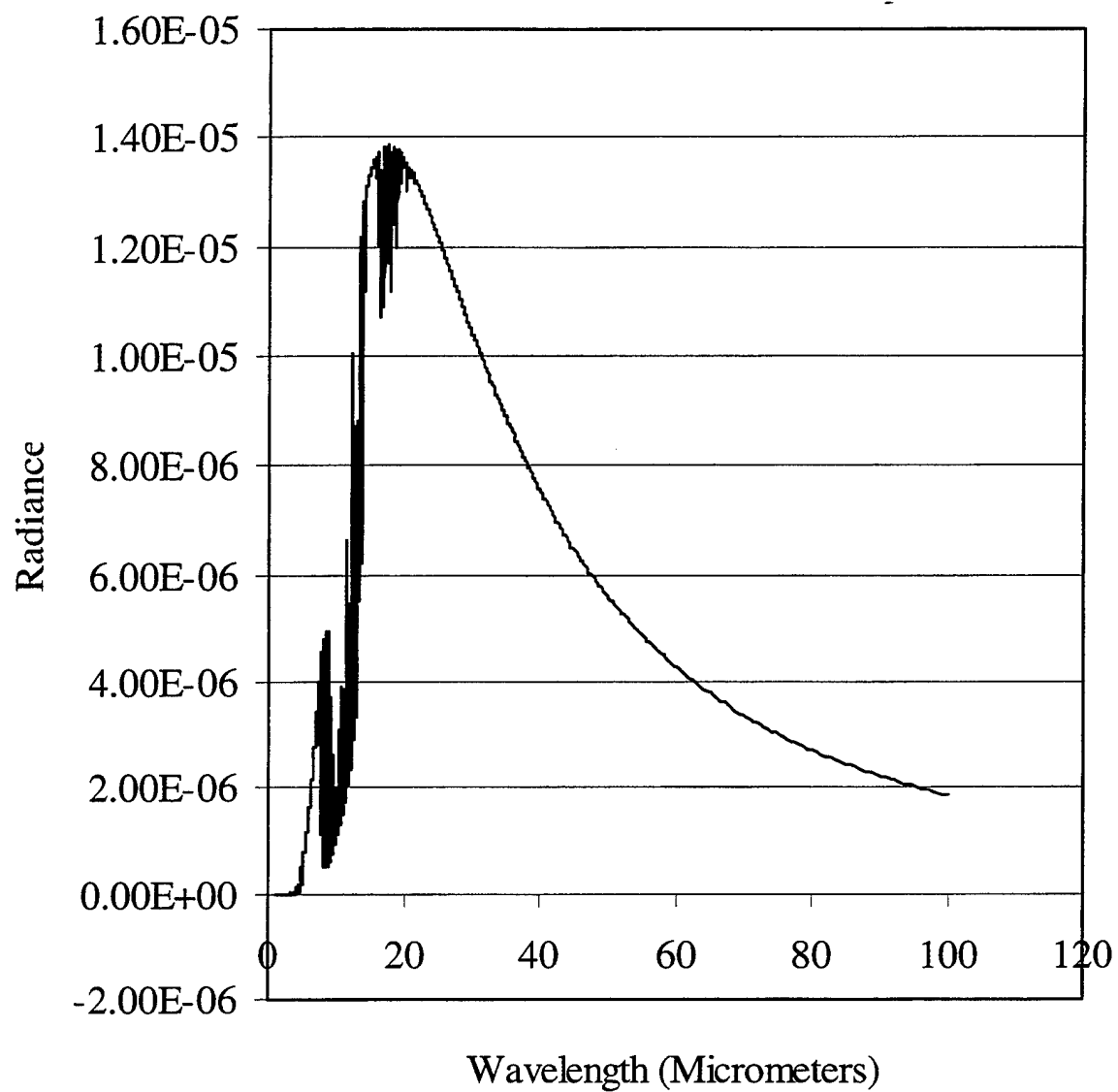


Figure 29: Radiance from 1.0 to 100.0 Micrometers.

The AIM $\alpha\beta\chi$.trn file gives the transmittance data used to generate the graphs in Figures 26 and 27. It is the “x” values that give the position along the wavelength scale and the “y” values gives the actual transmittance magnitudes, in percent of the whole originally emitted. It is these values which are convolved with the manufacturer’s data for the detector. The following illustrates the values on the first page of the AIM $\alpha\beta\chi$.trn file showing 40 of the approximately 2,000 points generated by this program:

1/cm	transmission	1/cm	transmission
10000	9.35E-01	10020	9.22E-01
10001	9.36E-01	10021	9.34E-01
10002	9.35E-01	10022	9.35E-01
10003	9.35E-01	10023	9.31E-01
10004	9.20E-01	10024	9.35E-01
10005	9.34E-01	10025	9.35E-01
10006	9.35E-01	10026	9.35E-01
10007	9.35E-01	10027	9.35E-01
10008	9.31E-01	10028	9.33E-01
10009	9.35E-01	10029	9.35E-01
10010	9.35E-01	10030	9.25E-01
10011	9.34E-01	10031	9.35E-01
10012	9.35E-01	10032	9.34E-01
10013	9.28E-01	10033	9.35E-01
10014	9.35E-01	10034	9.35E-01
10015	9.35E-01	10035	9.35E-01
10016	9.36E-01	10036	9.35E-01
10017	9.36E-01	10037	9.35E-01
10018	9.35E-01	10038	9.35E-01
10019	9.35E-01	10039	9.33E-01

A point of explanation needs to be made about the “Initial_Frequency” and “Final_Frequency.” The units are cm^{-1} or 1/cm which are converted from the input of

micrometers. The Initial_Frequency value, 10000 cm⁻¹ came from the 1 μm and the Final_Frequency value, 50000 cm⁻¹ came from 0.2 μm. [10000/cm → 1000000/m → 1.0 x 10⁻⁶ m → 1.0 μm]

The following represents the 0.2 to 2.0 μm file for the AIMαβχ.cpd file, which is the printout of the parameters going into the PLEXUS program.

```
[GENERAL]
AIM_Interface_Version=1.2
Date=04-29-1998
Code=AIM ;[CODE-C,F,M,S,U] C=CBSD F=FASCODE M=MODTRAN S=SHARC U=AIM
Special_Case_for_AIM=2 ;[ISPECIAL-U] 0=Full AIM 1=No NLTE Scat 2=Modtran Only
Problem_Definition_File=c:\plexus\aim\FIGURE4.CPD ;[PROBFILE-U]
User=FIGURE4 ;[UserName-U]
Title=FIGURE4 Day Z180,A001 ;[TITLE-F,M,S,U]
Plexus_Version=1.9

[IMAGE]

[SPECTRAL]
Initial_Frequency=5000.0000000000000000 ;[V1-F,M,S,U] (CM-1)
Final_Frequency=50000.0000000000000000 ;[V2-F,M,S,U] (CM-1)
Spectral_Resolution=1.000000000000000000 ;[FWHM-M,S] (CM-1)

[OUTPUT]
Execution_Mode=2 ;[IEMSCT-F(IEMIT),M,U] 0=T 1=T,R 2=SCAT 3=IRR
Flag_for_Multiple_Scattering=1 ;[IMULT-M,U] 0=NO 1=YES
Printing_Step_Size=1 ;[IDV-M] (CM-1)
Flag_for_Laser_Options=0 ;[ILAS-F,U] 0=NO 1=YES
Flag_for_Scanning_Function=0 ;[ISCAN-F,U] 0=NO 1=YES
Scanning_Function=0 ;[JFN-F,U] 0=RECT 1=TRIANG 2=GAUSS 3=SINC**2 4=SINC
Flag_for_Continuum= 1 ;[ICNTNM-F,U] 0=NO 1=YES
Flag_for_Line-by-Line_Function4= 1 ;[ILBLF4-F,U] 0=NO LBLF4 1=25 CM-1 2=5CM-1 aboutve 0.5 MB

[LOS]
Initial_Altitude=1.00000000 ;[H1ALT-F,M,S,U] (KM)
Initial_Latitude=45.43000000 ;[H1LAT-F,M,S,U] (DEGREE)
Initial_Longitude=12.07000000 ;[H1LON-F,M,S,U] (DEGREE)
Final_Altitude=0.00000000 ;[H2ALT-F,M,S,U] (KM)
Final_Latitude=45.43000000 ;[H2LAT-F,M,S,U] (DEGREE)
Final_Longitude=12.07000000 ;[H2LON-F,M,S,U] (DEGREE)
Earth_Radius=6371.00000000 ;[RO-F,M,S,U] (KM)
Tangent_Altitude=-999.99 ;[HMIN-S] (KM) -999.99=no tangent point in path
Tangent_Latitude=-999.99 ;[HMLAT-S] (DEGREE) -999.99=no tangent point in path
Tangent_Longitude=-999.99 ;[HMLON-S] (DEGREE) -999.99=no tangent point in path
Initial_Zenith_Angle=179.99456037 ;[ZENANG-F,M,S,U] (DEGREE)
Path_Azimuth_Angle_Earth=0.00000000 ;[PSIPO-M,U] (DEGREE)
Observer_Target_Distance=1.00000000 ;[RANGE-F,M,S,U] (KM)
Earth-Centered_Angle=0.00000085 ;[BETA-F,M,S,U] (KM)
Path_Long/Short_Index=0 ;[LEN-F,M,S,U] (0=SHORT 1=LONG)

[SOURCE]
Sun_Altitude=152089207.40 ;[SUNALT-U] (KM)
Sun_Latitude=22.87 ;[PARM3-M,U] (DEGREE)
Sun_Longitude=16.28 ;[PARM4-M,U] (DEGREE)
Moon_Latitude=-10.64 ;[PARM3-M,U] (DEGREE)
Moon_Longitude=134.23 ;[PARM4-M,U] (DEGREE)

[MODEL_ATMOSPHERE_PARAMETERS]
Model_Atmosphere=8 ;[MODEL-F,M,S,U]
```

```

Title_of_Model_Atmosphere=AIM Atmosphere for FIGURE4 ;SAG title
Modtran_Model_Atmosphere=c:\plexus\ATM_POP\AIM.MMA ;SAG output TAPE5 file
Sharc_Model_Atmosphere=c:\plexus\ATM_POP\AIM.SMA ;SAG output Sharc compatible file
Fascode_Model_Atmosphere=c:\plexus\ATM_POP\AIM.FMA ;Fascode atmospheric file
Solar_Flux_Index=120.0 ;[F107-G]
Solar_Flux_Index_Average=120.0 ;[F107A-G]
Geomagnetic_Activity_Index=15.0 ;[AP-G]
CO2_Mixing_Ratio= 360 ;[CO2MX-M,U] (PPMV) 0 = 330 PPMV

[TIME]
Greenwich_Time=11.00 ;[TIME-M]
Day_of_Year=185 ;[IDAY-M,U]
Time_of_Day=D ;[Select Day or Night Sharc Profile]
Observation_Date=4 7 1998 ;[OBSDATE-C] (DMS)
Observation_Time=11 0 0.00 ;[OBS TIME-C] (HMS)

[LOWER_ATMOSPHERE_ENVIRONMENTAL_PARAMETERS]
Boundary_Temperature=0.000 ;[TBOUND-F,M,U] (K)
Surface_Albedo_of_Earth=0.00 ;[SALB-M,U]
Ground_Altitude=0.00000000 ;[GNDALT-F,M,U] (KM)
Boundary_Aer._Extinction+Vis.=5 ;[IHAZE-F,M,U]
Surface_Meteorological_Range=23.0 ;[VIS-F,M,U] (KM)
Current_Wind_Speed=4.1 ;[WSS-F,M,U] (M/S)
Average_Wind_Speed=4.1 ;[WHH-F,M,U] (M/S)
Air_Mass_Character=3 ;[ICSTL-F,M,U]
Tropo.+Strato._Aer._Season=0 ;[ISEASN-F,M,U]
Cloud_or_Rain_Model=0 ;[ICLD-F,M,U]
Rain_Rate=0.00 ;[RAINRT-F,M,U] (MM/HR)
Cirrus_Thickness=0.00 ;[CTHIK-F,M,U] (KM)
Cirrus_Base_Altitude=0.00 ;[CALT-F,M,U] (KM)
Cirrus_Extc._Coeff._@_0.55_um=0.00 ;[CEXT-F,M,U] (KM-1)
Strato._Aer._Extinction+Profile=1 ;[IVULCN-F,M,U]
Type_of_Aer._Phase_Function=2 ;[IPH-M] 0=HENYEV-GREENSTEIN 1=USER 2=MIE
Asymmetry_Factor_for_H-G_Phase_Function=0 ;[G-M]

[UPPER_ATMOSPHERE_REGION_PARAMETERS]
Region_Total=2 ;[NREGT-S]
Amb_Pop_Filename=c:\plexus\ATM_POP\STD.POP ;[POP NAM(1, IREG)-S,U]
Amb_Pop_Save_Index=0 ;[ISAVE(1, IREG)-S,U] 0=NEW+NOT SAVED; 1=NEW+SAVED; 2=OLD
Aur_Pop_Filename=c:\plexus\ATM_POP\STD.POP ;[POP NAM(2, IREG)-S,U]
Aur_Pop_Save_Index=0 ;[ISAVE(2, IREG)-S,U]
Code/User_Auroral_Index=0 ;[IAUR(IREG)-S,U] 1=CODE 2=USER
Auroral_IBC_Index=0 ;[IBC(IREG)-S,U] 2=II 3=III 4=III+
Incident_e-_Energy_Spectrum=0 ;[IDGM(IREG)-S,U] 1=MAXWELLIAN(DIFFUSE) 2=GAUSSIAN(DISCRETE)
Total_e-_Energy_Flux=0.00 ;[QF(IREG)-S,U] (ERGS/CM2/S)
Characteristic_Energy=0.00 ;[EC(IREG)-S,U] (KEV)
Scale_Param._for_Gaussian_Dist.=0.00 ;[WG(IREG)-S,U] (KEV)
Auroral_Duration=0.00 ;[TDOSE(IREG)-S,U] (S)
Auroral_Observation_Time=0.00 ;[TOBS(IREG)-S,U] (S)
Latitude_of_Corner_1=4.00 ;[REGD(1,1,IREG)-S,U] (DEGREE)
Longitude_of_Corner_1=4.00 ;[REGD(1,2,IREG)-S,U] (DEGREE)
Latitude_of_Corner_2=-4.00 ;[REGD(2,1,IREG)-S,U] (DEGREE)
Longitude_of_Corner_2=4.00 ;[REGD(2,2,IREG)-S,U] (DEGREE)
Latitude_of_Corner_3=-4.00 ;[REGD(3,1,IREG)-S,U] (DEGREE)
Longitude_of_Corner_3=-4.00 ;[REGD(3,2,IREG)-S,U] (DEGREE)
Latitude_of_Corner_4=4.00 ;[REGD(4,1,IREG)-S,U] (DEGREE)
Longitude_of_Corner_4=-4.00 ;[REGD(4,2,IREG)-S,U] (DEGREE)
Top_of_Local_Region=0.00 ;[REGTOP(IREG)-S,U] (KM)
Bottom_of_Local_Region=0.00 ;[REGBOT(IREG)-S,U] (KM)

[SCREENS]
JulianDate=2450998.95833333 ;date and time together
WaveUnits=micron ;user preferences for spectral screens
IntervalUnits=cm-1 ;user preferences for spectral screens
DefaultMode=-1 ;user preferences for spectral screens
Screen_Calculation_Mode=0 ;user preferences for spectral screens
Expert_System_Warning="" ;[expert warning for selected code]
Surface Temperature Unit=K ;unit preference
Fog List Index=0 ;expert system parameter

```

Visibility List Index=4	;expert system parameter
Terrain Type List Index=0	;expert system parameter
Urban Industrial Influence List Index=0	;expert system parameter
Recent Weather Conditions List Index=0	;expert system parameter
Cloud Type List Index=0	;expert system parameter
Rain Rate List Index=0	;expert system parameter
Type of Aurora List Index=0	;expert system parameter
Aurora Base Altitude (km) List Index=5	;expert system parameter
Aurora Top Altitude (km) List Index=0	;expert system parameter
Aurora Duration (sec) List Index=1	;expert system parameter
Aurora Time of Observation (sec) List Index=1	;expert system parameter
Aurora Location (Near or Far) List Index=0	;expert system parameter
Observer Altitude Unit=KM	;user preference units for screen restoration
Observer Latitude Unit=Deg	;user preference units for screen restoration
Observer Longitude Unit=Deg +E	;user preference units for screen restoration
Final Altitude Unit=KM	;user preference units for screen restoration
Final Latitude Unit=Deg	;user preference units for screen restoration
Final Longitude Unit=Deg +E	;user preference units for screen restoration
Tangent Altitude Unit=KM	;user preference units for screen restoration
Tangent Latitude Unit=Deg	;user preference units for screen restoration
Tangent Longitude Unit=Deg +E	;user preference units for screen restoration
Initial Altitude Unit=KM	;user preference units for screen restoration
Tangent Azimuth Unit=Deg	;user preference units for screen restoration
Sensor Zenith Unit=Deg	;user preference units for screen restoration
Sensor Azimuth Unit=Deg	;user preference units for screen restoration
Sensor Range Unit=KM	;user preference units for screen restoration
Ground Altitude Unit=km	;user preference units for screen restoration
Infinity Flag=0	;Flag to compute range to Earth/Atmosphere Top
DateUnit=Gregorian Date	;unit preference
TimeUnit=Local A (+15E) 1.0	;unit preference
UserExperience=1	;used by expert system
ReferenceWavelength=0	;user preferences for spectral screens
Altitude Reference=1	;0=to ground 1=to Mean Sea Level
LOS Parameter Set=2Pt	;set of LOS parameters user selected

Two other files not shown are the AIM $\alpha\beta\chi$.bnd which gives the integrated radiance and the average transmittance, and the AIM $\alpha\beta\chi$.spc files. The AIM $\alpha\beta\chi$.bnd is a short file giving a summary of the transmittance and the radiance over the spectral range specified. The AIM $\alpha\beta\chi$.spc file gives the radiance values on a point by point basis. The printout values for the AIM $\alpha\beta\chi$.spc file looks like the AIM $\alpha\beta\chi$.trn file except that it gives radiance values for the second column (ordinate values) instead of the transmittance values.

There are 20,001 points generated by PLEXUS for the entire range from 0.4 μ m to 2.0 μ m and the "x" values are the independent values used in determining all other dependent values throughout the analysis. For analysis approaching the ultraviolet end of the spectrum the numbers of points generated greatly increase. For example, in the short spectral range from 0.2

through 0.4 μm approximately 25,000 points are generated and from 0.2 through 1.0 there are 40,000 points generated. These examples give a feel for the kinds of computer space necessary for an analysis.

The PLEXUS program will show the estimated number of points generated when the spectral range is established. Depending on the limitations of the spreadsheet program you may have to break this data set into sets of data so it fits into the spreadsheet for graphing and calculation purposes. Both Mathcad and Mathematica do not have limits in their programs. The only limits are those of your computer capacity.

APPENDIX B

SCANMAKER II PROCEDURAL DETAILS

Scanning of the manufacturer's detector response curves is performed so we can convolve these values as a function of "x" for each atmospheric transmittance value generated by PLEXUS. The Microtek ScanMaker II is a flatbed scanner that will take a picture and make a bitmap out of it and store it as a file on a zip drive with a .PCX extension. In the Corel Photo Paint-6 software program this scanner is called a Microtek ScanWizard.

The procedure for performing the scanning operations is as follows:

1. Go to the laboratory where the scanner is located and press the power button that should turn on both the computer and scanner.
2. After windows has produced the "desk-top screen" select the START button on the bottom left part of the screen that brings up a menu.
3. Select the Corel Photo Paint 6 program on the top of the menu and that program will become operable within a few moments.
4. Select the FILE menu on the top of the screen and the file menu will appear.
5. Select ACQUIRE IMAGE and two options will appear.
6. Select ACQUIRE and a setup menu with attached preview scan-screen will appear. The second option available was the SOURCE option that by default should already be set at Microtek ScanWizard. Do NOT select the Microtek ScanMaker III.
7. The smaller setup screen for the scanner details is on the left where the following options should be selected:
 - a. TYPES should be set at LINE ART

- b. RESOLUTION should be set at 300 dpi
 - c. Everything else should be set at default values although experimentation with other values for better clarity can be performed
8. Put graph in scanner such that the top of the graph is located in the lower left corner of the screen.
 9. From the toolbar on top of the right-hand worksheet select PREVIEW which in a few moments will produce the picture of the page in the scanner.
 10. The dotted square initially located around the entire picture can be re-sized and moved around using the mouse arrow. Select the portion of the picture or graph desired.
 11. Select SCAN from the toolbar located to the right of the PREVIEW button.
 12. Scanning may take a few minutes depending upon how many points are in the picture. For Line Art selected as a "type" on the left menu it takes less than a minute, but for some of the other selections for "type"; it could take several minutes.
 13. The picture of the graph will appear on the large screen under the two working screens. Press the "x" in the upper right corner to remove those screens from view with only the large graph picture on the screen.
 14. Select FILE from the top menu selection.
 15. Select SAVE AS which brings up the screen where the selection of file type is found.
 16. Type in the file name, saving location, and the .PCX extension as file type. A zip disk should be used since the files can be somewhat large and much file space is needed.
 17. Please note: The next step in the procedure is to digitize the response curve with the Un-Scan-It software program. This program is sensitive to lines that intersect with the original

curve it is digitizing. Any intersecting lines will result in the digitizer following the intersecting line. The solution is as follows:

- a. If the graph has grid lines they should be erased with the Paintbrush software program. This is accomplished by erasing a small section of the spurious line above and below the main curve.
- b. Likewise if the graph has two or more graph lines which intersect with each other than the curve that is not wanted should have a small portion of the curve above and below the desired curve erased. If both curves are to be digitized then save the new erased graph as a new file and then call up the original file. Go through the same procedure with the other curve by erasing those critical portions of that curve and save as another file name.

APPENDIX C

UN-SCAN-IT PROCEDURAL DETAILS

The curve that now exists as a bitmap file is just a picture file. It has no "x" and "y" values. To obtain "x" and "y" values the curve must be digitized. This is the purpose of the software program. The following procedure should be followed:

1. Select the Un-Scan-It program from the program list.
2. Select DIGITIZE from the main menu. Do not select file, as is customarily done.
3. Select the option, DIGITIZE NEW IMAGE PCX... which results in the list of files from the drive where those files are located.
4. Select the *.PCX file which was saved by the Corel Photo Paint-6 program. The graph appears with a set of menu screens overlaying the graph.
5. Scan Mode - Select AUTOMATIC LINE FOLLOW from the first set of choices.
6. Scale - Select the scale that the original graph utilized for the "x" and "y" axes.
7. Point Assignment - Select the third choice, MID-LINE* since it gives the best approximation for the true Y value and does correct for changing line thickness. As a result it will not cause peak heights to be lowered as often as the regular mid-line selection. This method does not work well with ragged, noisy data but a commercial detector response curve does not usually present that problem.
8. Line Follow Side - This selection depends upon which way the peaks in the graph point. If peaks point up then select FOLLOW TOP OF LINE. If peaks go down then select FOLLOW BOTTOM OF LINE.

9. Digitizing Speed – Select STANDARD that would show the x,y values as they are being digitized, and shows the movement of the crosshair. If the TURBO MODE is used it will show neither of these features and only shows a red dot at each data point. For this work it does NOT matter.
10. Line Follow Method – SLOPED METHOD is the faster of the two methods but does have a tendency to follow stray markers close to sharp points. NON-SLOPED method is slower but reduces chances of following stray marks, especially those close to sharp peaks.
11. Color Type – Select DIGITIZE A SINGLE DATA COLOR, which is used to determine the data the program should recognize. Since only one graph line at a time is being digitized this will usually be the option selected.
12. At this point the main digitizing screen appears displaying the entire PCX image. The zoom window must always be visible during automatic digitizing. The “zoom screen” and the “measure box” used to guide through the set-up can be easily moved using the mouse and dragging either around the screen so necessary parts of the graph are visible.
13. Locating Axes Points – The next eighty screens will require the placement of a graphics cross-hair on the lowest and highest tick mark on the X axis. After each cross-hair placement a prompt will also be given to type in the value of the cross-hair location. Do the same for the Y-axis as led to do by the prompt. A marker is located at each of the tick marks. Use the zoom screen to place the tick marker in the exact location for accurate results.
14. Notification of any tilt of the graph will be given along with the correction factor. This is automatically done and an ENTER is all that needs to be performed.
15. Locating Endpoint - A prompt will be given for the placement of the end point of the line, which is, where scanning will end on the graph line.

16. Defining Digitizing Window - The next two screens are used only for the Automatic Line Follow Mode where it will prompt the placement of the upper and lower limit, outside of which no data will be digitized. The first screen asks for the placement of lower axis point, which is usually the X-axis. Place the cross hair anywhere along the X-axis. The next screen will ask for the placement of the cross hair on some upper Y-axis tick point or anywhere above the highest point on the graph line. Always select OK after placing the cross hair as directed.
17. Line Thickness Prompt - This screen is also only used for the Automatic Line Follow Mode or Semi-Automatic mode where a prompt will ask for the placement of the cross hair slightly above the flat portion of the graph. This helps to measure the data line thickness to better calculate the digitized data.
18. Begin Scan - This screen is also only used for the Automatic Line Follow Mode or Semi-Automatic mode where a prompt will ask for the placement of the cross-hair to where you wish to begin digitizing on the graph line.
19. The cross hair will begin to move along the graph line and will be viewed in the zoom screen along with the X and Y digitized values shown in a data box.
20. When completed, a prompt will ask what is to be done with the digitized points of the graph. If everything has gone as planned select "Accept the *** points and exit."
21. Select from the FILE menu the Save As option. Save as an ASCII, tab delimited file.

Now that the digitized manufacturer's detector response curves are digitized it would be best to get a graph of each to be sure they have been properly digitized. Call the ASCII tab delimited file into Excel and obtain a graph. It will be assumed that the user of this document has a working knowledge of the Microsoft Office Software package and hence can

effectively use Excel. Note that a text file is being called and tab delimiting is the proper format. Use the “chart” option and obtain a graph as illustrated in Figure 6 for R-Scope 85345.

Save each file called into Excel with the appropriate file name. It may be best to save as a Comma Delimited file under the saving format: “CSV(Comma delimited)[*.csv]”.

APPENDIX D

PROCEDURAL DETAIL FOR DETERMINATION OF POLYNOMIAL FIT USING MATHEMATICA AND EXCEL FOR GRAPHING COMPARISONS

The next step of the procedure is to determine the polynomial fit of the manufacturer's detector response graph that has now been digitized. Using the Mathematica software program best performs this. However, Mathematica, version 3.0 is very particular of the kind of external file it will read. It must be a Space-Delimited file, with one or more spaces between the data values. It was found that Tab-Delimited files, although looking like the space-delimited format, would not be accepted. Likewise it was found that Excel's space-delimited file saving format, "Formatted Text[Space delimited][*.prn]", would not be accepted because there is no actual space between the data values. The data is run into each other in a text mode with no actual space between the numbers.

One solution to the problem is to load the ASCII text file with tab delimiting into Excel and save as a Comma Delimited file under the saving format: "CSV(Comma delimited)[*.csv]". This may have already been done upon completion of Un-Scan-It, where the files were called into Excel for graphing purposes. In either case call the comma-delimited file from Excel into Word Pad where the REPLACE function is used to replace the commas with one or more spaces. It can be saved with the same csv extension or use any other text extension available.

The reason the Tab Delimited saving format cannot be used in saving with Excel, when going into Word Pad, is that TAB cannot be read in trying to do a "replacement" of TAB with a space in the Word Pad program.

Now that a space delimited file is available for the digitized manufacturer's detector response curve the polynomial fit can be derived with Mathematica. Mathematica software program is not user friendly so it is suggested that the following statements be typed as you see them, and if understanding is desired, see the manual. This program is also case sensitive such that where upper case letters are used they must be typed as such and the same for small letters.

To illustrate the procedure the manufacturer's detection graph of R-Scope 85345 will be used. Using the digitized values saved in a text file, 85345.csv which is space delimited as discussed above, the data is read into Mathematica to get a plot of the data. Type the following:

```
ListPlot[ReadList["e:\85345.csv", Number, RecordLists -> True]]
```

where only e:\85345.csv is subject to change depending on the file name and where it is located.

This results in the graph shown in Figure 30 where the "In[2] :=" preceding the typed statement is automatically produced by Mathematica upon completion of the calculations along with Out[2] = -Graphics-.

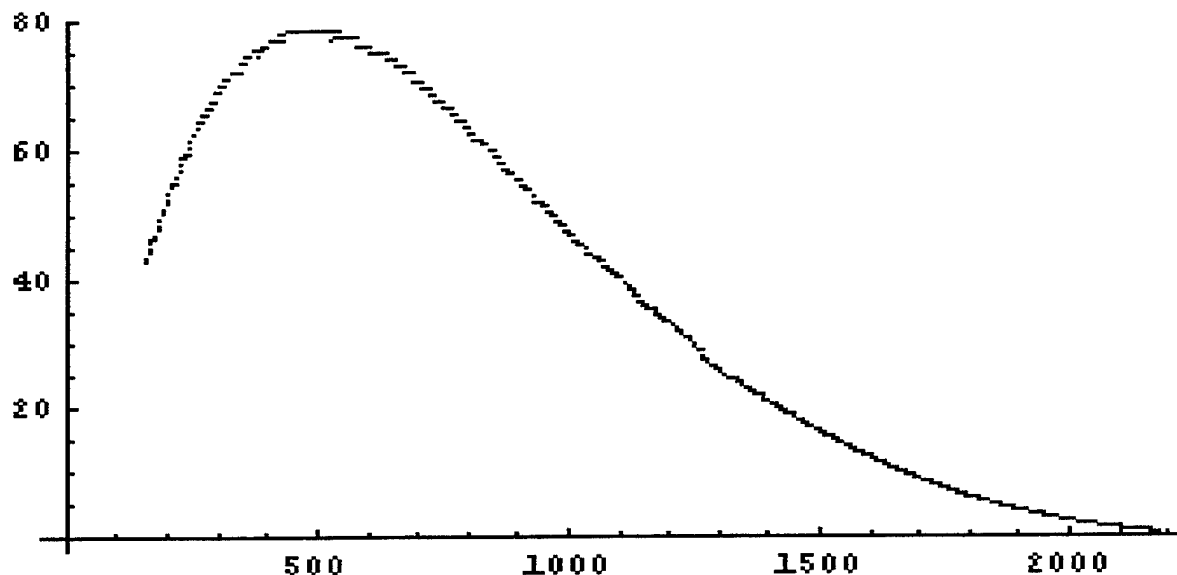


Figure 30: Mathematica Output Graph For The R-Scope 85345 Detector Response File.

To determine the polynomial fit from Mathematica type the following, assuming the file name is 85345.csv.

```
data := ReadList["e:\85345.csv", Number, RecordLists -> True]
```

```
Fit[data, Table[x^i, {i, 0, 3}], x]
```

The “3” in the Fit statement determines that there will be a third degree polynomial. The In[3] := and the Out[4] = are both produced by Mathematica upon completion of the calculations.

The polynomial equation $Y = 38.0556 + 0.148354 x - 0.000185853 x^2 + 5.12486 \times 10^{-8} x^3$, obtained from Mathematica, should be verified that it is a proper fit to the manufacturer's graph of R-Scope 85345. This is accomplished by taking the abscissa values to the digitized manufacturer's curve and use them as the “x” values of that equation to calculate the Y value. The results of the generated values from the equation are compared with the digitized values from the manufacturer's graph on a comparison graph using Excel. See Figure 31 for comparison of the fit for R-Scope 85345. Three comparison graphs for R-Scope 84499 are also shown in Figure 9 - 11 where it was reasoned that more polynomial terms may give a better fit but the opposite was found to be true. It was later learned that a good rule of thumb is to have one term for each hump or dip and that too many terms can give really skewed results as Figures 10 & 11 illustrate. It can be seen that none of the polynomial equations give a good fit to the manufacturer's detection response graphs.

Upon checking the Mathematica documentation the reason became obvious. Mathematica uses a linear “sum of polynomials.” The term linear is interpreted differently from the traditional meaning where $y = mx + b$. Here the largest power of “x” is one, hence it is linear. However, the concept of a linear sum of polynomials means that it may also have a linear factor such as $(x + a)$. Since we can solve for “x” it can be said that it is a linear polynomial. If a

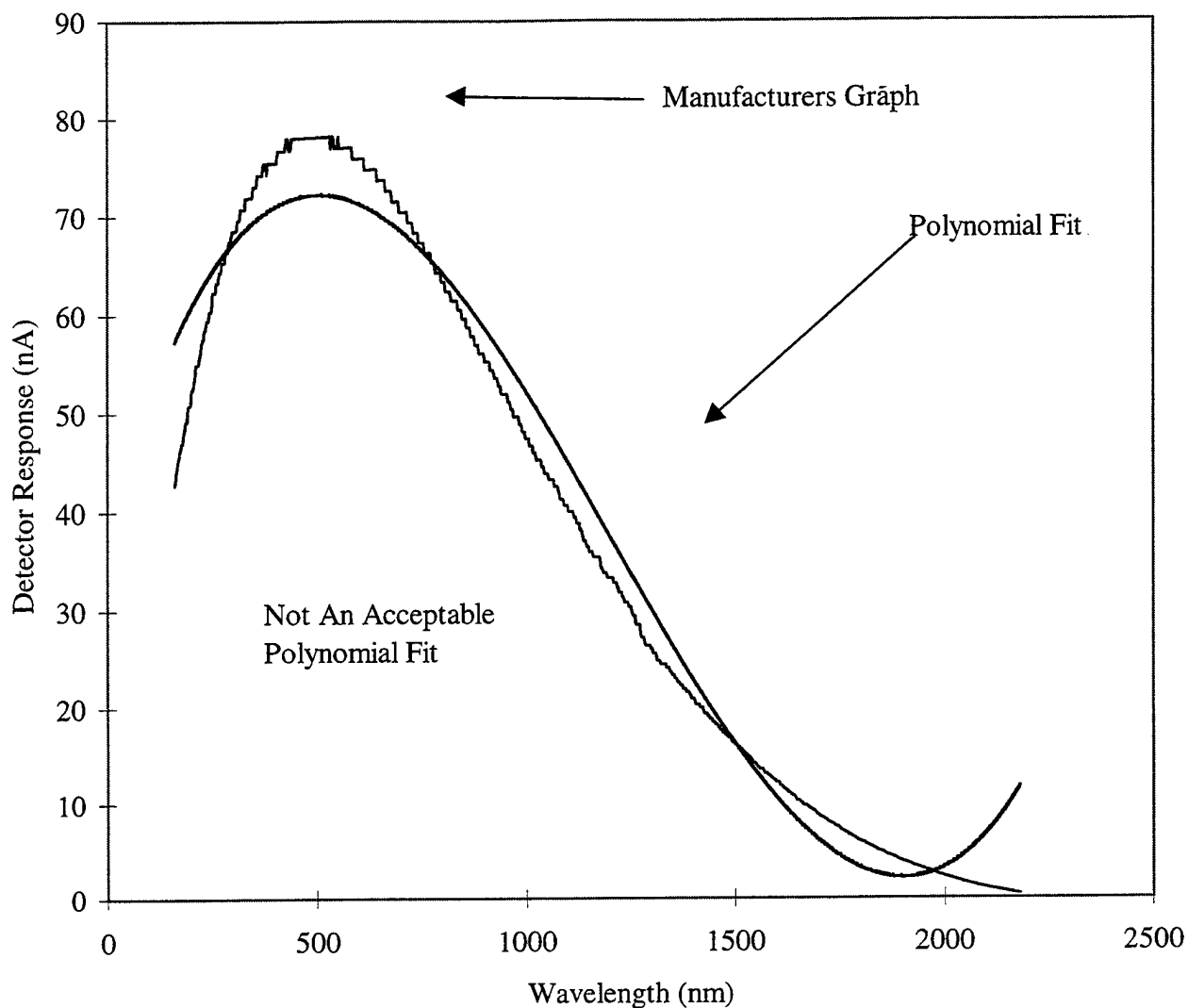


Figure 31 Comparison of R-Scope 85345 With Mathematica Polynomial Fit.

solution to the polynomial has an imaginary term it is nonlinear. The plotting of natural exponential functions " e^x ", logarithmic, and trigonometric functions are all example of nonlinear functions.

The solution to the problem is found in breaking the complex curves into smaller segments and then combining or stacking the segments together. This involved a lot of trial and error attempts as Figures 32 - 34 illustrate for the R-Scope 85345 and Figures 35 - 47 illustrate for R-Scope 84499.

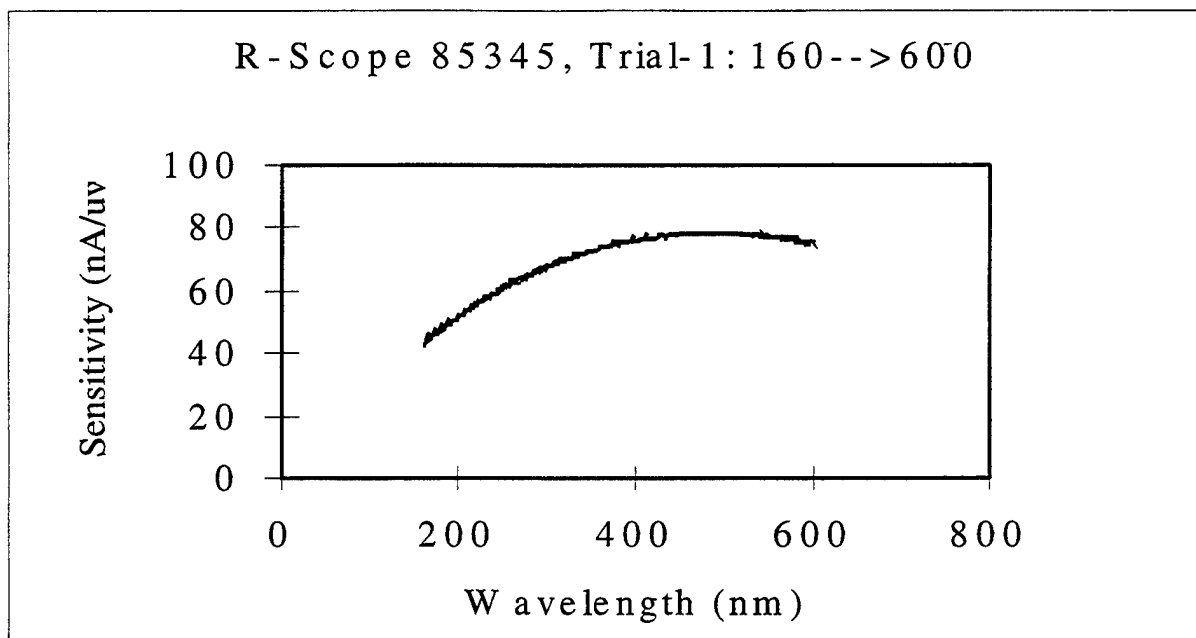


Figure 32: Trial 1 Match Of R-Scope 85345.

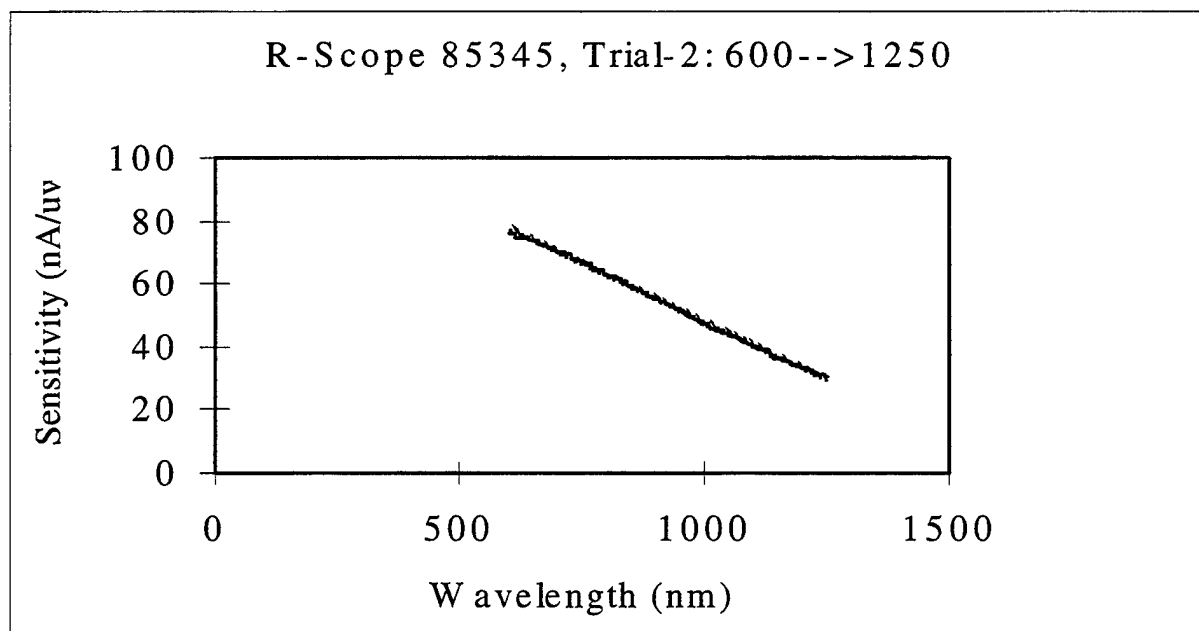


Figure 33: Trial 2 Match Of R-Scope 85345.

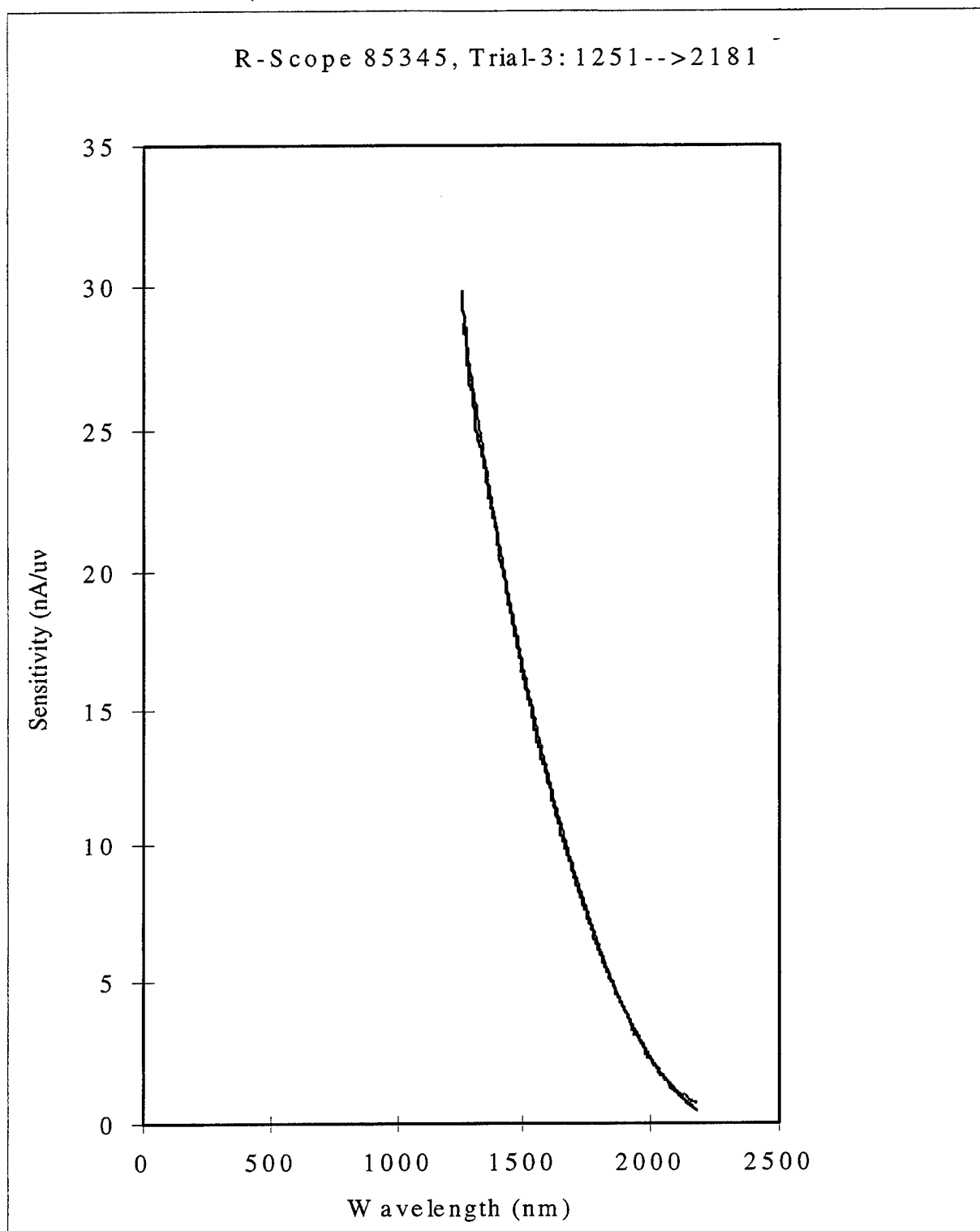


Figure 34: Trial 3 Match Of R-Scope 85345.

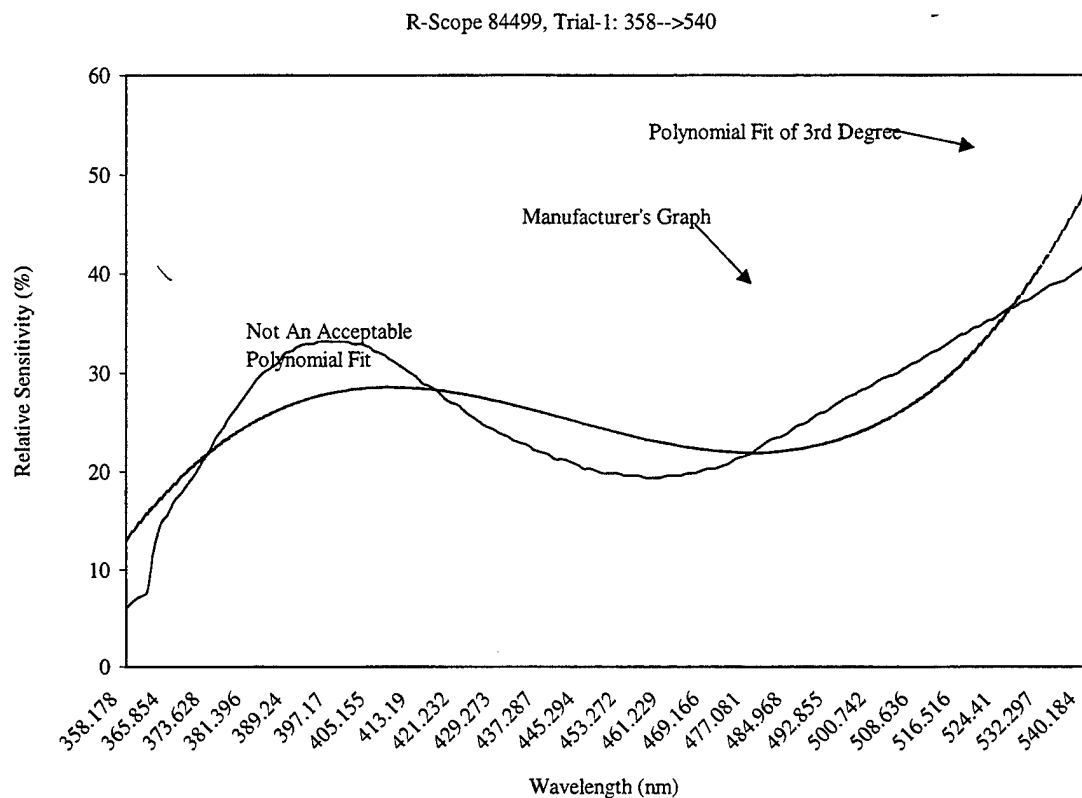


Figure 35: Trial 1 Match Of R-Scope 84499.

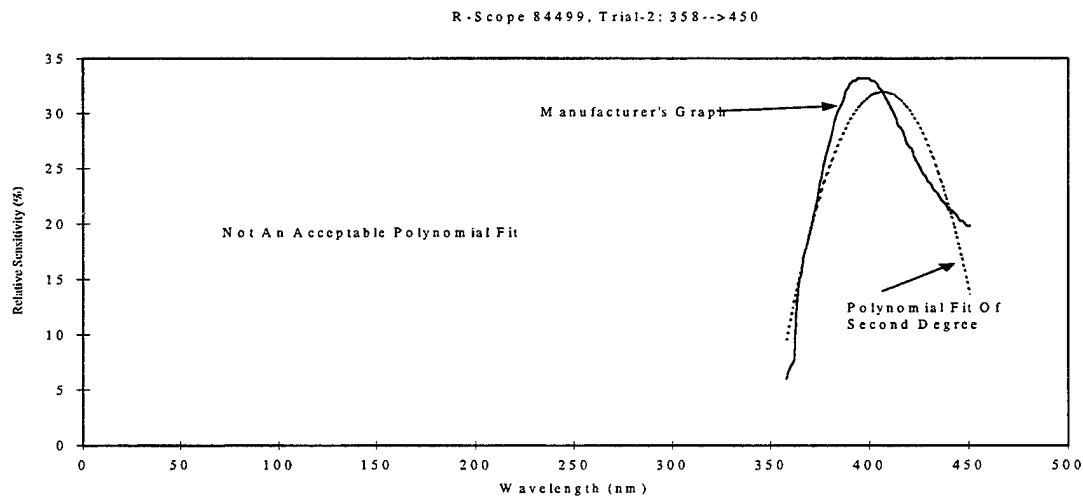


Figure 36: Trial 2 Match Of R-Scope 84499.

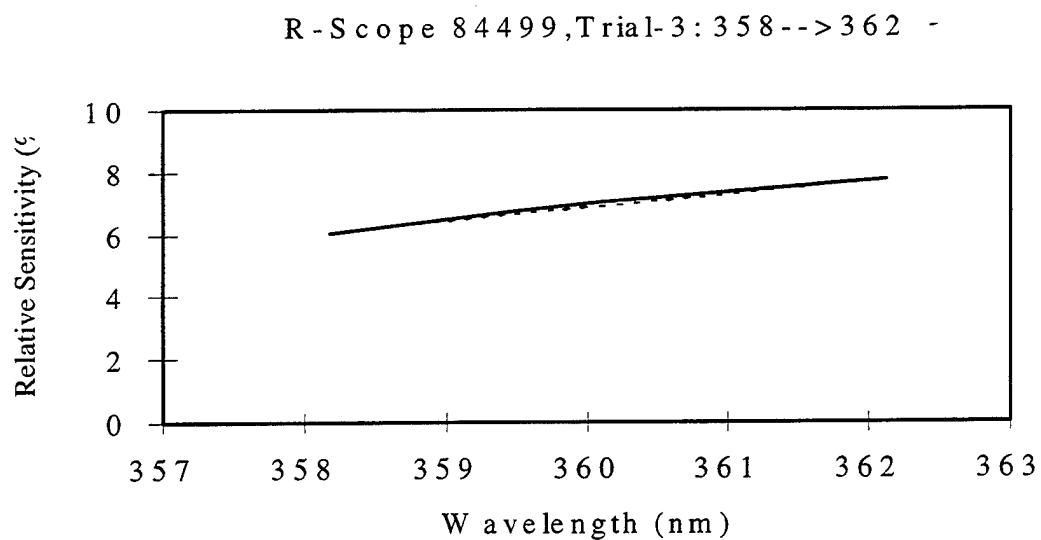


Figure 37: Trial 3 Match Of R-Scope 84499.

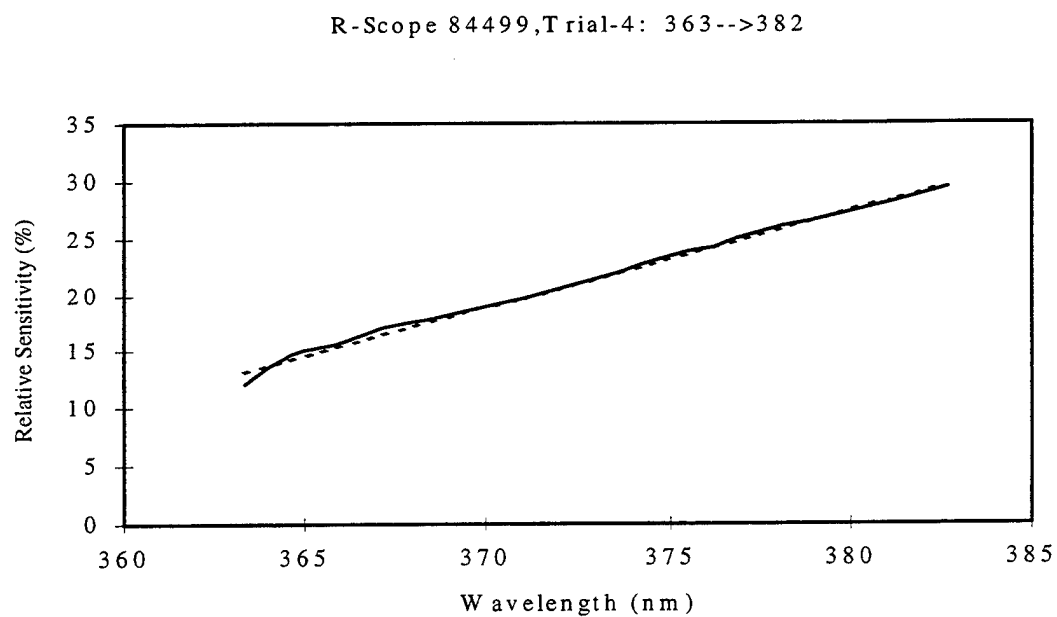


Figure 38: Trial 4 Match Of R-Scope 84499.

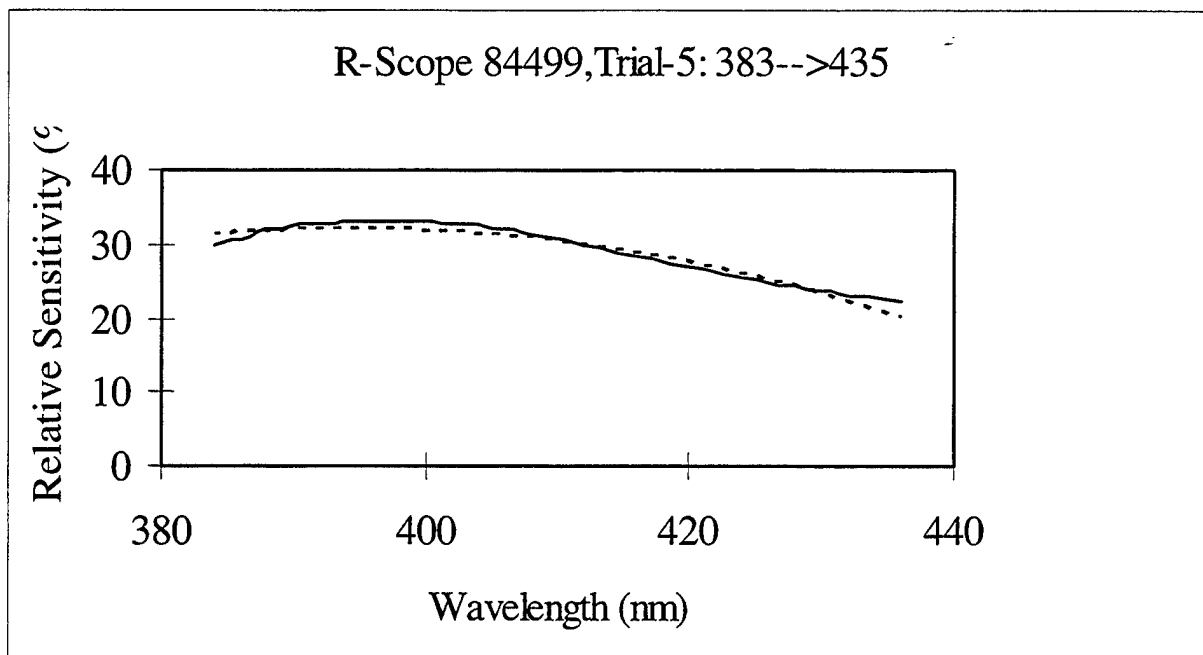


Figure 39: Trial 5 Match Of R-Scope 84499.

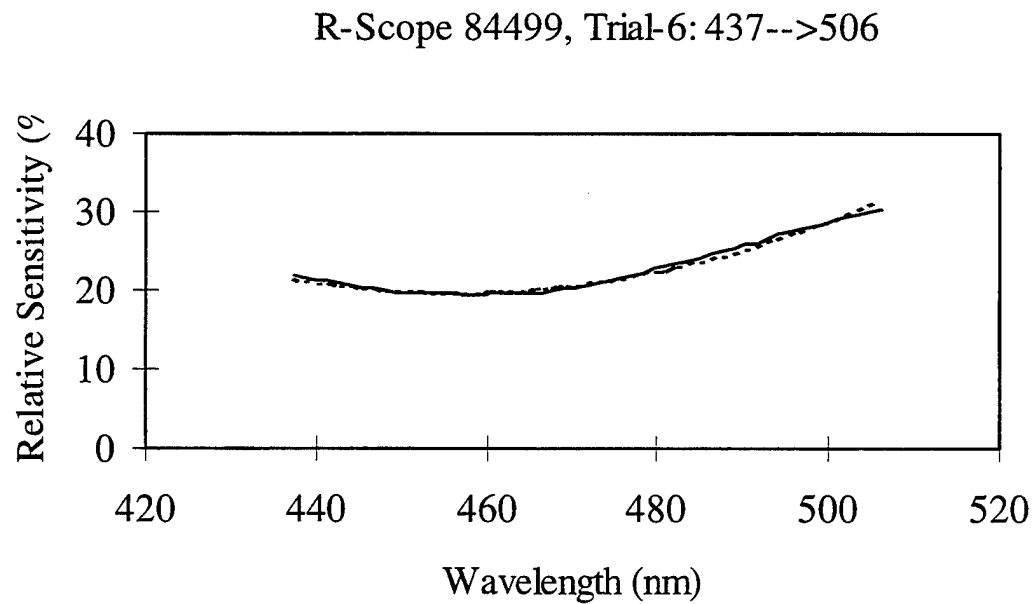


Figure 40: Trial 6 Match Of R-Scope 84499.

R-Scope 84499, Trial-7: 507-->966

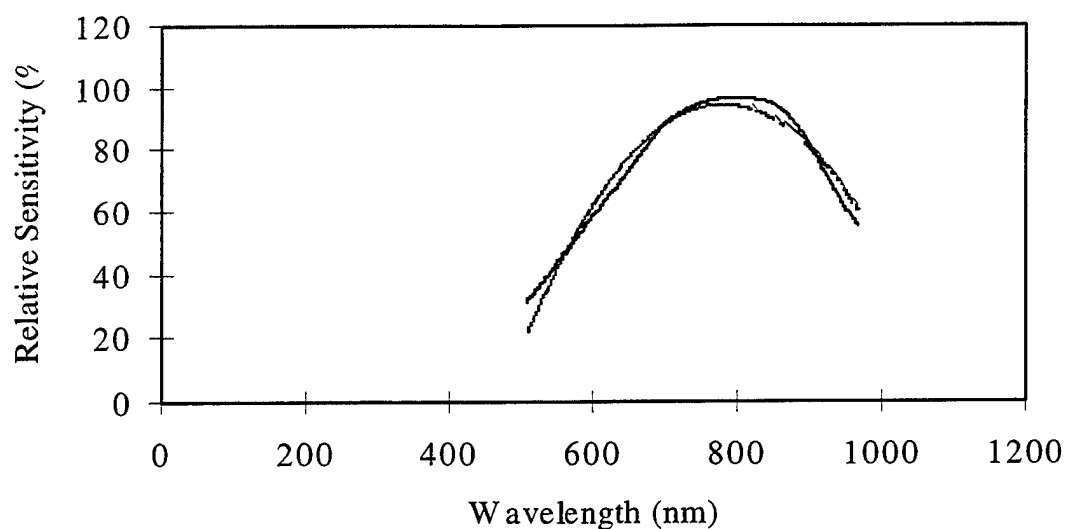


Figure 41: Trial 7 Match Of R-Scope 84499.

R-Scope 84499, Trial-8: 507-->676

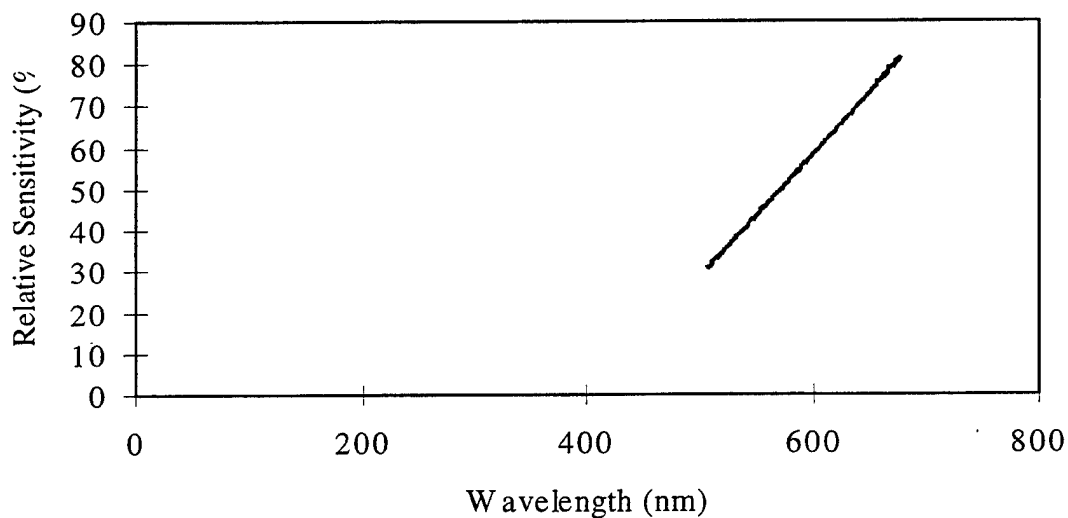


Figure 42: Trial 8 Match Of R-Scope 84499.

R-Scope 84499, Trial-9: 678-->899

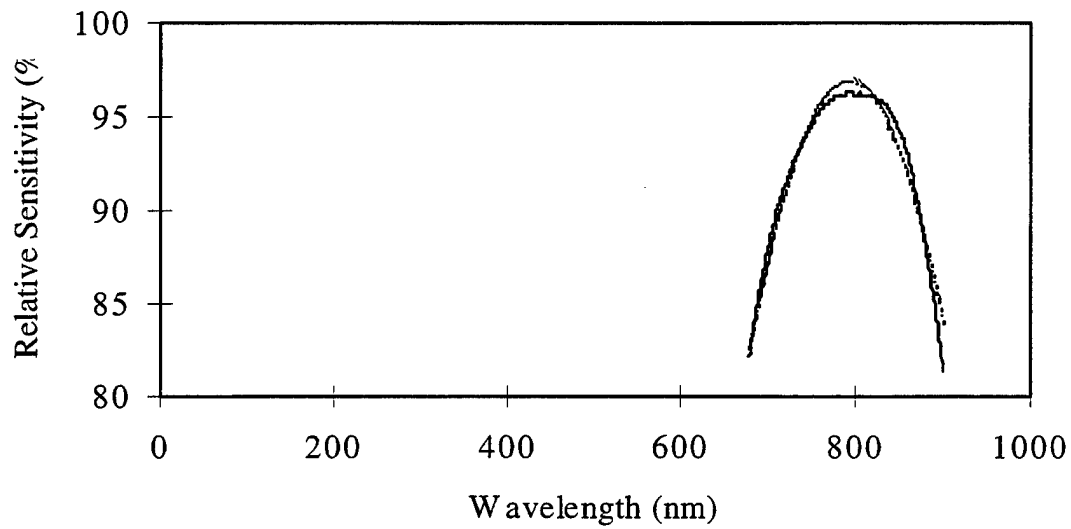


Figure 43: Trial 9 Match Of R-Scope 84499.

R-Scope 84499, Trial-10: 678-->860

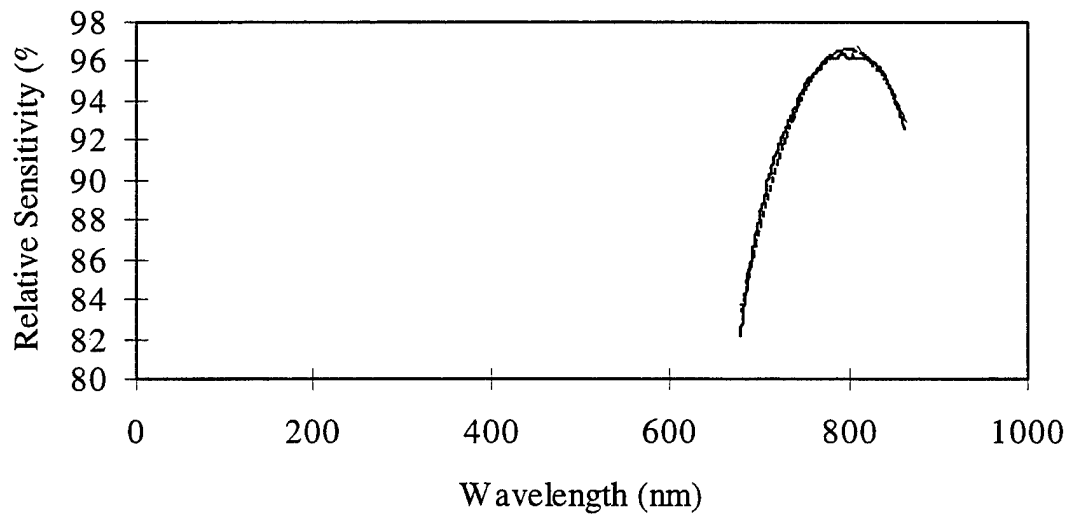


Figure 44: Trial 10 Match Of R-Scope 84499.

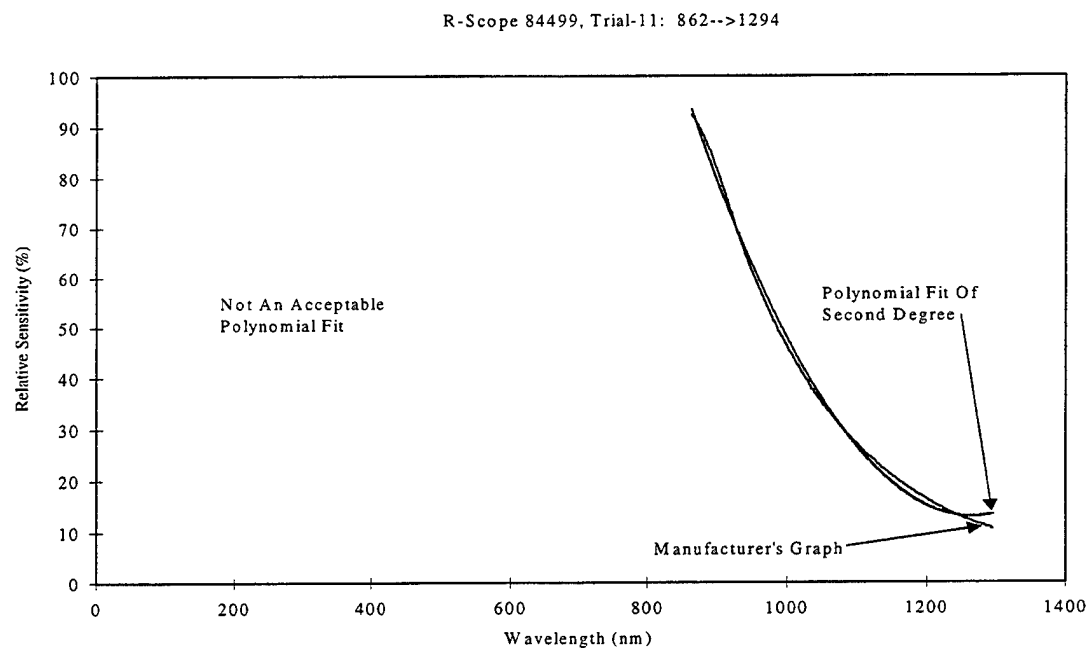


Figure 45: Trial 11 Match Of R-Scope 84499.

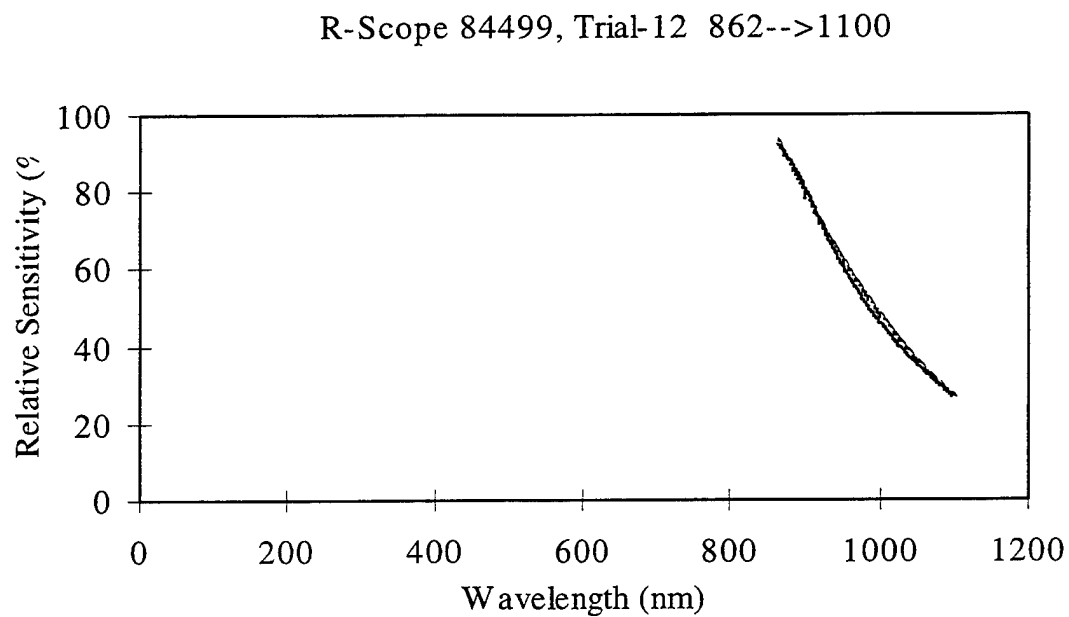


Figure 46: Trial 12 Match Of R-Scope 84499.

R-Scope 84499, Trial-13: 1101-->1295

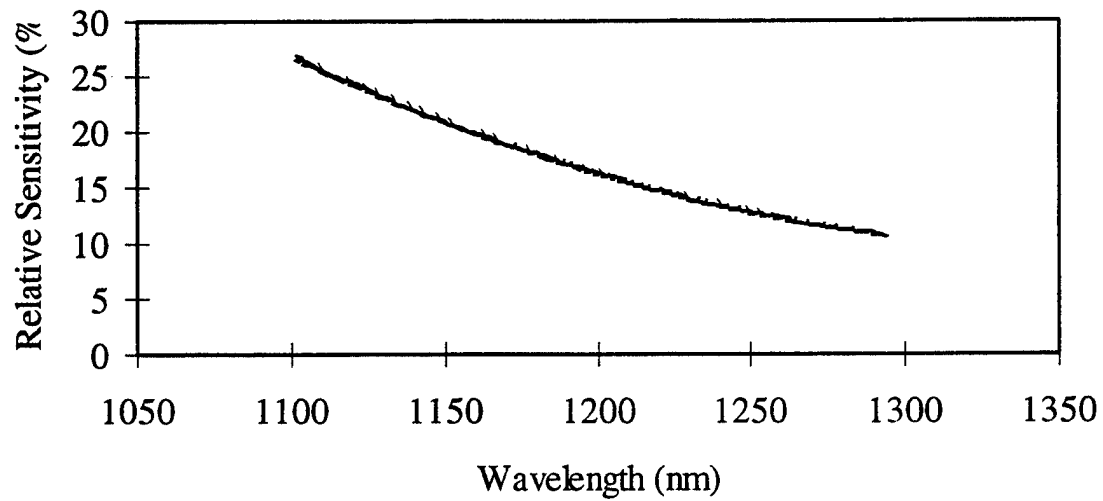


Figure 47: Trial 13 Match Of R-Scope 84499

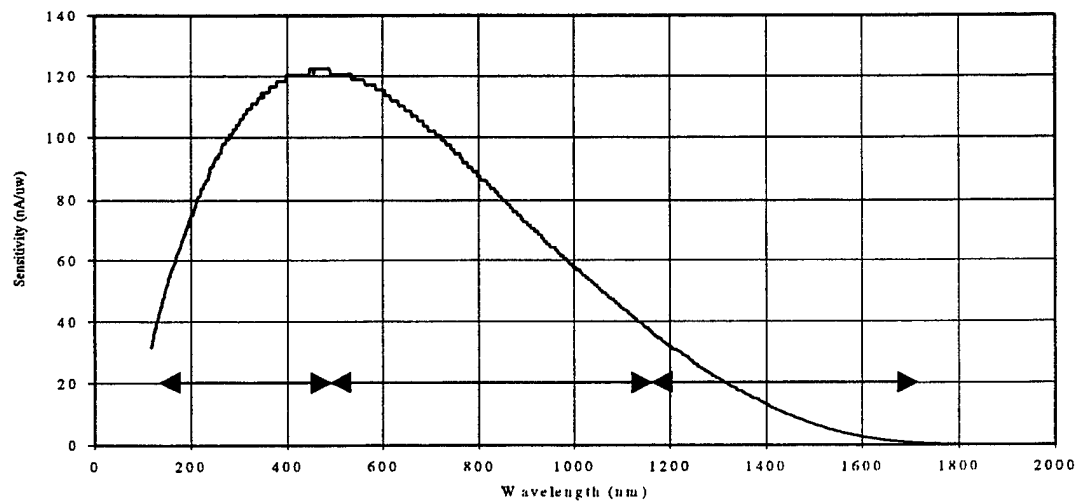


Figure 48: Overview Of 3 Trials For R-Scope 85345.

Figure 12 gives an overview for the trials for the R-Scope 84499 where only 8 of 13 trials were valid.

It is important that when applying the polynomial fit to a section of the “x” values from the AIM $\alpha\beta\gamma$.tm file (which have been converted into micrometers or nanometers) that judgement be made as to where one equation begins and another leaves off. The technique this researcher used was to extend the calculated “y” values for both equations each way beyond the point of intersection and find where the least difference occurs when switching to the next equation. This means the point of junction is arbitrary and care must be taken as to where one equation begins and another leaves off. This also implies that it is not critical at first where you choose to start or stop an equation when first establishing the equation range because adjustments will be made later.

APPENDIX E

PROCEDURES FOR CONVOLUTION AND FINAL RESULTS

The final phase of the analysis is the convolving of everything together and coming up with a graph of those results for each visibility range, for each detector. This is very simply performed when using the new version of Excel when all 20,001 points can be contained in one file, calculated, and graphed. However, since some may not have that capability the more complex approach will be discussed where the 20,001 points are divided into subsets of data. Although this researcher had 15 subsets of data the description will be performed with using only a "few" subsets of data, which follows:

2200nm-AIM85345--> VISIBILITY = 1.0 KM, "R-SCOPE, 85345, 2200nm"

AIM093 AIM093 AIM093 POLY-EQ ATM-DET

(nm)	(1/cm)	% TRAN	(nA/uw)	(nA/uw)	(nA/uw)
649.9837504	15385	3.94E-02	74.05025967	2.916099226	
649.9415053	15386	3.81E-02	74.05340452	2.824248742	
649.8992656	15387	3.92E-02	74.05654897	2.905682755	
649.8570315	15388	3.93E-02	74.05969301	2.9141008	
649.8148028	15389	3.93E-02	74.06283664	2.909928851	
649.7725796	15390	3.68E-02	74.06597986	2.725628059	
649.7303619	15391	3.89E-02	74.06912267	2.88062225	
649.6881497	15392	3.93E-02	74.07226507	2.909558572	
649.645943	15393	3.92E-02	74.07540707	2.902274449	
649.6037417	15394	3.88E-02	74.07854866	2.872766117	
649.561546	15395	3.92E-02	74.08168983	2.907558163	
649.5193557	15396	3.85E-02	74.08483061	2.853377251	
649.4771709	15397	3.73E-02	74.08797097	2.764222197	
649.4349916	15398	3.90E-02	74.09111092	2.887552866	
649.3928177	15399	3.92E-02	74.09425047	2.90138266	
649.3506494	15400	3.92E-02	74.09738961	2.905284549	
649.3084865	15401	3.91E-02	74.10052834	2.896663753	
649.266329	15402	3.65E-02	74.10366667	2.706562321	
649.2241771	15403	3.89E-02	74.10680458	2.882384164	
649.1820306	15404	3.91E-02	74.10994209	2.900440804	
649.1398896	15405	3.92E-02	74.1130792	2.901823503	
649.0977541	15406	3.84E-02	74.11621589	2.843839204	
649.0556241	15407	3.91E-02	74.11935218	2.895398373	
649.0134995	15408	3.90E-02	74.12248806	2.893297199	
648.9713804	15409	3.85E-02	74.12562353	2.851464486	
648.9292667	15410	3.86E-02	74.1287586	2.861295953	
648.8871585	15411	3.89E-02	74.13189326	2.886621792	
648.8450558	15412	3.78E-02	74.13502751	2.799783449	
648.8029585	15413	3.89E-02	74.13816136	2.887607247	
648.7608667	15414	3.88E-02	74.1412948	2.875421836	
648.7187804	15415	3.83E-02	74.14442783	2.838100408	
648.6766995	15416	3.89E-02	74.14756046	2.882708855	
648.6346241	15417	3.83E-02	74.15069268	2.840342283	

Columns 1 - 5, illustrate the following process as discussed in the following paragraphs. Columns #2 and #3 contain the data called in from the AIM045.trn file generated from PLEXUS. Column #2 needs to be converted into nanometers since that is the "x" unit used in the manufacturer's detector curve. Column #1 shows the results of this conversion using the procedure discussed previously in this report. This is only 33 of the 20,001 data points shown extending from 649.9838 nm to 648.6346 nm. Keep in mind that the whole spectrum analyzed went from 2.0 μm to 0.4 μm or 2,000 nm to 400 nm.

Column #4 is the result of using the polynomial equation determined by Mathematica and calculating the dependent value as a result of the value of "x" located in the 1st column. Column #4 is then multiplied by column #3, which is the atmospheric transmittance calculated by PLEXUS in file AIM045.trn. The product of columns #3 and #4 produce the result found in column#5 which is the convolution of the two bits of data for each value of "x" along the spectral range being analyzed. The above procedure is performed for each subset of data, for each file making up the entire spectral range, for each visibility range.

The next step in the process is to stack each subset of data on top of the other in order, from the largest to the smallest or visa versa for each visibility range. There will be one composite graph for each visibility, i.e., six graphs for each detector. Be sure to remove all headings and text such that it is a pure data file with no headings. If the spreadsheet being used is large enough then use it and obtain the graph from excel, which is the simplest route to take.

Obtaining a log graph is most desirable for the "y" axis values so be sure to eliminate all zeros. This is easily done in Excel where there is no actual zero. All that needs to be done is to

put column #5 data as an exponential number and all very small numbers will still exist as a nonzero number.

Since the researcher's spreadsheet is not large enough, Excel was used until it could hold no more and then the file was switched to a text document and called into WORD, the word-processor for Microsoft. The copy function was used to copy and paste the remaining data from the AIM $\alpha\beta\gamma$.trn files into the new WORD file. Be sure to delete all headings and nonnumerical data.

One additional calculation that was performed was to get a sum, a grand total of all the convoluted transmittance data of column #5 for each visibility range. For cases where Excel will not hold all the data be sure to take the sums of the smaller sets of data. This composite sum will be used for one composite graph comparing all the visibility ranges with each other for each detector at the very end of the analysis.

Once all subsets of data are combined into one large composite file, 20,001 "x" values in this case, the data is stored as a text file in WORD. This "text" file is now called into Mathcad and graphed in the following manner. Load Mathcad program

1. Select FILE from main menu. The file selected is only one of the 15 segments of the entire spectrum analyzed. The resulting graph at the end of this discussion is a straight line because of this being only a small section of data being used for this example for the reader to see. The whole composite file was NOT used.
2. Select ASSOCIATE FILENAME under FILE menu
3. Results in a box with options
 - a. Select the file you desire (file should be a tab-delimited text file)

- b. Type in the variable to associate with the desired file. "cccc" was used in this case.
 - c. Select ASSOCIATE
 - d. Select CLOSE
5. On blank screen type: any variable name, colon (which results in a :=),
 READPRN(associated name), enter

 Example → Var:=READPRN(cccc), press enter

 Where "Var" is any variable name I chose, "cccc" was any associated name from previous box declaration, ":=READPRN()" must be there.
6. This results in a green stripped box covering the equation. Wait a few moments and the cursor will drop down below the equation ready for the next step.
7. Type the variable name from the above equation and type an equal sign next to it, not a colon this time. Example: Var=
8. This will result in a large box with the first several rows of data from the file being called in and given the associated name cccc.
 - a. Put cursor right next to the right side of the box and press the left side of mouse. A movable data locator button will appear. Notice the number of the 1st and last data location on the left side of the table of values. (Hint, it starts with a "0" and ends with whatever the last data was numbered with.)
 - b. The box can be moved by depressing the left cursor button and begin circling the box. A black dotted line will form around the box that you can drag to the location desired.
9. Just below the box type in: i :=0..1307 and press enter

- a. This refers to the 1st and last digit
 - b. 1307 is not the last item of data but is the last location (i.e., there are 1307 lines of data). 10 is the last data location shown in the figure but as the data locator is moved on the left side of the table it can move to the end of the data (see discussion in #8 above).
 - c. Pressing enter results in the cursor dropping below that line being ready for the next step.
10. Put select the only graph in the upper menu (next to the equality and inequality icon).
- This results in another menu dropping down to the right of the screen.
11. Select the two-dimensional line graph (upper left corner). Results in a graphing box with three black squares on the left side and the bottom.
12. The left most square of the three on the ordinate side of the graph place the cursor there.
- a. Type in the variable name (name on the left side of original equation that defines the name of the file being called in). Type Var
 - b. Go to the top menu and select the matrix icon that is next to the graphing icon previously selected. Results in another box of mathematical menus dropping down
 - c. Select the 2nd math symbol down from the top left \rightarrow It has a upper case M with a less-than and greater-than symbol above it $\rightarrow M^{\diamond}$. This results in the \diamond being placed above the Var typed into the left of the graph.
 - d. Place the column number of the data desired to be the "y" values, the independent data, between the <and the>.

- 1) The 1st column is NOT one but is zero in numbering; therefore the 5th column is called column #4.
- 2) The variable name now to the left of the graphing square looks like this, using Var as the variable name: Var^{<4>}
 - e. Put the cursor on the Var^{<4>} and press the up arrow until a blue square box encloses the entire expression.
 - f. Press the left square bracket “[”. This will enclose the Var^{<4>} with a set of large parentheses with the cursor in position for a subscript to be placed below the parentheses.
 - g. Type in a small “i” as the subscript.
 - h. It now looks like this: (Var^{<4>})_i
13. Place the cursor over the Var and use the up arrow to bring about the blue square around entire expression.
14. Copy the entire expression and paste it on the middle black square at the bottom.
15. Go into the expression and change the 4 to a 0 so that it looks like this: : (Var^{<0>})_i . The “0” means that the data for the abscissa comes from the 1st column which is numbered the zeroth column according to Mathcad.
16. If a log graph put in the upper and lower limits in the top and bottom square on the left side
17. Since the “x” axis, the abscissa is not having a log scale the numbers will automatically be placed in the two black squares on the bottom for the upper and lower limits.
18. Press F9 and the graph is calculated and shown in the graphing square

19. Save the file as a bitmap file with one of several extensions, one being PCX.

20. Do this for each visibility range for each detector.

Now that the composite graph is established for each visibility range this graph should be printed out. This can be done a variety of ways. One method is selecting the graph, copy and paste it in a blank WORD page. This is performed as follows:

1. Depressing the left mouse button and dragging around the graph resulting in a black dotted line around the graph is Mathcad.
2. Select copy
3. Go to the WORD program and select a blank page to copy into
4. Paste the graph on that page by using SPECIAL PASTE
 - a. Select "Mathcad 6.0 Object"
 - b. Deselect [Float over Text] on left side of screen.
5. Save file with an appropriate name.
6. Print out the graph.

See Figures 13 - 24 for the resulting twelve graphs from the above procedure. These graphs represent the convoluted detector responses modified by atmospheric transmittance effects for the six visibility ranges for the two detectors analyzed in this study. The interpretation of these graphs is discussed in the conclusion section of this report. Figure 13 does have some transmittance but it is below the minimum shown.

The final graph created is a composite graph of all the summations of the convoluted atmospheric transmittance-detector response results for each visibility range. The summation value for each range came as a result of the final table in the convolution procedure where all of the convoluted values for each value of "x" along the spectral range analyzed was summed up.

That summation data was put into the Excel spreadsheet with one column for each detector. The visibility ranges of 0.2 km, 0.5 km, 1.0 km, 5.0 km, 23 km, and 50 km are the independent variables and are also place in one column. For each detector, record the sum of photon emission received by the detector for each range. Use that data to establish a graph/chart in Excel. See Figure 25 for the results of this analysis. Because of the large spread of numbers it may be best to put this into a log-log graph format.

END NOTES

This report covered data calculated from commercial brochures on infrared night vision scopes. Atmospheric transmission calculations were generated from the commercially available program PLEXUS (Phillips Laboratory Expert Assisted User Software). The meteorologist at Wright Patterson, and other U.S. Air Force facilities use the PLEXUS program provided information on the limitations of PLEXUS. PLEXUS has an overall validity in prediction of transmittance and radiance in our atmosphere of approximately 97% overall. In the infrared region, the validity of PLEXUS is even better than the shorter wavelength region. Results are especially predictable for altitudes of less than 80 km, because, the air is essentially a homogenous mixing of gases up to 80 km of altitude. PLEXUS could easily model the atmosphere for the visibility ranges from 0.2 km to 50.0 km. The spectral sensitivity data from the commercial night vision scopes were readily modeled mathematically, using the commercial software package Mathematica. The atmospheric data from 400nm to 2,000 nm was convolved with the night-vision, scope sensitivity that was modeled from the manufacturer's data. The data showed that enhanced infrared response increased the utility of the night vision scope under adverse visibility conditions.

The mathematical modeling using PLEXUS, Mathematica, Mathcad, Excel, and other software programs has proven to be a reliable way of predicting the behavior of detector responses under a variety of conditions. It is believed that the quantitative results, and predictions made, would be shown to be an accurate representation of any actual field-testing. Field testing is very expensive. The modeling technique described in this document should minimize the amount of testing necessary, thus, saving millions of dollars in field-testing.

The two-month time constraint limited the number of "infrared scopes" and possible scenarios considered. However, a methodology has been established and when specific detectors need to be evaluated, this tool is in place to facilitate the decision making process.